A Study on Transient Stability and Effective Use of Synchronous Inverter under Introduction of Renewable Energy in Power Systems

（　電力系統における再生可能エネルギー導入時の過渡安定度及び
同期化力インバータの効果的使用に関する研究　）

Yuki Nakamura

Graduate School of Engineering
Hiroshima University

March 2019

Contents

Chapter 1

Introduction: Power system on introduction of renewable energy

1.1 Background and purpose

The introduction of Renewable energy source (RES) is being advanced all over the world. Especially in Japan, we aim to introduce Photovoltaic power generation (PV) to 64 GW which corresponds to 7% of the total electricity generation amount, and the introduction volume is expanding rapidly [1]. However, there are various problems when they are connected to the electric power system [2]. One of them is difficult to forecast because the output depends on the weather, and proper operation of generators etc. is required for stable system operation. Therefore, the thesis proposes control by the generator and control of the inverter attached to PV.

1.2 Renewable energy source

RES means the energy extracted from among the recurring phenomenon in the natural environment, in contrast to fossil fuels and nuclear power, such as oil and coal, which have a risk of depletion. Specifically, it is new energy that is natural energy utilizing photovoltaic power, hydro power, wind power and biomass and recycled energy utilizing incineration heat of wastes. Because these energies do not emit greenhouse gases that are the cause of global warming at the time of power generation, it seems that there is a significant effect in reducing the CO2 concentration in the air.

1.2.1 Photovoltaic generation

Photovoltaic power generation (PV) is the power generation system that converts sunlight energy into electrical energy by using solar panels. The most often-used solar cells are silicon solar cells [3]. This is a cell superposed n-type and p-type silicon semiconductors that have different properties. Particles that have a positive charge (holes) and negative charge (electrons) are born when light strikes the solar cell, the electrons are

attracted toward the n-type silicon, holes are attracted toward the p-type silicon. As a result, an electromotive force is generated, and current flows through the external electrical circuit. In addition, the advantages and disadvantages of PV are shown as below.

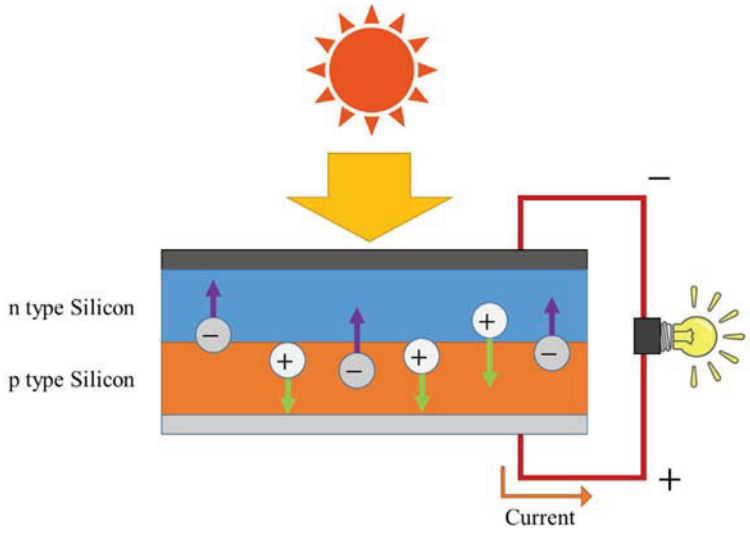

Fig.1-1 Principle of power generation of solar panel

<Advantages>

- There is no worry about depletion because it is an infinite energy source.
- It does not emit greenhouse gases during power generation.
- Transmission loss is small, because it can be installed to demand area.
- It is possible to generate power in the daytime that is much in demand.

<Disadvantages>

- It needs a vast area because the energy density is low.
- It cannot generate power at night.
- Output is unstable because depends on the weather.
- High equipment costs.

1.2.2 Confidence interval for PV

Since the output of PV generation varies with the amount of solar radiation, forecasting solar radiation amount is a very important task. Since it is extremely rare for prediction

to be 100% correct, some methods show a value including the prediction error. By giving this prediction error as a confidence interval, PV uncertainty is considered in this thesis. Fig.1-2 shows solar radiation forecast with confidence interval. Arrows indicate possible range of solar radiation at that time.

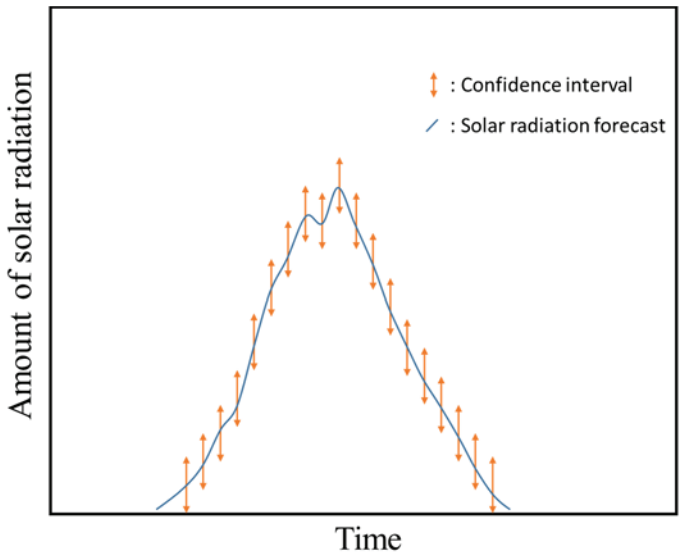

Fig.1-2 Example of solar radiation forecast with confidence interval

1.3 Power system

Power system intricately consist of a huge variety of power generator, transformer and load, etc. and its state is determined by supply and demand. Power systems are constantly exposed to any disturbances such as direct hit from lightning and contact with animals always. Under these circumstances, the phenomenon is power oscillation that cannot be avoided, and it can occur frequently. Suppressing this vacillation is necessary in order to ensure the reliability of the power system and supply stably economically.

A state that the power system is operated stably is to be maintained voltage and frequency within the specified value anywhere in the system and to be balanced both active power and reactive power [4]. However, there are many the elements interfering

with the stable operation of the power system, such as rapid load change. The stability means the strength of stable supply when state change of power system due to load changes or failure.

1.3.1 Synchronous mechanism of generator

Here, we discuss with transient stability in power system. The stability indicates an important measure that means to keep the stable power supply against system disturbances such as power equipment faults or demand fluctuations. It can be classified into the following: First is steady-state stability index. This is a measure to treat whether it is possible to operate stably in case of small disturbance has occurred. The other one is the transient stability. This means a degree to treat whether it is possible to return to normal operating in case of large disturbance has occurred such as sudden shut-down of generators. Furthermore, in consideration for the influence on the control system, these stability index are classified by transient region (0~1[sec]), intermediate region (1~60[sec]) and steady state region (1~[min]).

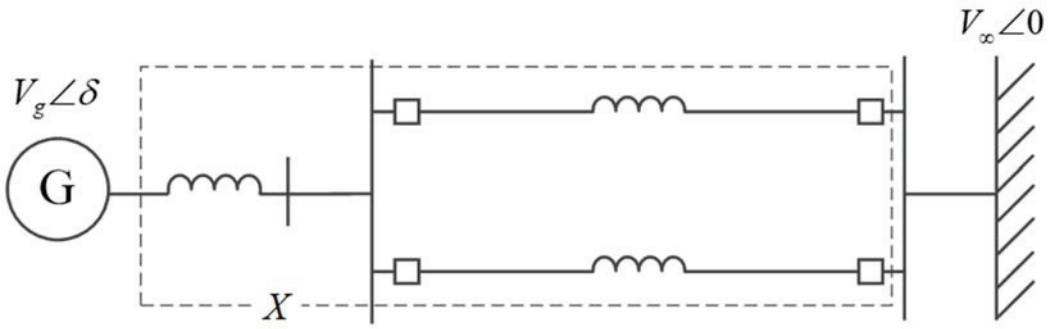

Fig.1-3 Single-machine infinite-bus systems

Next, we discuss the synchronizing power to use single-machine infinite-bus system shown in Fig.1-3. This is a model which one generator is connected to a large power system infinitely via power transmission line. The system as viewed from the generator

is regarded as a power supply which frequency and voltage is constant. The voltage of the infinite bus is set as the reference of the phase, and the difference between this reference phase and the phase angle of generator internal voltage is the phase difference δ. We assume that the resistance of power system equipment can ignore because it is very small compared with the reactance. The power equation is as follows:

$$P_e = \frac{V_g V_\infty \sin\delta}{X} \qquad (1\text{-}1)$$

Where, V_g is internal voltage of synchronous generator, V_∞ is the voltage at the infinite bus, X is the transmission line impedance including the internal reactance of the generator. Incidentally, the power swing equation expresses the state of a system with the differential equation. At one machine with infinite bus system, θ is regarded as internal phase of generator. The power swing equation is as follows.

$$M\frac{d^2\delta}{dt^2} = P_m - P_e \qquad (1\text{-}2)$$

Where, M is inertia constant, P_m is a mechanical input, P_e is an electrical output.

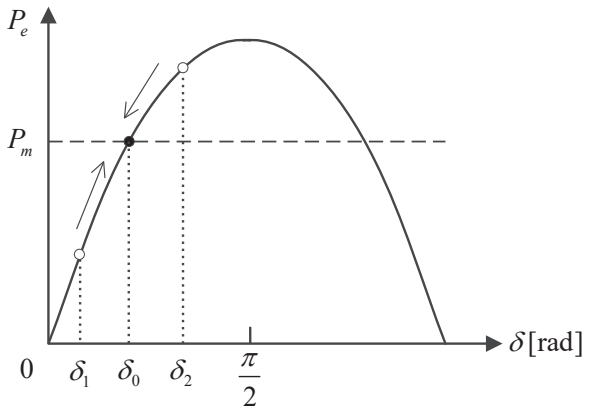

Fig.1-4 Transient Power-Angle Characteristics

Fig.1-4 shows transient power-angle characteristics which signifies the relation between the power output and phase difference. In the figure, the mechanical input is assumed to be constant. δ_0 is the phase difference when the mechanical input and electrical output is

equal. In this state, the generator is on the balanced operation. When it assumed to become $\delta_1 = \delta_0 - \Delta\delta$, Pm is larger than P_e, the generator may accelerate. Contrary to this, when it assumed to become $\delta_2 = \delta_0 + \Delta\delta$, Pm is smaller than P_e, the generator will slow down. Thus, we call this power the synchronizing power that the generator seeks to return to a steady state. The synchronizing power is signified by $dP/d\delta$. Then, the equation in order to maintain a synchronized operation must be satisfied. That is, the synchronizing power is the gradient in power-angle curve.

$$\frac{dP}{d\delta} > 0 \qquad (2\text{-}3)$$

1.3.2 System stability

Stability of the power system has stability of synchronization, voltage stability, frequency stability, and stable operation cannot be performed unless these three types of stability are maintained. Synchronization stability arises from the fact that the synchronous machine is used as the main generator of the electric power system and is generally called stability. In this system, the voltage phase angle of the generator in the system converges to a fixed value, and the stability is judged by whether or not the synchronous operation can be maintained. In addition, he N-1 security criterion, which assume that accidents occur on one line in two lines, has been used worldwide to maintain power system security and reliability [5-7]. Stability is largely classified into the following two.

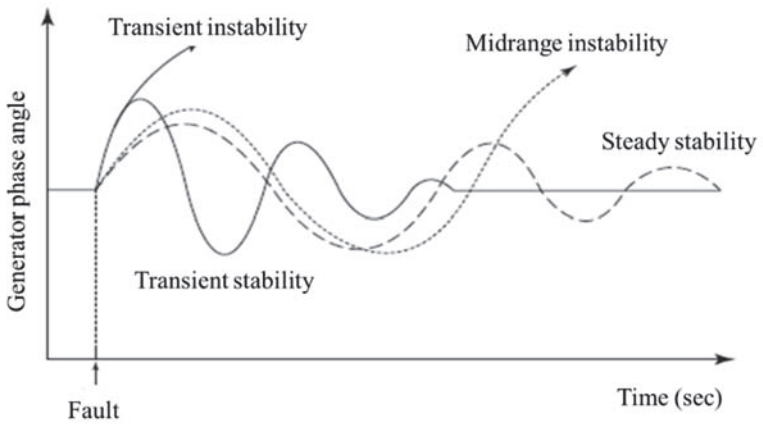

Fig.1-5 Examples of stability classification

1.3.2.1 Steady-state stability

It refers to the stability of whether or not the fluctuation falls back to the original state when the electric power system is in equilibrium operation state and extremely small disturbance is applied. It is the degree to which synchronous rotation can be maintained even if gentle load change occurs. Unlike the transient stability, stability is applied to a relatively long time domain of tens of seconds, so normally a linearly approximated differential equation is used for analysis, but nonlinearity sometimes becomes a problem.

1.3.2.2 Transient-state stability

It is the stability of the region where the disturbance applied to the strain is relatively large, the influence of the nonlinearity is large, and the elapsed time from the occurrence of disturbance is short. It is the degree to which synchronous rotation can be maintained even if a sudden disturbance such as a system accident occurs. We handle the phenomena in the first wave of rotor-to-rotor fluctuations or in the time domain of about 1 second (at most about 2 to 3 seconds).

1.4 Taoyaka Project

Since I belong to the graduate program of master and Ph. D course in the Hiroshima University, I solved the problem in the disadvantaged area using the technical field in the curriculum. My group proposed a new type of community center with the aim of smart village at Kodani, Takaya-cho in Higashi Hiroshima City, Japan [Appendix]. I worked on building a smart electric power system among them. We established Taoyaka Farm as a community center in the Kodani region of Higashi-hiroshima city as a test case.

Fig.1-6 About activities of the Taoyaka project

As a technical aspect, I decided to cover the power inside the Taoyaka from PV panels. There are solar panels, DC - DC converters with MPPT function, batteries, pumps for hydroponics and lights, and it is a system completely independent from the power grid. I only measured PV outputs and loads because project period is limited.

Future tasks for Taoyaka project

I am trying to stabilize the power system of remote islands and areas where the power system is weak with this inverter. In addition, it enables house interconnection since this inverter covers single phase voltage used in ordinary households. Therefore, it is possible to build a power system step by step against unelectrified areas. This conceptual diagram is shown in Fig.00.

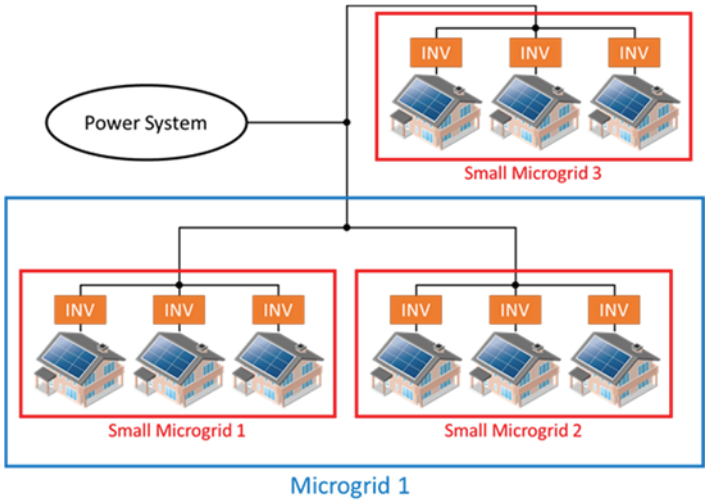

Fig. 1-7 Concept model for Taoyaka project from technical aspect

Eventually I aim to establish a microgrid by the proposed inverter. Microgrid means the system that allows small-scale power generation facilities to be interconnected within the region to stable power supply. As an actual experiment site, several small inverters are easily installed in the laboratory. In addition, because Taoyaka Farm was built within the Taoyaka Project and an independent system was built inside, testing of synchronous inverters is possible there as well.

1.4 Outline of the thesis

Chapter 2 explains the stability of power system and its analysis methods. Conventional stabilization control methods are also explained.

Chapter 3 proposes a novel approach, that is, the transient stability analysis and control methods based on CCTs. First, the characteristic of CCT is investigated when PV is introduced to conventional system. Then, the transient stability control through CCT is studied based on CCT-DF by controlling generator outputs. This chapter also discusses formulation and solution of robust optimization problem for secure power system operation against REs uncertainties. Then, the effectiveness is verified by simulation.

Chapter 4 proposes a new design of the synchronous inverter for improving power

system stability. Assuming the future situation, it is expected that synchronizing power also decreases with the decrease of synchronous generators in operation. Then, the synchronous inverter, which have synchronizing power similar to synchronous generator, is designed for improving power system stability. The conventional functions for voltage and frequency controls are also implemented in the inverter.

Chapter 5 concludes this thesis through each chapter discussion.

Chapter 2

Stabilization control for power system

2.1 Transient stability analysis

There is concern that deterioration of transient stability will be caused by massive introduction of RESs. If the transient stability gets worse, a little system failure will also cause a major blackout. Therefore, it is very important to monitor transient stability. Therefore, some transient stability analysis methods are introduced. In this thesis, the analysis is usually performed by time domain simulation method, where numerical integration of ordinary differential equation (ODE) is time consuming but can deal with numerous complex nonlinear phenomena [8,9]. Transient energy function (TEF) methods are an alternative approach, where system stability is assessed on the base of transient energy [10-17]. They provide fast and efficient stability assessment while certain disadvantage is related to the accuracy of stability judgment. The Boundary Controlling Unstable (BCU) equilibrium point method comprises a strong theoretical background and appears to be a credible approach [12] with improved computation of Controlling Unstable Equilibrium Point (CUEP) [15-17].

2.1.1 Critical clearing time

The system is divided into stable and unstable depending on the time to remove faults when a system fault occurs. The fault clearing time which is the boundary between stable and unstable is called Critical Clearing Time (CCT) as shown in Fig.2-1. If the fault clearing is fast, the system will return to the stable state. However, if it is later, it will shift to the unstable state. Normally, protection relay works after system fault occurs and fault clearing is performed automatically. In other words, if the CCT is shorter than this protection relay operation time, the system becomes unstable. Thus, the grid operator needs to operate the grid at the operating point where CCT is longer than this protection relay operation time. Also, since it is possible to determine whether the system is stable or unstable simply by checking the CCT as described above, it is an extremely easy-to-

use index for evaluating transient stability.

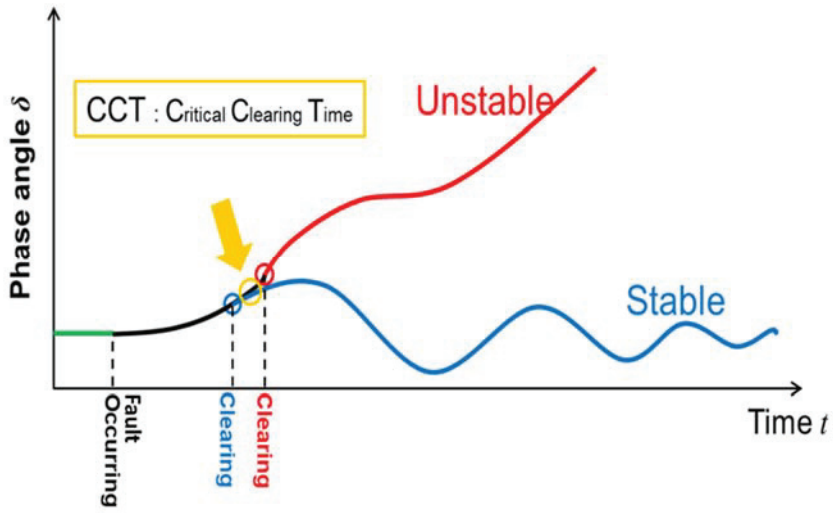

Fig.2-1 Relationship between Critical Clearing Time and stable/instability

2.1.2 Time domain simulation method

In the time domain simulation method, the state of the grid is sequentially calculated, and stability is determined from the behavior. In this method, since the state of the system can be strictly expressed, calculation can be performed also on detailed models considering the control system and the like. However, in the simulation method, the computation time increases sharply as model complexity and system size increase. Furthermore, in general, it is necessary to calculate the stability limit state in order to grasp the stability margin of the system. However, since this method is a method of setting the fault elimination time in advance and verifying stability / instability in that case, stable It is not suitable for computing the limit.

The numerical solution method by the simulation method will be explained below. Specifically, the numerical integration method used to sequentially calculate the state of the system will be explained. In general, the numerical integral method in the stability calculation is to integrate the equation (1-2) which is the oscillation equation of the

generator with a certain step size in order to know each state of the system. Especially in transient stability calculation, since nonlinear equations are handled, numerical integration method is an effective means. Here we describe representative numerical integration methods in power system simulations, which is the 4th order Runge-Kutta method.

4th order Runge-Kutta method

The 4th order Runge-Kutta method is a numerical solution of ordinary differential equations that can obtain numerical solutions with high accuracy. The fourth Runge-Kutta method can be expressed as follows, assuming that a given amount of x_n in the function $\dot{x} = f(x,t)$ is given as a known amount and the step size of the independent variable *t* is *h*.

$$t_{n+1} = t_n + h \tag{2-1}$$

$$x_{n+1} = x_n + \frac{1}{6}(k_1 + 2k_2 + 2k_3 + k_4) \tag{2-2}$$

Where,

$$\begin{cases} k_1 = h \cdot f\left(x_n, t_n\right) \\ k_2 = h \cdot f\left(x_n + k_1/2, t_n + h/2\right) \\ k_3 = h \cdot f\left(x_n + k_2/2, t_n + h/2\right) \\ k_4 = h \cdot f\left(x_n + k_3, t_n + h\right) \end{cases}. \tag{2-3}$$

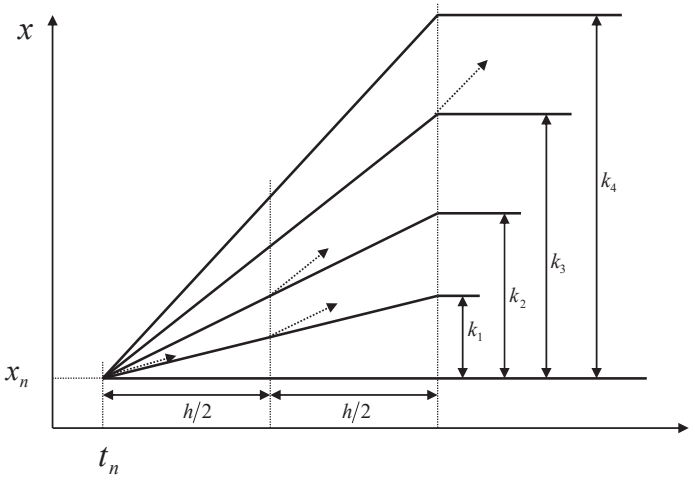

Fig.2-2 Conceptual diagram of the 4th order Runge-Kutta method

The calculation method by time domain simulation method is described. When systematic contraction is done, next, the same number of shaking equations as the number of generators will be sequentially solved by numerical integration. At that time, a slack generator is decided from among a plurality of generators, and the phase angle of the slack generator is used as a reference. Figure 2.15 shows the behavior of the system when a fault occurred at time 0 [s] and the fault was removed at 0.18 [s], δ_{21} is the generator 2 based on the phase angle of the generator 1 and δ_{31} is the phase angle of the generator 3.

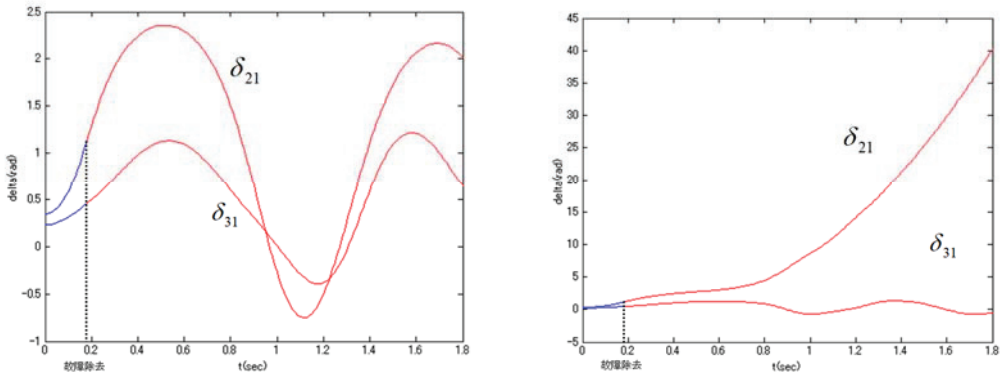

(a) Stable trajectory (b) Unstable trajectory

Fig.2-3 Shaking waveform of generator phase angle

As shown in Fig. 2-3(a), it is found that when the fault is removed at 0.18 s from the occurrence, the system is restored to the stable state. Fig. 2-3(b) is a diagram when fault removal is performed at 0.19 s. In Figure 2.16, the phase angle of the generator 2 is greatly divergent, indicating that the system becomes unstable. From this, CCT can be estimated to be between 0.18 [s] and 0.19 [s].

2.1.3 Transient energy function method

The energy function method is a method of comparing the transient energy value of the system at the time of fault clearing and the (critical) energy value at the stability limit to perform stability discrimination. The outline of the energy function method and the stability discrimination method will be described below.

In the energy function method, since the first fluctuation of the generator is targeted, a classical model is used as a generator. That is, for the generator under shaking, the following expression that does not consider the braking system is assumed to hold.

$$M\dot{\omega} = P_m - P_e \tag{2-4}$$

$$\dot{\theta} = \omega \tag{2-5}$$

Furthermore, in order to consider only the relative motion of the generator in the energy function method, we introduce the center of inertia (COI) reference axis expressed by the following equation.

$$\theta_0 = \frac{1}{M_T}\sum_{i=1}^{n} M_i\theta_i \tag{2-6}$$

$$\omega_0 = \frac{1}{M_T}\sum_{i=1}^{n} M_i\omega_i \tag{2-7}$$

Where, $M_T = \sum_{i=1}^{n} M_i$, n is the number of generator. Phase angle and angular velocity are redefined by COI.

$$\tilde{\theta}_i = \theta_i - \theta_0 \tag{2-8}$$

$$\tilde{\omega}_i = \omega_i - \omega_0 \tag{2-9}$$

Swing equation is expressed as follows.

$$M_i\dot{\tilde{\omega}}_i = P_{m_i} - P_{e_i}(\tilde{\theta}) - \frac{M_i}{M_T}P_{COA}(\tilde{\theta}) \tag{2-10}$$

$$\dot{\tilde{\theta}}_i = \tilde{\omega}_i \tag{2-11}$$

Where, $P_{COI}(\tilde{\theta}) = \sum_{i=1}^{n}(P_{m_i} - P_{e_i}(\tilde{\theta}))$, $P_{e_i}(\tilde{\theta}) = {E_i}^2 G_{ii} + \sum_{j=1, j\neq i}^{n} E_i E_j (G_{ij}\cos\tilde{\theta}_{ij} + B_{ij}\sin\tilde{\theta}_{ij})$.

Add both sides for all generators and integrate with the phase angle to obtain the energy

function of the generator group.

$$
\begin{aligned}
V &= \frac{1}{2}\sum_{i=1}^{n} M_i \tilde{\omega}_i^{\,2} + \sum_{i=1}^{n}\int_{\tilde{\theta}_i}^{\tilde{\theta}_i^s} (P_{e_i}(\tilde{\theta}) - P_{m_i} + \frac{M_i}{M_T} P_{COI}(\tilde{\theta}))d\tilde{\theta}_i \\
&= \frac{1}{2}\sum_{i=1}^{n} M_i \tilde{\omega}_i^{\,2} - \sum_{i=1}^{n} P_i(\tilde{\theta}_i - \tilde{\theta}_i^s) - \sum_{i=1}^{n-1}\sum_{j=i+1}^{n} E_i E_j B_{ij}(\cos\tilde{\theta}_{ij} - \cos\tilde{\theta}_{ij}^s) \qquad (2\text{-}12) \\
&= V_K(\tilde{\omega}) + V_P(\tilde{\theta})
\end{aligned}
$$

Here, the ideal energy function does not change temporally with constant oscillation without braking system and is constant. In the energy function method, stability is determined from the energy value at the time of fault removal, which is very fast. However, in general there is a problem with accuracy because there is a damping system.

2.2 Conventional stabilization control

There are various loads in the power system. The load includes electric lights used in ordinary households, home appliances such as air conditioners, electric furnaces used in factories, electric machines for work and the like. These loads are generally designed to exhibit the best performance when used at rated voltage. Therefore, if the voltage deviates from the rated value when using the equipment, it will adversely affect the accuracy, efficiency and life of the equipment. In order to use these devices with high accuracy and safe, it is necessary to stably supply high-quality electric power. Furthermore, it is a matter that cannot be written to keep the power receiving end voltage of the customer load at the specified value. The three main methods are described below.

(1) Adjust the field voltage of the generator to adjust the internal induction machine power of the generator.

(2) Adjust the transformation ratio by operating each tap control transformer.

(3) Open and close the conditioning equipment (power condenser and shunt reactors).

Each of the above-mentioned voltage control capabilities has its own characteristics and limitations, and by complementing each other, the voltage of each place is maintained at

an appropriate value. In addition to these three, we also summarize the control using FACTS equipment using power electronics technology using high-speed controllable devices.

2.2.1 Stabilization by generator

Voltage control method by the power generator is time schedule method determined the target voltage and power factor by system demand for each time, and it is often used. Target voltage is controlled by Automatic Voltage Regulator (AVR), and target power factor is controlled by Automatic Power Factor Regulator (APFR). By controlling excitation current of the generator automatically, the AVR controls terminal voltage and the APFR controls power factor. Moreover, reactive power Regulator (AQR) are also control the reactive power output of the generator.

<Characteristics>

- Voltage can be continuously controlled.
- If the online control, the voltage can be controlled at a high speed.

<Problems>

- It is easy to control the system overall voltage, but it is difficult to control local voltage.
- Since apparent power increase with the increasing reactive power consumption of transmission lines and transformers, active power losses of resistance of transmission lines and generator also increase.
- There are hard restrictions on voltage, reactive power and power factor, because of constraints due to mechanical problems with the insulation of equipment and generators.

2.2.1.1 AVR (Automatic Voltage Regulator)

AVR is a device that keep voltage of synchronous generator constant with high accuracy automatically. AVR is installed in the exciter of the synchronous generator to maintain the voltage during load fluctuations and improve the dynamic stability by adjusting the reactive power. it is possible to suppress the voltage rise at the time of load rejection by using the ability to quickly recover voltage when voltage changes suddenly and that improves the transient stability. AVR can increase the generator internal voltage by increase exciting voltage when the terminal voltage drops. As a result, it can increase generator output. In other words, if increasing quickly exciting voltage when the generator is accelerated by system fault, synchronizing power are enhanced and acceleration of generator can be suppressed. Transient stabilities also can be improved. In particular, it is possible to further improve the transient stability by improving the response speed and increasing the maximum excitation voltage of AVR. Therefore, AVR is required to be small voltage variation rate (control deviation), sufficiently fast response and sufficiently stable controllability.

2.2.1.2 PSS (Power System Stabilizer)

Although adoption of the ultra-fast response excitation type AVR are progressed, if response of AVR is speeded up, there is a case that the braking force is reduced while synchronizing power is increased. This has become a problem. When the synchronization power is enhanced by AVR, it is possible to more strongly suppress the amplitude of the first wave. However, characteristics become more oscillatory, and damping force of second wave and its later is decreased. Thus, power oscillation is in danger of expanding. PSS is one of the solutions. The PSS is the controller attached to excitation system of the generator. PSS performs the auxiliary input to the AVR. PSS generate a positive damping torque against a negative damping torque generated from AVR. PSS performs phase

compensation. As a result, PSS increase damping force and stabilize power system. There are ΔP type, $\Delta\omega$ type and $\Delta P + \Delta\omega$ type, etc. the $\Delta\omega$ type PSS is effective in the long-period fluctuation compared with ΔP type PSS.

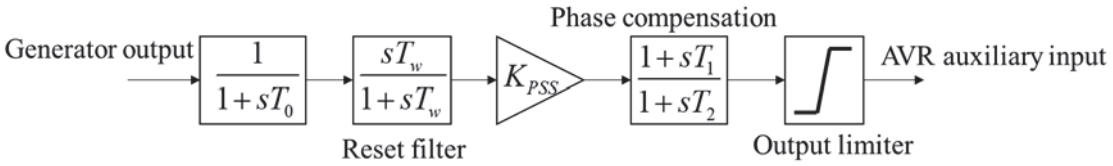

Fig.2-3 PSS block diagram

2.2.2 Stabilization by FACTS

FACTS (Flexible AC Transmission Systems) equipment is a power electronics technology that combines three technologies of electronic, electric power and control, and it is used to enhance the function of the electric power system. When FACTS equipment is installed at a specific position in the electric power system, this technology allows the FACTS equipment to respond quickly to the control input and change the voltage, phase and impedance of the grid. Therefore, high-speed control of voltage control and control similar to phase becomes possible, and the stability of the power system is improved. FACTS controllers are increasingly used in power system operation that requires stability up to now. Due to the characteristics of FACTS equipment, improvement of voltage stability can be expected especially in heavily loaded systems. The main FACTS equipment will be explained here. The outline is shown in Table 2-1.

Table 2-1 Classification of FACTS

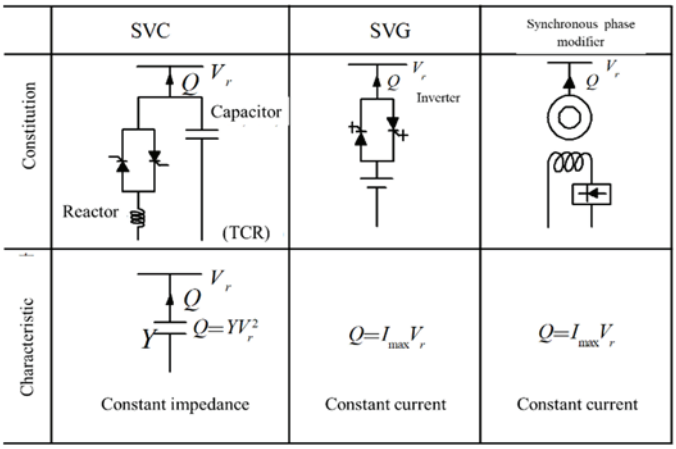

SVC: Static Var Compensator (Static reactive power compensator)

Generally, it consists of a step-down transformer, a series reactor, a phase advancing capacitor, and a high-voltage large capacity thyristor device, and by reactive power being continuously changed in a load state by high-speed control using a thyristor, reactive power with fast response speed Compensation can be done. Basic methods of SVC include a TCR (Thyristor Controlled Reactor) method, a TCT (Thyristor Controlled Transformer) method, and a TSC (Thyristor Switched Capacitor) method. The TCR system consists of a series connection of a thyristor device and a reactor, and by continuously controlling the thyristor firing angle, the reactor current is continuously and rapidly changed from zero to the rated value. Therefore, like the simple power capacitor, the constant impedance characteristic changes reactive power output in proportion to the square of the voltage. In addition, a device that performs reactive power control using a self-commutated converter is called STATCOM (STATic synchronous COMpensator).

SVG: Static Var Generator (self-excited SVC)

Adjust voltage and power factor by supplying reactive power. Since the output is adjusted by the self-excited inverter, the response speed is fast.

Synchronous phase modifier

Synchronous motor operated with no load. By adjusting the field current, it is possible to continuously adjust reactive power over a wide range from supply of reactive power to absorption. In addition, since the self-voltage is established by the internal induced voltage, constant reactive power can be supplied even when the system voltage drops. Therefore, for the purpose of improving the system voltage stability, a synchronous phase shifter may be adopted instead of a power capacitor.

Although the above three control the voltage and reactive power by installing it at the load end, there are FACTS equipment which is effective by installing it other than the load end. Examples are shown below.

TCSC (Thyristor Controlled Series Capacitor): Thyristor controlled series capacitor

This can directly control the impedance by controlling the series capacitor and parallel reactor with a thyristor. By installing in the power transmission facility, it is possible to compensate the reactance of the transmission line at all times, and to control the reactance so as to suppress power oscillation at the time of fluctuation to stabilize the system at high speed and in a wide range. The TCSC has a thyristor switch type composed of a series capacitor and a reactor with an inverse parallel thyristor connected in parallel to it and a self-excited type which applies a voltage in phase with the line voltage by a self-commutated inverter using a series transformer.

UPFC (United Power Flow Controller)

It consists of a parallel inverter via a transformer connected in parallel to the transmission line, a series inverter via a series connected transformer, and a DC capacitor

connecting these two inverters to each other There. Since the inverter can independently control the active power and the reactive power, it is possible to supply and absorb active power and reactive power to the system by using these two inverters. By absorbing the parallel inverter from the system by the amount of active power supplied by the series inverter, the voltage fluctuation of the capacitor of the DC link part is prevented. In other words, the UPFC is a device that can perform flexible control by adjusting the magnitude and phase angle of a voltage by a series inverter, and the current by a parallel inverter.

2.3 Conventional transient stability control

Until now, the transient stability has been maintained by Japan's very excellent lineage outage / accident prevention relay. This is a relay system that automatically removes a fault after a system accident and prevents it from widening even if it becomes unstable. However, due to the rapid increase in RES, situations cannot be dealt with by such emergency control. As a conventional study, transient stability control method using transient energy function method has been proposed, but there was a problem that the system model was limited and the error became very large [18]. Although some studies aimed at reducing errors by using this transient energy value in simulation methods, the error is not small [19] because critical energy values are used. Therefore, the thesis proposes the transient stability control method using CCT directly in chapter 3.

2.4 Stabilization control by inverter

The inverter is a DC-AC power conversion device, which is widely used as one of parts in fluorescent lamps, Power Conditioning System (PCS) of PV, household appliances such as air conditioner, EVs and industrial drive device. The inverter has aspects of the equipment which controls the energy with the energy devices and it is power electronic device having a power conversion function.

Inverters are categorized into center tap, half-bridge, bridge type, single-phase, multi-phase, multi and three-level type, etc. according to circuit configuration. Moreover, a self-excited inverter that voltage required for commutation is given from the components of the inverter and a separately-excited inverter that voltage is given from outside of the inverter are existed. The self-excited inverter has forced commutation method and device commutation method. The forced commutation method is to be tacked on a commutation circuit composed of capacitors and reactors to main circuit consist of thyristor, which is three- terminal semiconductor element that current flows between anode and cathode when apply current from gate to cathode. The device commutation method is to be used on-off control devices such as IGBTs, power MOSFETs, power transistors and GTO thyristors, etc. The separately excited inverter has power commutation method which is given commutation by an AC power source and load commutation method which is given by the induced voltage of the load machine.

Power MOSFET (Metal Oxide Semiconductor Field Effect Transistor)

The power MOSFET is a MOSFET that can handle relatively large power. It has high switching speed (~several [MHz]) compared with the conventional bipolar transistors (A type of transistor, there are two types of junction structure of the npn and pnp type, it has a current amplified and switching function. Mainly in the power, npn type is used.) and it is lower on-resistance at the low voltage (~200[V]). Thus Currently, it is widely used in small and medium capacity power supply such as a switching power supply for AC-DC converter and a DC-DC converter. However, the on-resistance of inverters that have 300 ~ 400V of breakdown voltage abruptly increases.

IGBT (Insulate Gate Bipolar Transistor)

By compounding a MOSFET and a bipolar transistor, IGBT is a power device that utilizes the advantages of both functions. It is a device of voltage controlled type by the

insulated gate, and it has high speed switching and a low on-resistance. Moreover, It has a lower on-resistance and a higher breakdown voltage more than that of the bipolar transistor. Since it has excellent characteristics as described above, it is widely used as devices of home electronics such as air conditioner, refrigerator, washing machine, microwave and electromagnetic cooker, etc. and Industrial and large-scale plant equipment such as general-purpose inverters, large motor control inverter, robot and uninterruptible power system, etc. In present study, I make a model by using the IGBT transistor.

Basically, if output is positive and negative of DC power source alternately, AC output can be obtained from the DC input. Since the direction of the current is reversed, the output can be considered as an AC. However, the forms of the AC power are variety. There are single-phase two-wire, single-phase three-wire, three-phase three-wire and three-phase four-wire system, etc. Furthermore, it is also necessary to consider values of frequency, voltage and current of the AC power. The inverter is more a equipment that can control the form of AC power than a generator.

2.4.1 Principles of inverters

Basically, if output is positive and negative of DC power source alternately, AC output can be obtained from the DC input. Since the direction of the current is reversed, the output can be considered as an AC. However, the forms of the AC power are variety. There are single-phase two-wire, single-phase three-wire, three-phase three-wire and three-phase four-wire system, etc. Furthermore, it is also necessary to consider values of frequency, voltage and current of the AC power. The inverter is more a equipment that can control the form of AC power than a generator.

2.4.1.1 Single phase inverter

Basically, the inverter controls the power by cutting current or voltage with the switch. I explain the principles that converts DC power to AC power of single-phase. It refers to the circuit shown in Fig.2-4 as H-bridge, it is connected with resistance R. When S1 and S4 are turned on, turn off S2 and S3. On the other hand, when S2 and S4 are turned on, turn off S1 and S4. By doing this operation alternately, it appears the voltage as shown in Fig.2-4 across the resistor R connected as a load.

As shown, the positive and negative voltage is applied. An AC voltage across the resistor is a rectangular wave with ± E amplitude and T period. The current that flows resistance in this case is also rectangular wave with ± E/R amplitude and T period. Power consumption of resistance P is always constant, and it is as following equation.

$$P = E \cdot I = E \cdot \frac{E}{R} = (-E) \cdot \left(-\frac{E}{R}\right) = \frac{E^2}{R} \tag{2.13}$$

Thus, it is possible to obtain a single-phase AC power of a rectangular wave by using this H-bridge.

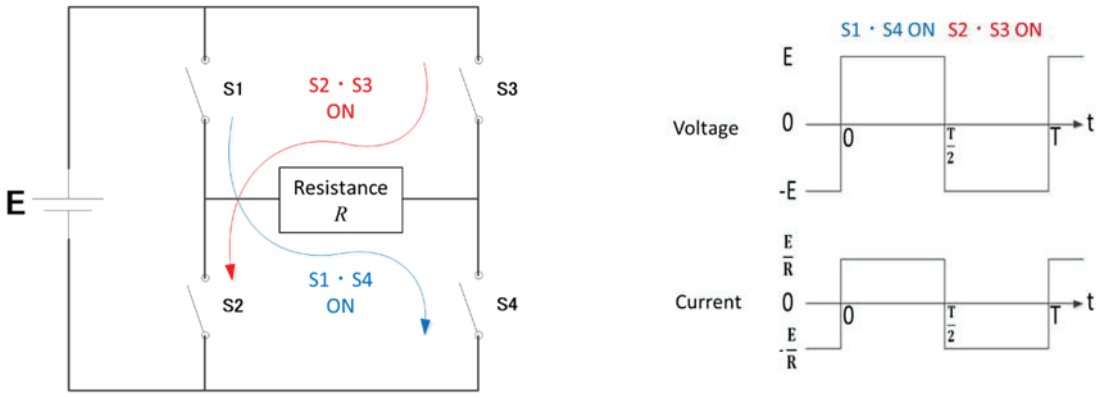

(a) H-bridge circuit (b) Voltage and current waveform

Fig.2-4 Single-phase DC-AC conversion (H-bridge)

2.4.1.2 Three Phase Inverter

Here, I will explain how to make the three-phase AC from a DC source by using the circuit consist of rectifying elements as shown in Fig.2-5. The case of three phase, it is

assumed that source voltage of the DC power source is ± E / 2 and it has neutral point. It regards neutral point of the power supply as ground potential reference potential of phase voltage of inverter output. In this figure, RL three-phase load by star connection is connected. The switching operation of the inverter which is composed of six switches is shown in Fig.2-6.

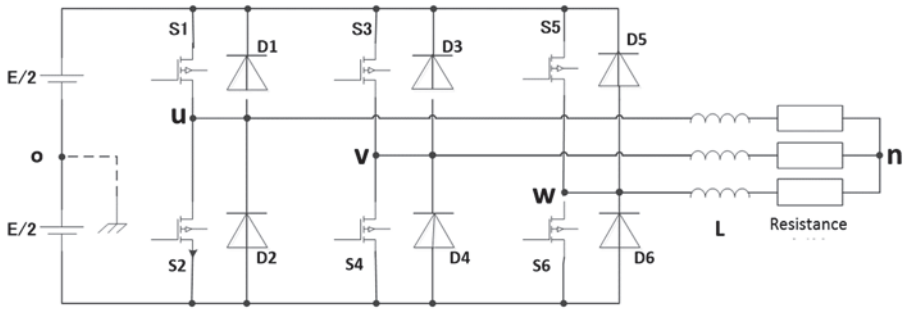

Fig.2-5 Circuit of the three-phase inverter

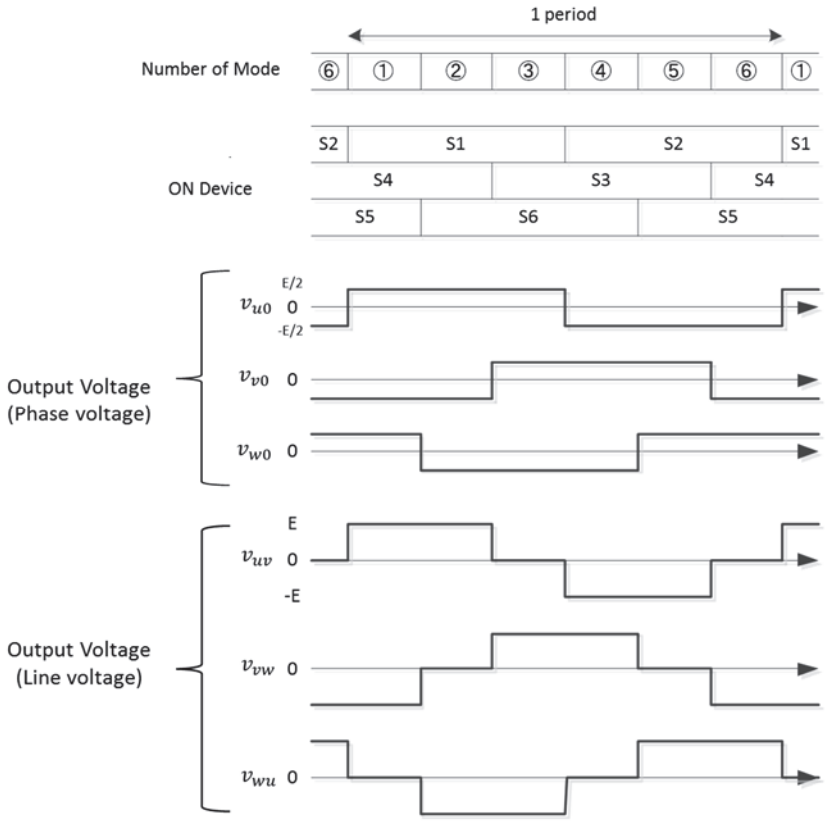

Fig.2-6 The voltage waveform due to switching

2.4.1.3 Voltage and current Source inverter

Load that is powered by the inverter is either a voltage type load or a current type load. The voltage source applies a voltage to the current type load and the current source apply a current to the voltage type load.

VSI (Voltage Source Inverter)

The power source is voltage source that can supply voltage continuously. Since impedance of the inverter is low when it is viewed from the AC output side, DC voltage is not changed suddenly. Since the current flowing through the power rapidly changes, it is necessary to connect the capacitor to the power source in parallel. Energy stored in the capacitor is supplied to the load as a voltage, the inverter controls the output voltage by the switching. The output voltage is a square wave pulse, and the current is a wave close to a sine wave. By connecting the feedback diode in parallel with the thyristor, delay current component of the inductive load is fed back to the DC power supply. Because the capacitor used in the voltage source is small and light, it is used in inverter that is medium and small capacity. Furthermore, since it is designed on the assumption to be connected to a commercial power source, voltage inverter has less problem for the load.

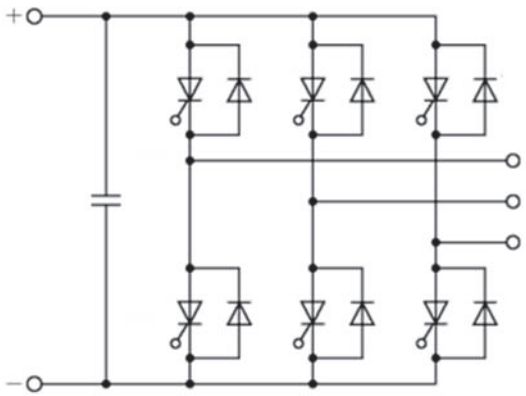

Fig.2-7 Circuit of VSI

CSI (Current Source Inverter)

The power source is current source that can supply current continuously. Since impedance of the inverter is high when it is viewed from the AC output side, DC current is not changed suddenly. The output voltage is a wave close to a sine wave, and the current is a

square wave pulse. Thus, since current only flows in one direction, feedback diodes are not required. However, it is necessary to connect the device (series diode) having a reverse blocking function because there are periods in which the reverse voltage is applied to the device.

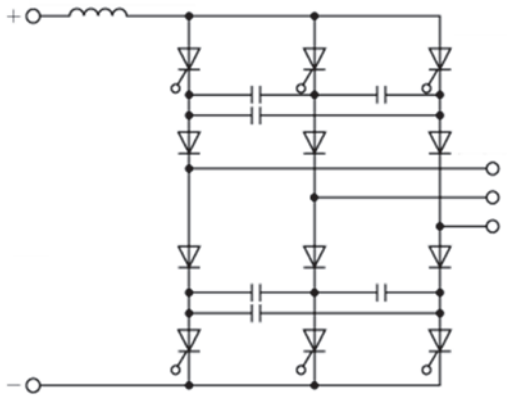

Fig.2-8 Circuit of CSI

Because it is assumed the power conditioner (to be described later) and simulated the inverter connected the power systems, I verify model and simulation used the voltage inverter.

2.4.1.4 PWM (Pulse Width Modulation)

The PWM is a typical method for controlling the inverter output. Since the inverter is the switching element, amplitude of output pulse waveform is constant. Thus, pulse width need to be controlled. The PWM is able to control the magnitude of the output voltage by changing the duty ratio of the pulse. Furthermore, it is also possible to approximate the output waveform by the sine wave when using following method.

Triangular Wave Comparison Method

This method is the most widely used with PWM. This is a control method that produces a pulse by comparing magnitudes of a triangular wave which is high frequency and a sine wave which is a desired signal. A triangular wave is called carrier wave and a sine wave

is called modulation wave. The principle of the triangular wave comparison method is shown in Fig.2-9.

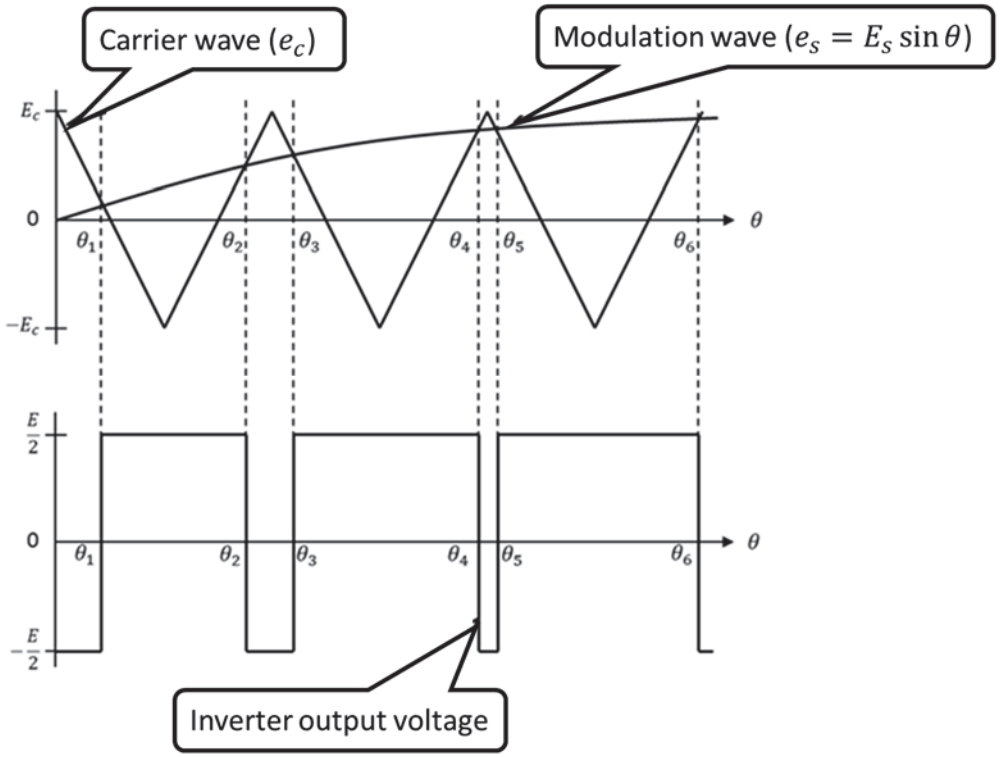

Fig.2-9 Principles of PWM

- Switch is on, when $e_s > e_c$
- Switch is off, when $e_s < e_c$

Here, as shown in Fig.2-10, we introduce the modulation factor M that is amplitude ratio between modulation wave and carrier signal.

$$M = \frac{E_s}{E_c} \tag{2-14}$$

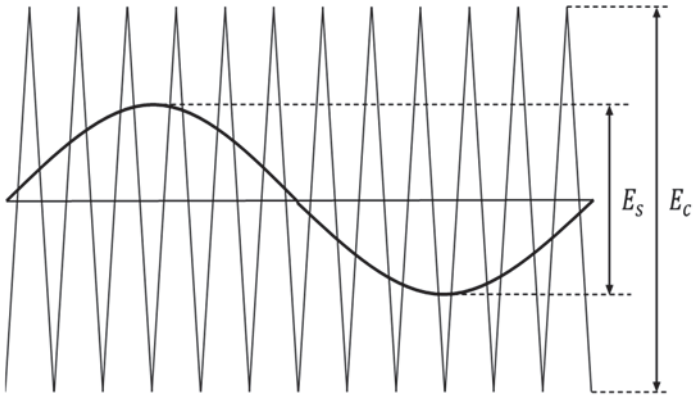

Fig.2-10 Modulation factor

Fundamental effective value of the output line voltage is shown as follows.

$$V_{rms} = \sqrt{\frac{3}{2}} M \frac{E}{2} \tag{2-15}$$

Thus, the inverter output voltage is controllable by modulation factor M.

2.4.1.5 PCS (Power Conditioning System)

PCS is a device that converted DC power generated by PV into AC power in order to connect with power system.

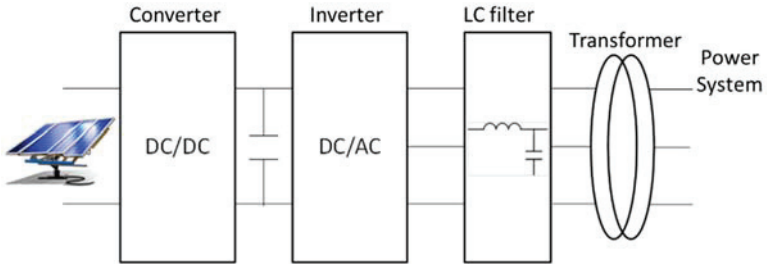

Fig.2-11 Basic circuit of the PCS

Basic Configuration

✓ Efficiency Control Unit of PV

It is a DC-DC converter that converts an unstable DC output voltage of PV to a stable

DC high voltage. There are MPPT (Maximum Power Point Tracking) control and automatic start-stop control. MPPT is a control method that tracks the maximum power point of solar cells by changing output voltage in order to compensate for the low conversion efficiency of solar cells.

✓ Inverter Control Unit

It is a DC-AC inverter that convert a DC high voltage of the DC-DC converter output a three phase or single phase AC power. it is performed high-efficiency control and adjusts the output voltage and frequency.

✓ System Interconnection Protection Unit

It has a system interconnection controller to be connected with grid and features to protect power system PV and PCS from short circuit and ground fault. Further, there is a protection relay to ensure the safety of the system side in the event of a power failure.

Comparison with conventional method

When the power source such as PV and buttery with inverters are introduced in large quantities near demand area, power systems are received a large negative impact by a reduction of various stability. In particular, the inverter has a feature that would automatically stop because of instantaneous voltage drop and power failure, when the equipment failures and disturbances are occurred in the system side. In other words, these power sources do not contribute to system disturbances. Therefore, in the future synchronizing power of the entire system is reduced, and situation that stable supply cannot be performed satisfactorily is expected. Recently, DVS (Dynamic Voltage Support) function to dynamically maintain the voltage and FRT (Fault Ride Through) function that is one of multi-functionality have been made.

As research trend on inverter model including a synchronizing power, there is something as follows. The method of feedback control in case of deriving phase angle in addition to the swing equation of a synchronous generator [20]. The cooperative control

method with traditional synchronous generator applying load frequency control in order to realize a stable control in the independent system [21]. Meanwhile, the method of stabilizing control using the inverter with the synchronizing power is also proposed to the High Voltage Direct current (HVDC) transmission system in overseas [22]. The above mentioned, the control method or the inverter with the synchronizing power is called Virtual Synchronous Generator (VSG) or INertia Emulation Control (INEC) [23-33]. Researches by the viewpoint from a control drive have done in every direction.

2.5 Summary

In this Chapter, we explained stabilization control. First, we introduce the simulation method and the energy function method for the transient stability analysis method, and summarized their calculation method, advantages and disadvantages, respectively. We also introduced control to improve transient stability by using generator, FACTS. Regarding FACTS, we mainly explained the inverter. Proposed control methods for generators and inverters will be described in detail in the following chapters.

Chapter 3

Transient stability analysis and control for power system by using CCT

3.1 Influence of renewable energy on power system

In West Japan Interconnected System, transient stability (TS) is a most important security factor limiting power transfer, while rapid increase in PV generations are causing uncertain power flows. The situation requires analysis of possible critical power flows for TS. The IEEJ West Japan standard model is used for this purpose, which is given in Fig. 3-1

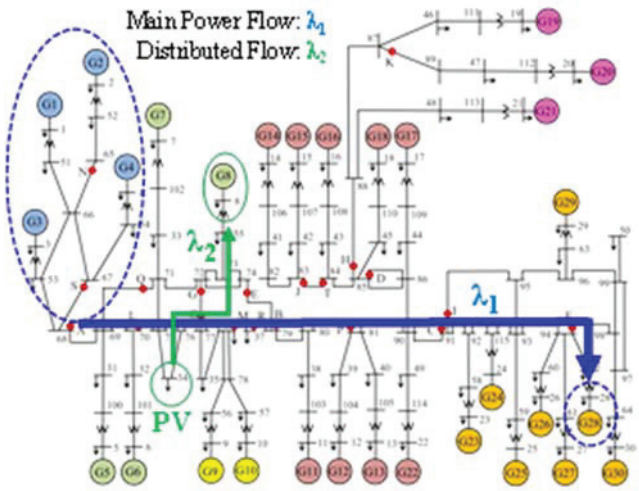

Fig. 3-1 IEEJ West Japan 30-Gen. Model (Total generation 100 GW)[40].

We propose the use of critical clearing time (CCT) as an index for TS. CCT is the critical value of fault clearing time for system stability. The reasons of using CCT as an index are: (1) CCT directly indicates the degree of TS; (2) CCT is useful for system control; (3) There are several options for the computation of CCT. The first option is the bisection method where conventional TS analysis tool is repeatedly used until required precision of CCT is obtained. The method is accurate but time consuming. The transient energy function methods are another options to obtain CCT. The methods are fast but errors are large. Thus, TDS method is used to compute CCTs in this thesis.

We analyze TS using the west Japan system model in Fig. A. We assume two kind of additional power flows, λ_1 and λ_2, from the original loading condition (100.2 GW

loading). λ_1 implies additional main power flow from west to east, which is increased form 0 to 1.0 GW, while λ_2, local power flow caused by PV generation, which is changed from 0 to 1.4 GW. Note that increase in λ_2 caused by PV generation makes the system light loading but unstable as is studied below.

Table 3-1 Transient Stability Assessment in terms of CCT.

	0.0	0.2	0.4	0.6	0.8	1.0
A	0.143	0.129	0.115	0.101	0.088	0.074
B	0.246	0.230	0.214	0.198	0.182	0.166
C	0.477	0.485	0.492	0.498	0.504	0.526
D	0.237	0.236	0.234	0.233	0.231	0.229
E	0.309	0.295	0.281	0.268	0.254	0.241
F	0.310	0.333	0.352	0.360	0.374	0.384
G	0.285	0.271	0.257	0.245	0.232	0.220
H	0.251	0.251	0.251	0.245	0.244	0.243
I	0.478	0.486	0.492	0.498	0.502	0.507
J	0.241	0.241	0.241	0.241	0.241	0.241
K	0.291	0.291	0.291	0.291	0.291	0.291
L	0.239	0.223	0.207	0.191	0.174	0.157
M	0.281	0.274	0.265	0.257	0.247	0.237
N	0.176	0.165	0.153	0.141	0.129	0.118
O	0.298	0.285	0.273	0.259	0.245	0.231
P	0.237	0.236	0.235	0.233	0.232	0.231
Q	0.215	0.203	0.190	0.176	0.161	0.146
R	0.332	0.321	0.309	0.297	0.284	0.272
S	0.130	0.120	0.109	0.098	0.088	0.078
T	0.251	0.251	0.251	0.251	0.250	0.250
U	0.367	0.367	0.366	0.366	0.365	0.364
V	0.292	0.292	0.291	0.291	0.290	0.290

	0.0	0.2	0.4	0.6	0.8	1.0	1.2	1.4
A	0.074	0.075	0.074	0.072	0.069	0.066	0.062	0.058
B	0.166	0.176	0.184	0.189	0.191	0.190	0.186	0.180
C	0.526	0.526	0.526	0.525	0.525	0.509	0.507	0.504
D	0.229	0.229	0.229	0.229	0.229	0.229	0.229	0.228
E	0.241	0.258	0.271	0.281	0.285	0.281	0.270	0.254
F	0.384	0.391	0.391	0.391	0.390	0.390	0.390	0.390
G	0.220	0.230	0.235	0.235	0.231	0.221	0.209	0.194
H	0.243	0.243	0.243	0.242	0.241	0.241	0.240	0.238
I	0.507	0.522	0.522	0.511	0.510	0.509	0.507	0.504
J	0.241	0.241	0.241	0.241	0.241	0.242	0.242	0.242
K	0.291	0.291	0.291	0.291	0.291	0.291	0.291	0.291
L	0.157	0.157	0.156	0.152	0.147	0.140	0.132	0.123
M	0.237	0.246	0.252	0.254	0.252	0.247	0.235	0.220
N	0.118	0.118	0.117	0.116	0.115	0.111	0.106	0.101
O	0.231	0.239	0.242	0.241	0.235	0.224	0.210	0.195
P	0.231	0.231	0.231	0.231	0.231	0.231	0.231	0.231
Q	0.146	0.146	0.144	0.141	0.136	0.129	0.122	0.113
R	0.272	0.285	0.294	0.300	0.300	0.295	0.281	0.262
S	0.078	0.079	0.079	0.077	0.075	0.072	0.068	0.064
T	0.250	0.250	0.250	0.250	0.250	0.250	0.250	0.250
U	0.364	0.364	0.364	0.364	0.364	0.364	0.364	0.364
V	0.290	0.290	0.290	0.290	0.290	0.290	0.290	0.290

We compute CCTs for various contingencies using bisection method, where we use the Xd' generator model with damping. The computed CCTs are given in Fig. 3-2(a), where λ_1 is changed from 0 to 1.0 GW with λ_2=0. It is observed that CCTs are decreased as additional power flow λ_1 is increased. The system is still stage since all CCTs' are greater than the operation time of fault clearing relay, 0.07 [s]. Fig. 3-2(b) shows CCTs for variable λ_2 with fixed λ_1=1.0 GW. The system becomes unstable for fault A when distributed power flow is deviated due to increase in PV output, λ_2>0.8 GW.

From the above examination, it is observed that the increase in PV output may cause instability for TS. An important issue is that various patterns of such critical power

flows for TS may exist caused by PV generations, and it is a fact that accurate PV outouts prediction is difficult. Therefore, an effective mointoring and control method is highly required.

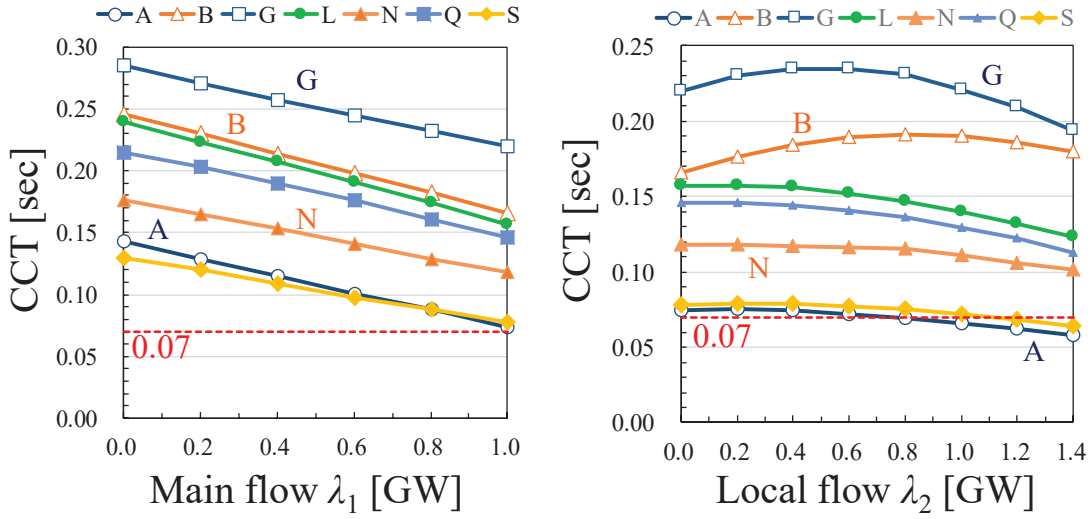

(a) (b)

Fig.3-2 Transient Stability Assessment in terms of CCT.

3.2 Sensitivity analysis of CCT

Distribution Factor (DF) which is widely used in power system is also applied to CCT and we name CCT-DF. A CCT-DF represents the sensitivity of CCT at a certain operating point and it is defined as follows.

$$CD_{Pj}^{(n)} = \frac{\Delta CCT^{(n)}}{\Delta P_j} \tag{3-1}$$

Where, $CD_{Pj}^{(n)}$ is CCT-DF, ΔP_j is the amount of generator's minimal output change, $\Delta CCT^{(n)}$ is the amount of change in CCT, subscript n is contingency (fault conditions), subscript j is generator number. Here, ΔP_j is an arbitrary value. Each CCT-DF is calculated by slightly changing the output of each generator. The slack generator absorb

the tiny changes to maintain the supply-demand balance.

$$\Delta P_j + \Delta P_{slac} = 0$$

By performing the same processing, it is possible to calculate the CCT-DF for the load and the RE.

In this paper, the bisection method is applied to compute CCT and CCT-DF as well. The following algorithm is used.

Step1: Initial setting of stable CT (SCT) and unstable CT (UCT).

Step2: Check TS stability for TestCT=(SCT+UCT)/2.

If stable SCT=TestCT, otherwise, UCT=TestCT.

Step 3: If UCT-SCT>eps, specified precision, goto Step 2.

Step 4 CCT is obtained as TestCT.

The advantage of the bisection method is that the accurate CCT is obtainable using conventional TS simulation tools, while the disadvantage is computational burden, which will discuss later. CCT-DF is computed based on equation (3-1) in which CCT is obtained by the above algorithm.

Table 3-2 CCT Distribution factor for fault A

Gen #	1	2	3	4	5	6	7	8	9	10
CD	-0.07	-0.06	-0.07	-0.07	-0.04	-0.03	-0.03	-0.01	-0.01	-0.01
Gen #	11	12	13	14	15 slack	16	17	18	19	20
CD	0.02	0.02	0.02	0.00	0.00	0.00	0.00	0.00	0.00	0.00
Gen #	21	22	23	24	25	26	27	28	29	30
CD	0.00	0.00	0.00	0.00	0.00	0.00	0.00	0.00	0.00	0.00

We select an operating point at (1=1.0,2=0.6) and evaluate CCT-DF for all generators j = G1 to G30 as given in Table 3-2, where G15 is the slack generator and the corresponding CCT-DF is set to zero. Fig. 3 compares the estimated deviations of CCTs by CCT-DF with the actual simulated values for several selected generators. As is observed, the errors in CCT-DF are small enough to be used for TS control problem.

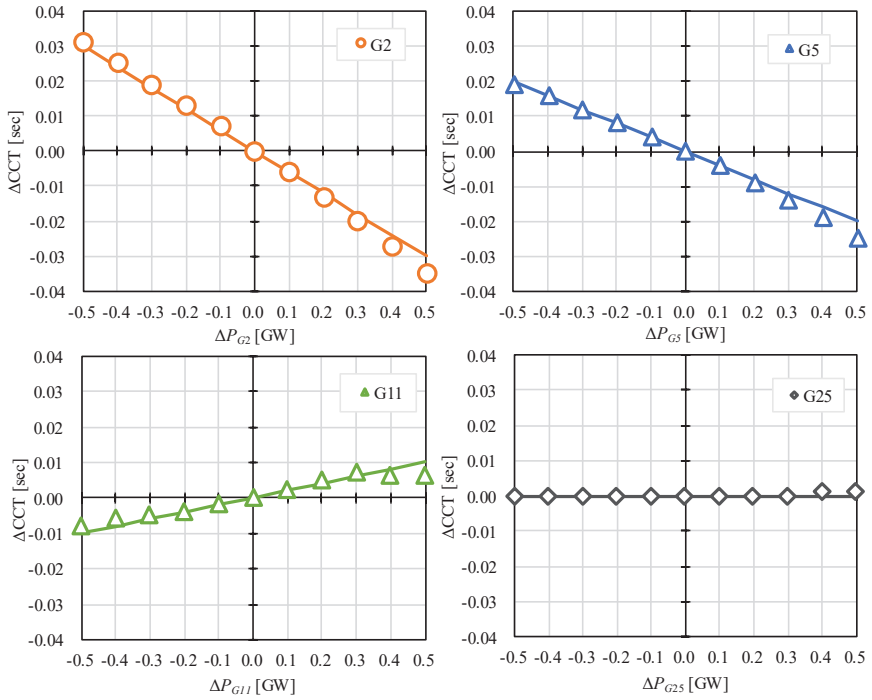

Fig. 3-3 Comparison of the estimated CCTs by CCT Distribution factors with the actual simulated values

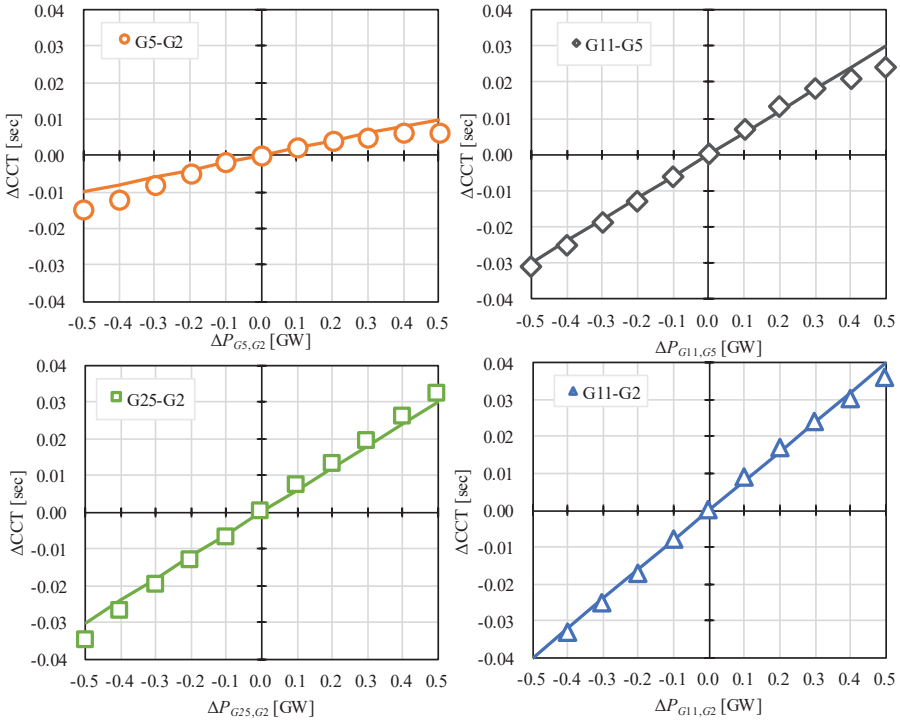

Fig. 3-4. Comparison of estimated and actual control effects

3.3 Transient stability control using CCT-DF

3.3.1 Formulation of planning problem

A TS control method against uncertainty is formulated. For this purpose, the following objectives are selectively used.

$$F_1(u) = \sum_i c_i \mid u_i - u_{0i} \mid \tag{3-2}$$

$$F_2(u) = \sum_i c_i (u_i - u_{0i})^2 \tag{3-3}$$

u_i is control variable, u_{0i} is its initial value. Here, c_i is 1. The minimization of the controlled variable is defined as the objective function.

Next, constraint set is defined. Based on a DC power flow problem, node injection vector is represented as:

$$y = l_0 + L_G u + L_p p \tag{3-4}$$

where $y \in R^{N_B}$ is node injection vector of active power; $l_0 \in R^{N_B}$ is constant vector; $L_G \in R^{N_B \times N_G}$ is a constant matrix whose elements are unity or null; $L_P \in R^{N_B \times N_p}$ is a constant matrix; $u \in R^{N_G}$ is control vector consisting of controllable generator outputs with upper and lower bounds:

$$\underline{u} \le u \le \overline{u} \tag{3-5}$$

and there is a rate of change constraint:

$$-\delta \le u - u_0 \le \delta \tag{3-6}$$

$p \in R^{Np}$ is uncertain uncontrollable vector. p is predictable but it has uncertainty with confidence interval:

$$\underline{p} \le p \le \overline{p} \tag{3-7}$$

N_B is the number of bus / node, N_G is the number of generator and N_p is the number of

uncertain parameter.

Typical system operation constraints for the economic load dispatch problem are assumed as follows:

Demand & Supply balance: $e^T \cdot y = 0$ (3-8)

Line Flow Limit: $\underline{P}_{TL} \le S \cdot y \le \overline{P}_{TL}$ (3-9)

where $e = [11...1]^T$, P_{TL}, $P_{TL} \in R^{N_l}$ is lower and upper line flow limits, $S \in R^{N_l \times N_B}$ is a transformation matrix from active power to line power flow and N_l is the number of line. Given an operating point, (u_0 , p_0) at which p_0 is the predicted value of uncertain parameter, we assume an operating condition where TS constraint is violated ($CCT_0 < Thresh$) and that CCT-DF has been computed. Then, we set the following TS constraint to determine future operating point u satisfying stability.

$$CCT_0 + CD_u^{(n)} \cdot (u - u_0) + CD_p^{(n)} \cdot (p - p_0) > Thresh \quad (3\text{-}10)$$

Then, constraint set is defined as a set of linear constraints, (3-4)-(3-10). They are represented by the following form.

$$Ap + Bu \le b \quad (3\text{-}11)$$

Here, u must be found which satisfies the constraint condition under any uncertain parameter p.

$$\begin{aligned} &\min_u \ F(u) \\ &\text{s.t} \ \ Ap_0 + Bu \le b \end{aligned} \quad (3\text{-}12)$$

where p_0 is forecasted /predicted value of p.

3.3.2 Robust optimization problem

Therefore, the following two step optimization is proposed to obtain an optimum u.

$$
\begin{aligned}
&\max_{p} \quad F(u) \\
&\text{s.t} \quad Ap + Bu \le b \\
&\qquad u \in \arg\min_{u} F(u) \\
&\qquad \text{s.t} \quad Ap + Bu \le b
\end{aligned}
\tag{3-13}
$$

The above type of problem can be transformed into MILP problem which will be solved by CPLEX in this thesis.

We describe the conversion of two-level programming problems (BLP: Bi-level programming problems) [8-10] into MILP problem [16,17,19,36]. Consider the following planning problem.

(BLP)

$$
\begin{cases}
\max\limits_{x,y} \; c^{1t}x + d^{1t}y \\
\text{s.t.} \quad A^1x + B^1y \le b^1 \\
\qquad x \ge 0 \\
\qquad y \in \arg\max\limits_{y} c^{2t}x + d^{2t}y \\
\qquad \text{s.t.} \quad A^2x + B^2y \le b^2 \\
\qquad\qquad y \ge 0
\end{cases}
$$

At this time, all variables are assumed to be nonnegative. First, it transforms to Generalized Linear Complementarity Problem (GLCP) using complementarity theorem for BLP.

(GLCP)

$$
\begin{cases}
\max\limits_{\tilde{x}} \; \tilde{c}\tilde{x} \\
\text{s.t.} \quad \tilde{A}\tilde{x} \le \tilde{b} \\
\qquad M\tilde{x} + q \ge 0, \tilde{x} \ge 0 \\
\qquad \tilde{x}^t(M\tilde{x} + q) = 0
\end{cases}
\qquad
\tilde{x} = \begin{bmatrix} x \\ y \\ \lambda \end{bmatrix}, \tilde{b} = b^1, \tilde{c} = \begin{bmatrix} c^1 \\ d^1 \\ 0 \end{bmatrix}, q = \begin{bmatrix} 0 \\ -d^2 \\ b^2 \end{bmatrix}
$$

$$
\tilde{A} = \begin{bmatrix} A^1 & B^1 & 0 \end{bmatrix}, M = \begin{bmatrix} 0 & 0 & 0 \\ 0 & 0 & B^{2t} \\ -A^2 & -B^2 & 0 \end{bmatrix}
$$

Convert to MILP by introducing a binary vector for GLCP secondary constraints.

(MILP)

$$\begin{cases} \max\limits_{\tilde{x}} \ \tilde{c}\tilde{x} \\ s.t. \quad \tilde{A}\tilde{x} \le \tilde{b} \\ \qquad M\tilde{x}+q \ge 0, \tilde{x} \ge 0 \\ \qquad M\tilde{x}+q \le L(1-u), \tilde{x} \le Lu \\ \qquad u: binary\ vector, L = \{\max \| \tilde{x}^* \|_\infty, \| M\tilde{x}^* + q \|_\infty\} \end{cases}$$

We explain in detail in order. Here we use the complementarity theorem to transform from BLP to GLCP. First, if $x = \hat{x}$ (constant), the objective function of BLP's second-level problem become following.

$$y \in \arg\max_y (c^{2t}\hat{x} + d^{2t}y) \ \Leftrightarrow \ y \in \arg\max_y d^{2t}y$$

Therefore, the main problem (P) of BLP's second-level problem and the dual problem (D) of BLP's second-level problem can be expressed as follows.

(P)

$$\begin{cases} \max\limits_{y} \ d^{2t}y \\ s.t. \quad B^2 y \le b^2 - A^2 x \\ \qquad y \ge 0 \end{cases}$$

(D)

$$\begin{cases} \min\limits_{\lambda} \ \lambda^t (b^2 - A^2 x) \\ s.t. \quad \lambda^t B^2 \ge d^{2t} \\ \qquad \lambda \ge 0 \end{cases}$$

From the above equation,

$$d^{2t}y \le \lambda^t B^2 y \le \lambda^t (b^2 - A^2 x)$$

From the strong duality theorem, it assume the optimal solution of (P) is y^* and the optimal solution of (D) is λ^*,

$$d^{2t}y \le \lambda^t B^2 y \le \lambda^t (b^2 - A^2 x) \Leftrightarrow d^{2t}y^* = \lambda^{t^*} B^2 y^* = \lambda^{t^*} (b^2 - A^2 x)$$

$$\Leftrightarrow \begin{cases} (d^{2t} - \lambda^{t^*} B^2) y^* = 0 \\ \lambda^{t^*} (b^2 - A^2 x - B^2 y^*) = 0 \end{cases} .$$

That is, the following relationship holds.

$$(d^{2t} - \lambda^{t^*} B^2) y^* = 0 \Leftrightarrow \{(d^{2t} - \lambda^{t^*} B^2) y^*\}^t = 0$$
$$\Leftrightarrow y^{*t}(d^2 - B^{2t}\lambda^*) = 0$$
$$\Leftrightarrow y^{*t}(B^{2t}\lambda^* - d^2) = 0$$

From the above, it can be rewritten as follows.

$$\begin{cases} y^{*t}(B^{2t}\lambda^* - d^2) = 0 \\ \lambda^{t^*}(-A^2 x - B^2 y^* + b^2) = 0 \end{cases}$$

(GLCP)

$$\begin{cases} \max\limits_{x,y} \ \tilde{c}\tilde{x} \Leftrightarrow \begin{bmatrix} c^{1t} & d^{1t} & 0 \end{bmatrix} \begin{bmatrix} x \\ y \\ \lambda \end{bmatrix} \Leftrightarrow c^{1t}x + d^{1t}y \\ s.t. \quad \tilde{A}\tilde{x} \le \tilde{b} \Leftrightarrow \begin{bmatrix} A^1 & B^1 & 0 \end{bmatrix} \begin{bmatrix} x \\ y \\ \lambda \end{bmatrix} \le b^1 \Leftrightarrow A^1 x + B^1 y \le b^1 \\ \quad \tilde{x} \ge \Leftrightarrow 0x \ge 0, \ \ y \ge 0, \ \ \lambda \ge 0 \\ \quad M\tilde{x} + q \ge 0 \Leftrightarrow \begin{bmatrix} 0 & 0 & 0 \\ 0 & 0 & B^{2t} \\ -A^2 & -B^2 & 0 \end{bmatrix} \begin{bmatrix} x \\ y \\ \lambda \end{bmatrix} + \begin{bmatrix} 0 \\ -d^2 \\ b^2 \end{bmatrix} \ge 0 \Leftrightarrow \begin{cases} B^{2t}\lambda - d^2 \ge 0 \\ -A^2 x - B^2 y + b^2 \ge 0 \end{cases} \\ \quad \tilde{x}^t (M\tilde{x} + q) = 0 \\ \Leftrightarrow \begin{bmatrix} x^t & y^t & \lambda^t \end{bmatrix} \left(\begin{bmatrix} 0 & 0 & 0 \\ 0 & 0 & B^{2t} \\ -A^2 & -B^2 & 0 \end{bmatrix} \begin{bmatrix} x \\ y \\ \lambda \end{bmatrix} + \begin{bmatrix} 0 \\ -d^2 \\ b^2 \end{bmatrix} \right) = 0 \\ \Leftrightarrow \begin{bmatrix} x^t & y^t & \lambda^t \end{bmatrix} \begin{bmatrix} 0 \\ B^{2t}\lambda - d^2 \\ A^2 x - B^2 y + b^2 \end{bmatrix} = 0 \\ \Leftrightarrow y^t (B^{2t}\lambda - d^2) + \lambda^t (-A^2 x - B^2 y + b^2) = 0 \end{cases}$$

Here, focus on. $\tilde{x}^t(M\tilde{x}+q)=0$ and define as follows.

$$\tilde{x}=\begin{pmatrix}\tilde{x}_1\\ \tilde{x}_2\\ \vdots\\ \tilde{x}_i\\ \vdots\\ \tilde{x}_n\end{pmatrix},(M\tilde{x}+q)=\tilde{X}=\begin{pmatrix}\tilde{X}_1\\ \tilde{X}_2\\ \vdots\\ \tilde{X}_i\\ \vdots\\ \tilde{X}_n\end{pmatrix},u=\begin{pmatrix}u_1\\ u_2\\ \vdots\\ u_i\\ \vdots\\ u_n\end{pmatrix},\qquad \tilde{x},\tilde{X},u\in\mathbb{R}^{n\times 1},\quad i=1,2\cdots n$$

$\tilde{x}^t(M\tilde{x}+q)=0$ can be rewritten as follows.

$$\begin{aligned}&\tilde{x}^t(M\tilde{x}+q)=0\\ \Leftrightarrow\ &\tilde{x}^t\tilde{X}=0\\ \Leftrightarrow\ &\begin{pmatrix}\tilde{x}_1\tilde{X}_1\\ \tilde{x}_2\tilde{X}_2\\ \vdots\\ \tilde{x}_i\tilde{X}_i\\ \vdots\\ \tilde{x}_n\tilde{X}_n\end{pmatrix}=0\Leftrightarrow\begin{cases}\tilde{x}_i=0\\ \text{or}\\ \tilde{X}_i=0\end{cases}\end{aligned}$$

Here, we transform by using $u:binary\,vector$.

$$\begin{cases}\tilde{x}_i=0\\ \text{or}\\ \tilde{X}_i=0\end{cases}\Leftrightarrow\begin{cases}\tilde{x}_i=0,\tilde{X}_i\le L\quad(\text{if } u_i=0)\\ \text{or}\\ \tilde{X}_i=0,\tilde{x}_i\le L\quad(\text{if } u_i=1)\end{cases}$$

$$\Leftrightarrow\begin{cases}\tilde{x}\le Lu\\ \text{and}\\ \tilde{X}\le L(1-u)\end{cases}$$

Where, $L=\{\max\|\tilde{x}^*\|_\infty,\|M\tilde{x}^*+q\|_\infty\}$. However, we cannot know the value. Thus, we define L as follows.

$$L\ge\{\max\|\tilde{x}^*\|_\infty,\|M\tilde{x}^*+q\|_\infty\}$$

(BLP)

$$\max_{u,p} \alpha = \sum_i c_i \mid u_i - u_{0i} \mid$$
$$s.t. \quad u \in \arg\min_u \ \alpha$$
$$s.t. \ \ Ap + Bu \le b$$

At this time, all variables are assumed to be nonnegative. First, it transforms to Generalized Linear Complementarity Problem (GLCP) using complementarity theorem for BLP.

(GLCP)

$$\max_{u,p,\lambda} \alpha = \sum_i c_i \mid u_i - u_{0i} \mid$$
$$s.t. \quad \begin{bmatrix} B^t\lambda + c \\ -Ap - Bu + b \end{bmatrix} \ge 0$$
$$\begin{bmatrix} u^t\left(B^t\lambda + c\right) \\ \lambda^t\left(-Ap - Bu + b\right) \end{bmatrix} = 0$$
$$\lambda \ge 0$$

Convert to MILP by introducing a binary vector for GLCP secondary constraints.

(MILP)

$$\max_{u,p,\lambda} \alpha = \sum_i c_i \mid u_i - u_{0i} \mid$$
$$s.t. \quad \begin{bmatrix} B^t\lambda + c \\ -Ap - Bu + b \end{bmatrix} \ge 0$$
$$\begin{bmatrix} B^t\lambda + c \\ -Ap - Bu + b \end{bmatrix} \ge L \begin{bmatrix} 1 - u_{bin} \\ 1 - \lambda_{bin} \end{bmatrix}$$
$$p \le Lp_{bin}, u \le Lu_{bin}, \lambda \le L\lambda_{bin}$$
$$\lambda \ge 0$$
$$p_{bin}, u_{bin}, \lambda_{bin} \in \{0,1\}$$

Here, L is a sufficiently large value, and in this paper 50,000 was set. As described above, BLP was converted to MILP.

3.4 Simulation

Here, the effectiveness of the proposed method is confirmed using the IEEJ WEST 30 generators model in Fig. 3-1. It is assumed that PV is installed at evry load and the individual PV capacities are 10% of the loads. PVs are generating 50% of their capacities and they have 10% uncertainty. This implies that each PV output is in the interval of 45 to 55% of each capacity. Two cases are examined as follows.

Case 1 : without uncertainty (deterministic PV prediction)

Case 2 : with uncertainty (PV prediction with confidence interval)

In case 1, TS control by CCT-DF is demonstrated. In case 2, the effectiveness of the proposed control is verified under uncertainty.

Table 3-3 shows CCT and CCT-DF for each fault point at a certain operating point. Since the fault clearing time of power system in Japan is 0.07 [sec], 0.17 is assumed in this paper as a threshold of CCT. Therefore, it is required for TS that CCT is not less than this value. It is observed from Table that the minimum value of CCT is 0.147 [sec] for fault S, and the second is 0.163 [sec] for fault A. Therefore, the TS control is necessary so that *Thresh* is set to 0.170 [sec] as TS constraint in (3-10). In order to perform the proposed control, CCT-DFs have been preliminary calculated using $\Delta P_j = 0.1$ [GW] in (3-1), which are listed in Table 3-3; positive and negative values are marked red and blue, respectively. CTT can be effectively controlled by adjusting the combination of generators with positive and negative CCT-DFs. It is recommended that not too small ΔP_j should be selected to avoid linearization errors of ΔCCT.

Table 3-3 CCT and CCT-DF for all faults (Normal condition of IEEJ WEST30)

Fault point	A	B	C	D	E	F	G	H	I	J	K	L	M	N	O	P	Q	R	S	T	U	V
CCT [sec]	0.163	0.274	0.513	0.258	0.338	0.333	0.309	0.270	0.514	0.264	0.309	0.269	0.307	0.197	0.327	0.262	0.238	0.364	0.147	0.271	0.314	0.310
CCT-DF [sec]																						
G1	-0.08	-0.09	-0.01	0.02	-0.06	-0.01	-0.05	-0.01	-0.01	-0.02	0.00	-0.09	-0.04	-0.06	-0.08	-0.01	-0.06	-0.07	-0.06	0.00	0.00	0.00
G2	-0.07	-0.09	-0.01	0.02	-0.06	-0.01	-0.05	-0.01	-0.01	-0.02	0.00	-0.08	-0.04	-0.09	-0.07	-0.01	-0.06	-0.07	-0.05	0.00	0.00	0.00
G3	-0.08	-0.09	-0.01	0.02	-0.06	0.00	-0.06	-0.01	-0.01	-0.02	0.00	-0.09	-0.05	-0.06	-0.08	0.00	-0.06	-0.07	-0.06	0.00	0.00	0.00
G4	-0.08	-0.09	-0.01	0.02	-0.06	0.00	-0.06	-0.01	-0.01	-0.02	0.00	-0.09	-0.05	-0.05	-0.08	0.00	-0.06	-0.07	-0.06	0.00	0.00	0.00
G5	-0.05	-0.11	-0.01	0.02	-0.09	0.00	-0.09	-0.01	-0.01	-0.02	0.00	-0.13	-0.06	-0.05	-0.11	0.00	-0.08	-0.09	-0.04	0.00	0.00	0.00
G6	-0.04	-0.11	-0.01	0.02	-0.08	0.00	-0.08	-0.01	0.00	-0.02	0.00	-0.12	-0.06	-0.04	-0.10	0.00	-0.06	-0.09	-0.03	0.00	0.00	0.00
G7	-0.04	-0.13	-0.01	0.02	-0.11	0.00	-0.13	-0.01	-0.01	-0.02	0.00	-0.11	-0.08	-0.04	-0.15	0.00	-0.13	-0.11	-0.03	0.00	0.00	0.00
G8	-0.03	-0.16	-0.03	0.02	-0.24	0.00	-0.21	-0.01	-0.02	-0.02	0.00	-0.06	-0.10	-0.04	-0.14	0.00	-0.04	-0.16	-0.03	0.00	0.00	0.00
G9	-0.02	-0.09	0.00	0.02	-0.05	0.00	-0.04	-0.01	0.00	-0.02	0.00	-0.02	-0.11	-0.02	-0.06	0.00	-0.01	-0.12	-0.02	0.00	0.00	0.00
G10	-0.02	-0.10	0.00	0.02	-0.06	0.00	-0.05	-0.01	0.00	-0.02	0.00	-0.03	-0.13	-0.02	-0.07	0.00	-0.01	-0.14	-0.02	0.00	0.00	0.00
G11	0.02	0.03	0.02	0.02	0.03	0.00	0.04	-0.01	0.02	-0.02	0.00	0.03	0.03	0.03	0.06	0.00	0.02	0.04	0.02	0.00	0.00	0.00
G12	0.01	0.03	0.02	0.02	0.03	0.00	0.03	-0.01	0.02	-0.02	0.00	0.03	0.03	0.02	0.05	-0.15	0.02	0.04	0.02	0.00	0.00	0.00
G13	0.01	0.02	0.02	0.02	0.03	0.00	0.03	-0.01	0.02	-0.02	0.00	0.02	0.02	0.02	0.05	-0.03	0.02	0.03	0.01	0.00	0.00	0.00
G14	0.00	0.00	0.01	-0.02	0.00	0.00	0.00	-0.02	0.00	-0.27	0.01	0.00	0.00	0.00	0.00	0.00	0.00	0.00	0.00	-0.07	0.00	0.00
G15	0.00	0.00	0.00	0.00	0.00	0.00	0.00	0.00	0.00	0.00	0.00	0.00	0.00	0.00	0.00	0.00	0.00	0.00	0.00	0.00	0.00	0.00
G16	0.00	0.00	0.00	-0.03	0.00	0.00	0.00	-0.02	0.00	-0.02	0.01	0.00	0.00	0.00	0.00	0.00	0.00	0.00	0.00	-0.13	0.00	0.00
G17	0.00	0.01	-0.01	0.03	0.01	0.00	0.00	0.00	-0.01	-0.01	0.00	0.00	0.00	0.00	0.00	0.00	0.00	0.00	0.00	0.00	0.00	0.00
G18	0.00	0.00	0.00	-0.10	0.00	0.00	0.00	-0.16	0.00	-0.01	0.01	0.00	0.00	0.00	0.00	0.00	0.00	0.00	0.00	-0.01	0.00	0.00
G19	0.00	0.00	0.00	-0.01	0.00	0.00	0.00	-0.01	0.00	-0.01	-0.27	0.00	0.00	0.00	0.00	0.00	0.00	0.00	0.00	0.00	0.00	0.00
G20	0.00	0.00	0.01	0.00	0.00	0.00	0.00	-0.01	0.01	-0.01	-0.02	0.00	0.00	0.00	-0.01	0.00	0.00	-0.01	0.00	0.00	0.00	0.00
G21	0.00	0.00	0.00	-0.02	0.00	0.00	0.00	-0.01	0.00	-0.01	0.00	0.00	0.00	0.00	0.00	0.00	0.00	0.00	0.00	-0.01	0.00	0.00
G22	0.00	0.01	-0.03	0.03	0.01	0.00	0.01	0.00	-0.03	-0.02	0.00	0.00	0.01	0.00	0.01	0.00	0.01	0.01	0.00	0.00	0.01	0.00
G23	0.00	0.01	-0.10	0.03	0.01	0.00	0.00	-0.01	-0.11	-0.02	0.00	0.00	0.00	0.00	0.00	0.00	0.00	0.00	0.00	0.00	0.01	0.00
G24	0.00	0.01	-0.55	0.03	0.01	-0.01	0.01	0.00	-0.61	-0.02	0.00	0.00	0.00	0.00	0.00	0.00	0.00	0.00	0.00	0.00	-0.50	0.00
G25	0.00	0.01	-0.14	0.03	0.01	-0.02	0.00	-0.01	-0.14	-0.02	0.00	0.00	0.00	0.00	0.00	0.00	0.00	0.00	0.00	0.00	-0.99	0.00
G26	0.00	0.00	0.41	0.02	0.00	-0.06	0.00	-0.01	-0.05	-0.02	0.00	0.00	0.00	0.00	0.00	0.00	0.00	0.00	0.00	0.00	0.00	0.00
G27	0.00	0.00	0.41	0.02	0.00	-0.09	0.00	-0.01	-0.05	-0.02	0.00	0.00	0.00	0.00	0.00	0.00	0.00	0.00	0.00	0.00	0.00	0.00
G28	0.00	0.00	0.41	0.02	0.00	-0.15	0.00	-0.01	-0.05	-0.02	0.00	0.00	0.00	0.00	0.00	0.00	0.00	0.00	0.00	0.00	0.00	0.00
G29	0.00	0.00	0.40	0.02	0.00	-0.03	0.00	-0.01	-0.06	-0.02	0.00	0.00	0.00	0.00	0.00	0.00	0.00	0.00	0.00	0.00	0.00	0.00
G30	0.00	0.00	0.40	0.03	0.00	-0.05	0.00	-0.01	-0.06	-0.02	0.00	0.00	0.00	0.00	0.00	0.00	0.00	0.00	0.00	0.00	0.00	-0.20

3.5 Result

Case 1 without uncertainty

Table 3-4 and Fig. 3-5 as well show predicted CCTs computed by conventional optimization (3-12), and resulted CCTs by TS control, which have been obtained by the bisection method after the control. The resulted CCTs are given for two cases: One is for the PV prediction without prediction error, while the other is for the PV outputs with the worst case of prediction error. For the former case, it is confirmed that the CCTs for all faults are larger than *Thresh* = 0.17 by the TS control. However, for the latter case, some CCTs violate the TS stability condition since they do not take into account the uncertainty

of PV prediction. Thus the conventional optimization requires to include uncertainty. This will be discussed in Case 2.

In order to investigate the difference in the objectives, Table 3-5 shows generator outputs after TS control. It is observed from the column of "Objective F_1", only two generators, G4 and G11, change thier outputs to satisfy CCT condition, while the others keep constant outputs. On the other hand, in "Objective F_2," multiple generators change their outputs to meet the stability condition.

The error of CCT is very small in both cases. However, when the necessary amount of control becomes larger, the discrepancy between the predicted and resulted CCTs tends to increase due to the linearization error. In this sense, it is expected that QP is more reliable than LP.

Table 3-4 CCT after TS control without uncertaninty

	Objective F_1 (LP)			Objective F_2 (QP)		
	Predicted CCT [sec]	Resulted CCT [sec]	Resulted CCT at worst case [sec]	Predicted CCT [sec]	Resulted CCT [sec]	Resulted CCT at worst case [sec]
A	0.192	0.191	0.245	0.192	0.193	0.246
B	0.309	0.308	0.380	0.322	0.323	0.391
C	0.522	0.523	0.214	0.542	0.507	0.196
D	0.258	0.259	-	0.253	0.254	-
E	0.364	0.355	0.381	0.377	0.366	0.392
F	0.333	0.334	0.189	0.327	0.327	0.182
G	0.338	0.323	0.337	0.346	0.332	0.346
H	0.270	0.269	0.034	0.268	0.267	0.028
I	0.523	0.522	0.232	0.500	0.506	0.216
J	0.264	0.264	-	0.261	0.259	-
K	0.309	0.309	0.106	0.304	0.303	0.093
L	0.304	0.305	0.345	0.311	0.312	0.352
M	0.330	0.325	0.363	0.336	0.331	0.368
N	0.220	0.219	0.268	0.224	0.224	0.275
O	0.367	0.377	0.391	0.373	0.373	0.394
P	0.262	0.261	0.275	0.255	0.256	0.267
Q	0.261	0.258	0.267	0.269	0.266	0.277
R	0.396	0.395	0.446	0.405	0.404	0.453
S	0.170	0.170	0.214	0.170	0.170	0.215
T	0.271	0.271	-	0.267	0.269	-
U	0.384	0.386	0.241	0.358	0.362	0.229
V	0.310	0.310	0.232	0.307	0.306	0.223

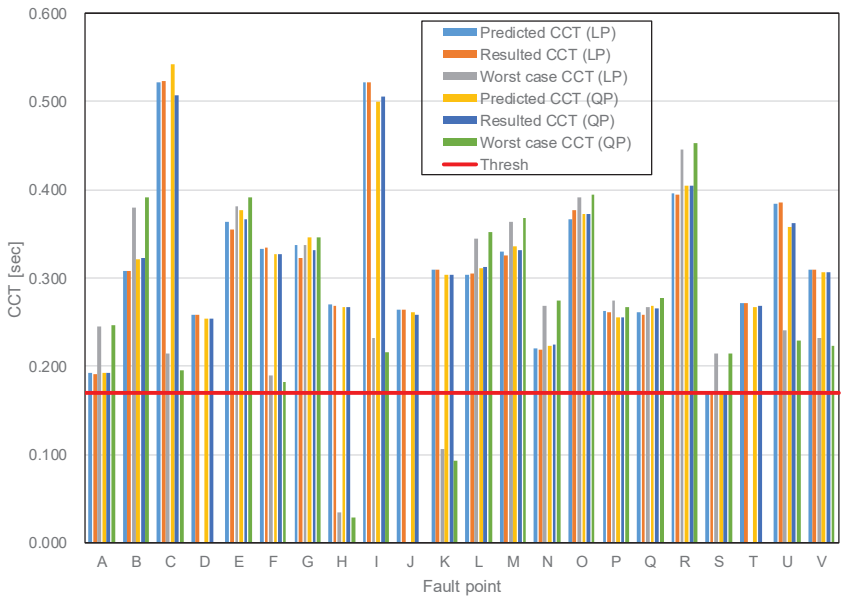

Fig.3-5 CCT after TS control without uncertaninty

Table 3-5 Generator outputs after TS control without uncertainty

	Generator output before TS control [pu]	**Objective F_1 (LP)**		**Objective F_2 (QP)**	
		Generator output before TS control [pu]	Amount of change	Generator output before TS control [pu]	Amount of change
G1	7.90	7.90	0.00	7.83	-0.07
G2	4.32	4.32	0.00	4.26	-0.06
G3	2.95	2.95	0.00	2.87	-0.07
G4	3.32	3.03	-0.29	3.24	-0.07
G5	1.69	1.69	0.00	1.65	-0.04
G6	2.62	2.62	0.00	2.59	-0.03
G7	1.14	1.14	0.00	1.11	-0.03
G8	2.06	2.06	0.00	2.03	-0.03
G9	3.90	3.90	0.00	3.88	-0.01
G10	4.76	4.76	0.00	4.75	-0.01
G11	2.91	3.19	0.29	2.95	0.05
G12	4.47	4.47	0.00	4.51	0.05
G13	6.30	6.30	0.00	6.33	0.03
G14	2.10	2.10	0.00	2.12	0.02
G15	3.63	3.63	0.00	3.64	0.02
G16	3.29	3.29	0.00	3.30	0.02
G17	2.72	2.72	0.00	2.73	0.02
G18	3.14	3.14	0.00	3.15	0.02
G19	1.73	1.73	0.00	1.75	0.02
G20	4.40	4.40	0.00	4.42	0.02
G21	0.97	0.97	0.00	0.99	0.02
G22	1.43	1.43	0.00	1.44	0.02
G23	7.58	7.58	0.00	7.60	0.02
G24	0.71	0.71	0.00	0.73	0.02
G25	0.36	0.36	0.00	0.38	0.02
G26	1.86	1.86	0.00	1.88	0.02
G27	2.45	2.45	0.00	2.47	0.02
G28	4.99	4.99	0.00	5.01	0.02
G29	3.14	3.14	0.00	3.16	0.02
G30	2.64	2.64	0.00	2.66	0.02
total	95.45	95.45	0.00	95.45	0.00

Case 2: with uncertainty

Table 3-6 shows predicted CCTs computed by proposed optimization (3-13) as well as the resulted CCTs, which are depicted in Fig. 3-6. The results have been computed in condition that the system reliability is preserved even for the worst possible case caused by PV prediction error. It is observed in Fig. 3-6 that the CCTs for all the situations satisfy the TS stability constraint, which is different from Case 1. Thus, it is confirmed that the

proposed method provides the reliable control against uncertainties.

Table 3-7 shows generator output deviations after the TS control, which is compared with Table 3-5. The same tendency of generator controls for different objectives is obtained. Note also that the supply and demand balances are satisfied in all the cases for the target PV outputs.

The supply and demand balance is reliably dealt with by the Economic Load Dispach Ploblem (ELDP). The ELDP computes generator dispatch taking into account all the major constraints with uncertainty except the TS constraint, while the proposed method is responsible for the TS control under the consistent constraint set as a complement to the existing method.

Table 3-6 CCT after TS control with uncertaninty

	Objective F_1 (LP)			**Objective F_2 (QP)**		
	Predicted CCT [sec]	Resulted CCT [sec]	Error	Predicted CCT [sec]	Resulted CCT [sec]	Error
A	0.179	0.266	-0.087	0.188	0.208	0.020
B	0.252	0.479	-0.227	0.235	0.267	0.032
C	0.489	0.602	-0.113	0.874	0.638	-0.236
D	0.369	0.218	0.151	0.354	0.221	-0.133
E	0.378	0.393	-0.015	0.345	0.370	0.025
F	0.307	0.370	-0.063	0.209	0.289	0.080
G	0.389	0.345	0.044	0.340	0.324	-0.016
H	0.234	0.262	-0.028	0.186	0.236	0.050
I	0.505	0.598	-0.093	0.323	0.437	0.115
J	0.170	0.279	-0.109	0.170	0.264	0.094
K	0.242	0.304	-0.062	0.175	0.244	0.069
L	0.317	0.407	-0.090	0.313	0.433	0.120
M	0.344	0.435	-0.091	0.291	0.358	0.067
N	0.240	0.274	-0.034	0.226	0.327	0.102
O	0.481	0.454	0.027	0.408	0.420	0.013
P	0.170	0.196	-0.026	0.170	0.202	0.032
Q	0.270	0.268	0.002	0.264	0.256	-0.008
R	0.427	0.555	-0.128	0.364	0.487	0.123
S	0.170	0.221	-0.051	0.170	0.191	0.021
T	0.269	0.259	0.010	0.236	0.256	0.020
U	0.380	0.391	-0.012	0.280	0.301	0.021
V	0.308	0.318	-0.010	0.276	0.292	0.016

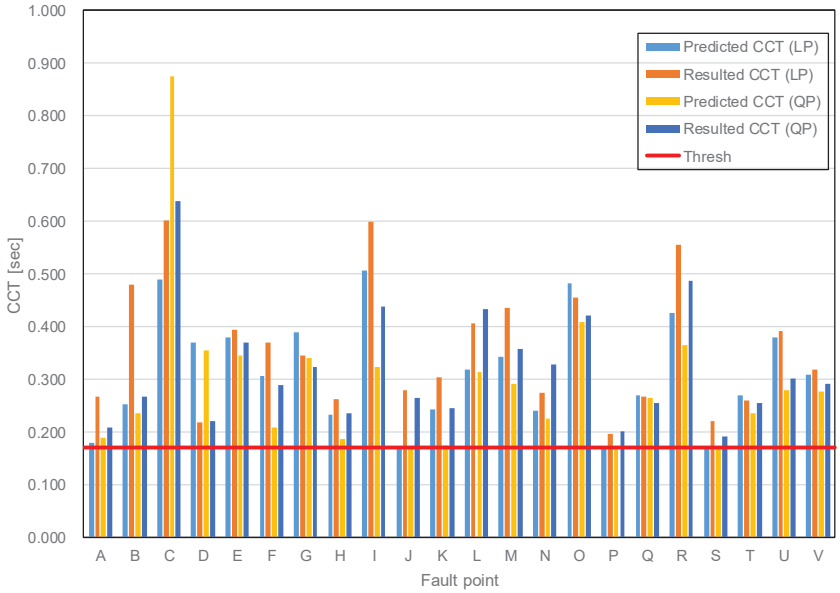

Fig.3-6 CCT after TS control with uncertaninty

Table 3-7 Generator outputs after TS control with uncertainty

	Generator output before TS control [pu]	Objective F_1 (LP)		Objective F_2 (QP)	
		Generator output after TS control [pu]	Amount of change	Generator output after TS control [pu]	Amount of change
G1	7.90	7.53	-0.38	7.64	-0.27
G2	4.32	4.32	0.00	4.16	-0.16
G3	2.95	2.95	0.00	2.68	-0.26
G4	3.32	3.32	0.00	3.05	-0.26
G5	1.69	1.69	0.00	1.63	-0.06
G6	2.62	2.62	0.00	2.67	0.04
G7	1.14	1.14	0.00	1.18	0.04
G8	2.06	2.06	0.00	2.11	0.04
G9	3.90	3.90	0.00	4.04	0.15
G10	4.76	4.76	0.00	4.91	0.15
G11	2.91	4.50	1.59	3.46	0.56
G12	4.47	4.78	0.32	4.94	0.47
G13	6.30	7.50	1.20	6.74	0.44
G14	2.10	1.95	-0.15	1.88	-0.22
G15	3.63	5.49	1.86	4.02	0.40
G16	3.29	3.29	0.00	3.50	0.21
G17	2.72	2.72	0.00	3.09	0.37
G18	3.14	3.14	0.00	3.40	0.27
G19	1.73	1.73	0.00	2.00	0.27
G20	4.40	4.90	0.50	4.77	0.37
G21	0.97	0.97	0.00	1.30	0.33
G22	1.43	1.43	0.00	1.78	0.35
G23	7.58	7.58	0.00	7.93	0.35
G24	0.71	0.71	0.00	0.75	0.04
G25	0.36	0.36	0.00	0.45	0.09
G26	1.86	1.86	0.00	2.21	0.35
G27	2.45	2.45	0.00	2.60	0.15
G28	4.99	4.99	0.00	5.30	0.31
G29	3.14	3.14	0.00	3.40	0.26
G30	2.64	2.64	0.00	2.80	0.16
total	95.45	100.40	4.94	100.40	4.94

The CPU time for the proposed method is listed in Table 3-8. Intel(R) Core(TM) i7-6700HQ CPU @ 2.60GHz is used in this examination. It is understood that the proposed TS control is very fast. On the other hand, the computation of CCT-DF is extremely time consuming since the bisection method is applied, although the CPU time is acceptable. The following characteristics are useful in reducing the computation time of CCT-DF.

Table 3-8 CPU time for the proposed method

		CPU time [sec]
CCT computation		40.263
CCT-DF computation		2885.468
TS control without uncertainty	Objective F_1 (LP)	0.006
	Objective F_2(QP)	0.017
TS control with uncertainty	Objective F_1 (LP)	0.149
	Objective F_2(QP)	0.183

As is observed in Table 3-3, there are many zeros in CCT-DFs, which are without colors. Those generators with zero CCT-DF are not important in the optimal TS control and rarely selected. Therefore, the CCT-DFs of those generators are no need to recompute unless the system condition is largely changed. In other words, the number of useful generators for control are quite limited, which can reduce the computational burden even though an effective computation of CCT-DF belongs to the future problem.

3.6 Summary

Development of countermeasure against the uncertainty of RE is critically important in the operation of power system in these days. In particular, it has been clarified that these uncertainties have a great influence on TS. In this chapter, an improved robust control method for TS is proposed by using CCT-DF. By solving two bi-level optimization problems with uncertainty of RE, it provides the worst case optimal solution. It is shown that the solution can guarantee reliable power system operations against uncertainty. Although CCT has been an important index in existing TS studies, its practical use is quite limited due to the difficulty of its computation. Therefore, an efficient computation method for CCT-DF is also presented in this chapter.

Chapter 4

Stabilization control by synchronous inverter

4.1 Synchronizing power of synchronous generator

The basic controller of the SSI is based on the swing equation (4-1).

$$M_{inv}\frac{d^2\theta_{inv}}{dt^2}+D_{inv}\frac{d\theta_{inv}}{dt}=P_m-P_e \tag{4-1}$$

where M_{inv} is virtual inertia constant; D_{inv} is virtual damping coefficient; Pm is virtual mechanical input; P_e is electrical output. While Pm is equal to P_e in a steady-state, the difference (P_m—P_e) is not zero by disturbance. Depending on the right hand side of (4-1), SSI automatically synchronizes with the grid. This synchronization method using the active power output P_e is called “power synchronization [34]”. The power synchronization can avoid instability of phase locked loop (PLL) in the weak grid. This kind of synchronization technique can achieve a stable performance free from the difficulties of PLL, which always requires sufficient grid voltage at the connection point even during the disturbance. In particular, the power synchronization method can be effective in the islanded microgrid operation without rotating synchronous machines.

For a linearized controller, the linearized expression of (4-1) around the equilibrium point is used. θ_{inv} is calculated by the variation $\Delta\theta_{inv}$. The linearized swing equations with governor are given as follows:

$$\theta_{inv}=\omega_{inv}t+\Delta\theta_{inv} \tag{4-2}$$

$$\Delta\omega_{inv}=\frac{d\Delta\theta_{inv}}{dt} \tag{4-3}$$

$$\omega_{inv}=\omega_{ref}+\Delta\omega_{inv}=\frac{d\theta_{inv}}{dt} \tag{4-4}$$

In SSI, it is assumed that an electric power storage device that simulates rotational energy is installed in the direct current link portion in order to exchange rotational energy of the rotating machine with the system. Therefore, we consider a system as shown in Fig.4-1.

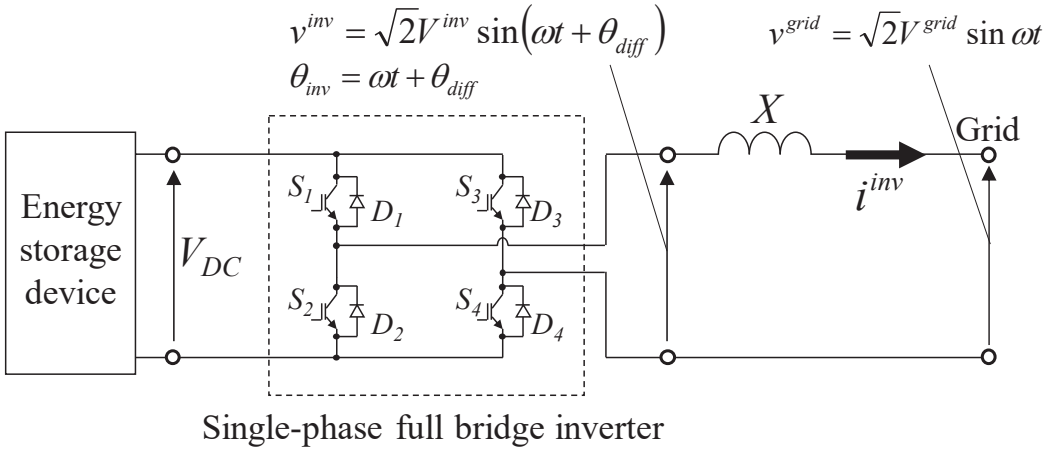

Fig.4-1 Main circuit

4.2 Implementing synchronizing power to inverter

In this chapter, we propose a single-phase full-bridge inverter circuit that converts DC link voltage VDC to AC voltage v_{inv} as shown in Fig.4-1. In the AC output, only the inductance L is used and the capacitance C is not used. Fig. 4-2 shows a block diagram of the controller developed. The core part includes the synchronization circuit, governor, AVR, and FFC functions described in next section, and the outside corresponds to the shell part. In this chapter we will describe the details of the shell.

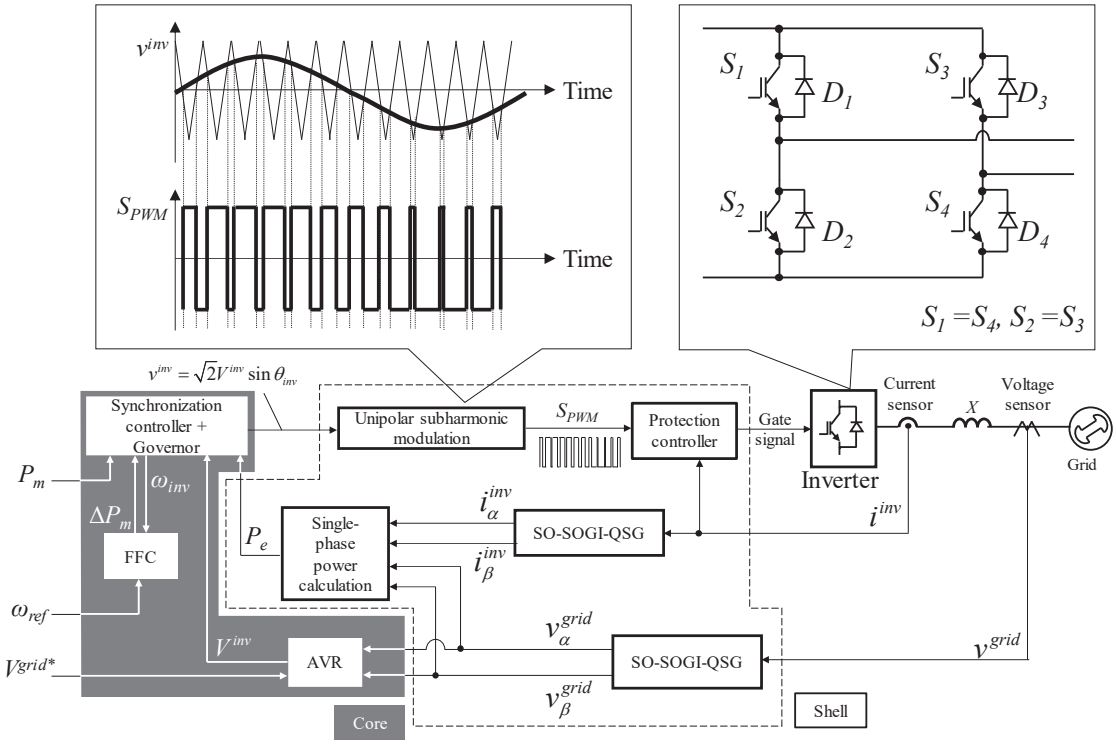

Fig.4-2 Proposed controller.

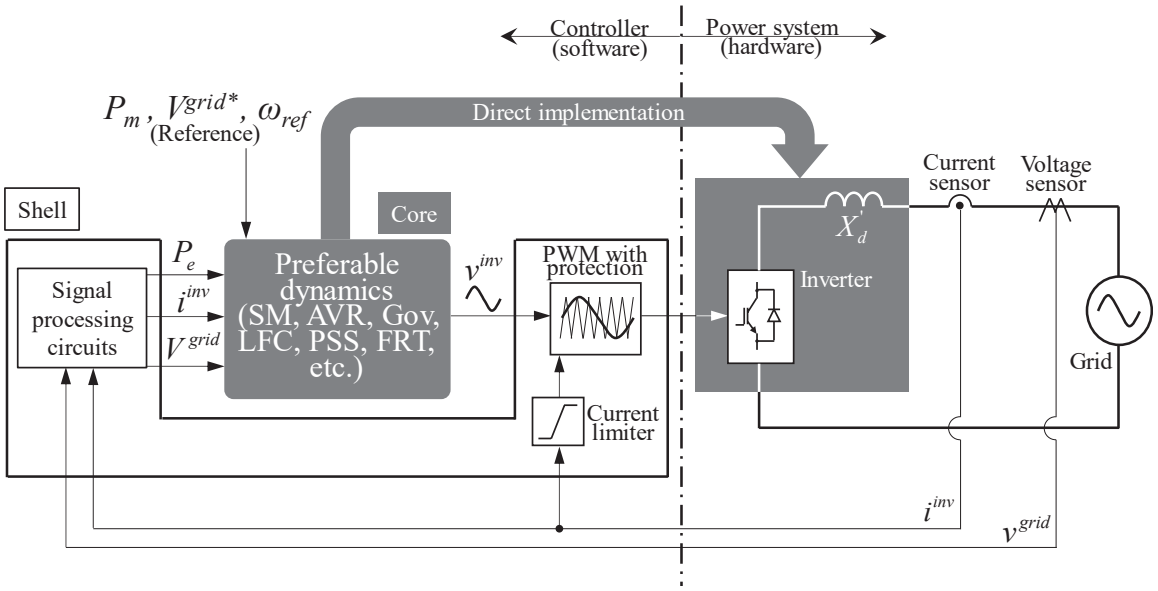

Fig.4-3 Proposed core-shell model.

Fundamental concept in our previous studies, since the SI control system was built using Multi Feedback Loop (MFB) as the standard design method for inverter control, we faithfully made the core dynamic characteristics. It could not be reproduced on the inverter. That is, even if the optimum design of the core is performed, it is difficult to realize desired performance as a result, and it operates merely as an inverter with inertia. Therefore, putting a feedback control system in the shell part may greatly change the characteristics of the control system in principle, so we adopt the design philosophy of avoiding it as much as possible. In this section, we propose the idea of shell construction of SI inverter and concrete construction method of optimal shell making full use of existing design technology.

Signal processing circuit for realizing design dynamic characteristics. When the frequency is ω_0, instantaneous active power vibrates at $2\omega_0$ unlike a three-phase circuit. Since SSI is synchronized based on active power output P_e, vibration of active power output deteriorates synchronization performance. In order to avoid this unstable synchronization, the active power output calculation using the stationary coordinate system is adopted. In the stationary coordinate system, the single-phase active power P_e is calculated by equation (4-5).

$$P_e = \frac{v_\alpha^{grid} i_\alpha^{inv} + v_\beta^{grid} i_\beta^{inv}}{2} \tag{4-5}$$

Here, subscripts α and β represent α-axis component and β-axis component calculated by orthogonal coordinate transformation. In the previous study, second order generalized integrator based quadrature signal generation (SOGI - QSG) has been adopted [35]. However, SOGI - QSG may cause computational errors when the input voltage or current contains direct current components or harmonic components. Furthermore, if the gain of SOGI - QSG is not appropriate, the synchronous machine characteristics of the designed SSI are obstructed. In order to accurately implement the designed synchronous machine characteristics on the SSI, the single-phase active power output P_e should not be

obstructed by noise etc. Therefore, in order to generate an orthogonal signal for a single-phase circuit, as shown in Fig. 4 The second order SOGI-QSG (SO-SOGI-QSG) [36] shown in Fig.4-4. From this, it is possible to realize a design idea that a stable signal can be generated while avoiding the influence on the dynamic characteristics of the time constant region away from the inverter operation frequency 60 Hz in the signal generation in the shell, and the dynamic characteristics of the core are not disturbed.

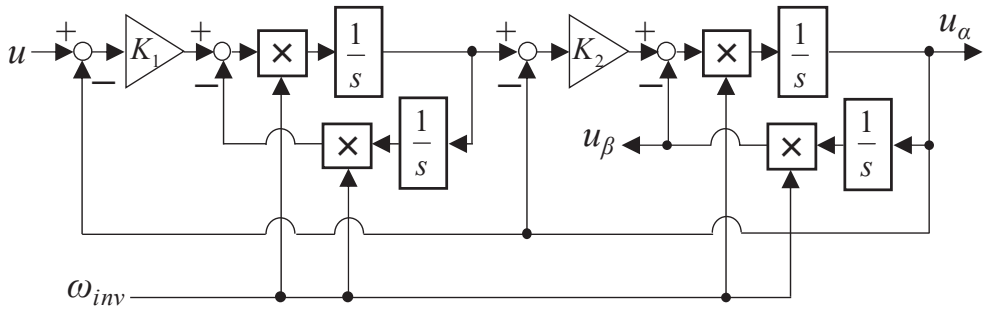

Fig.4-4 SO-SOGI-QSG

4.3 Protection circuit

Fig. 4-5 shows the principle of overcurrent suppression in this paper. Circle I^{max} indicates the range of allowable inverter current. When a short-circuit occurs due to a failure in the power system, the potential difference between V^{inv} and V^{grid} sharply increases as shown in Fig. 4-5 (a), causing the overcurrent to flow, and the inverter output current I^{inv} is located outside the circle of I^{max}. At this time, the single phase synchronous inverter accelerates due to the sudden decrease of P_e, and the phase opens with respect to the grid voltage V_{grid}. Although it is possible to set the inverter output current i^{inv} to 0 in principle by matching V^{inv} with V^{grid}, this control system, which does not disturb the dynamic characteristics of the swing equation, avoids directly interfering with V^{inv} and directly controlling its vector. In that case, since the pseudo rotor angle θ_{inv} of the inverter is automatically determined by the swing equation, the controllable physical quantity is only the voltage magnitude $|V^{inv}|$. Therefore, as shown in Fig. 4-5 (b), $|V^{inv}|$ is made equal to the system side voltage $|V^{grid}|$ when overcurrent is detected. As a result, the inverter output current i^{inv} is suppressed.

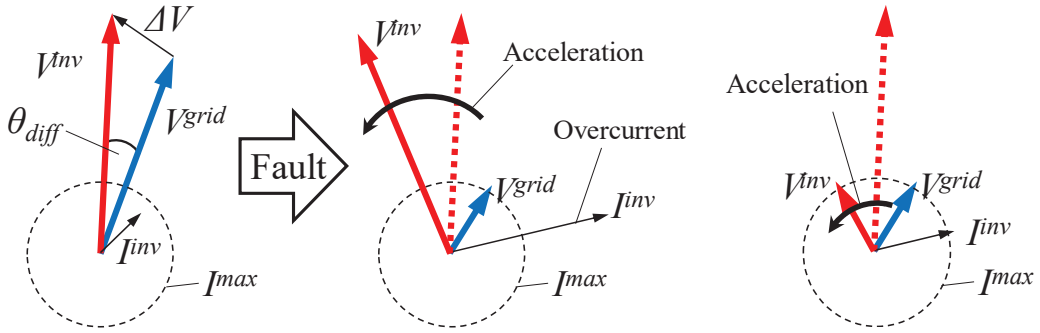

(a) At the fault (b) Current suppression

Fig. 4-5 Protection scheme from overcurrent.

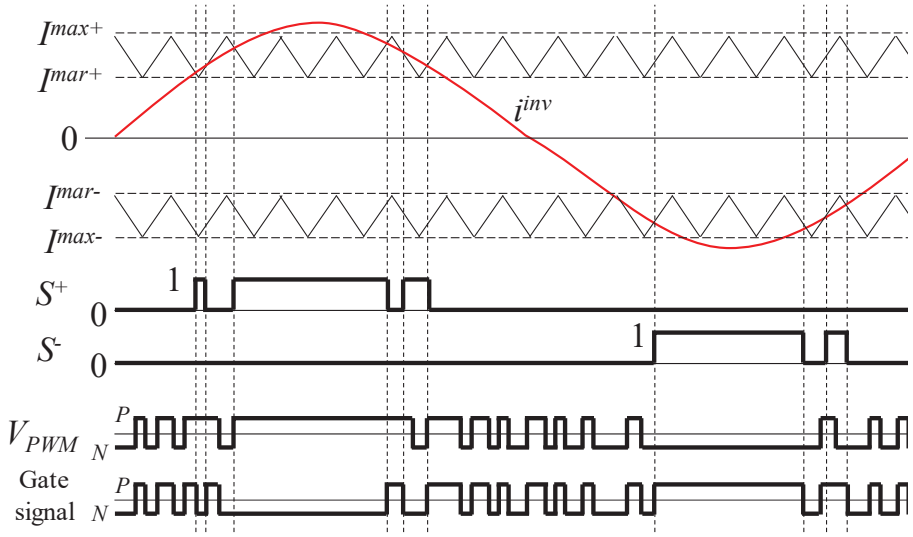

(a) Signal

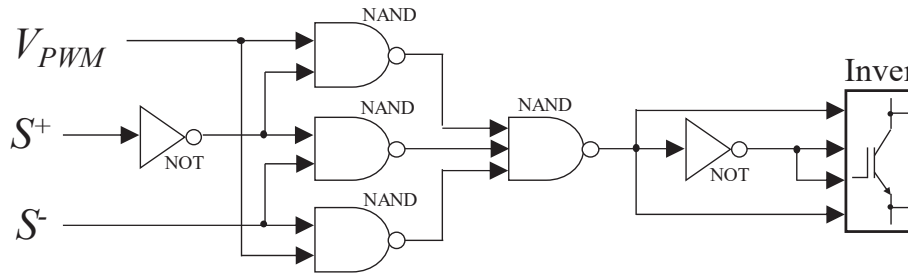

(b) Logical blocks

Fig. 4-6 Protection gate signal generation by current PWM

Although suppression of the inverter output current i^{inv} can be realized by reducing the output voltage, it is not guaranteed that I^{inv} will fit inside the circle of I^{max} since the phase

of V^{inv} is controlled by the oscillating. Therefore, the gate signal V_{PWM} after performing the PWM modulation on the voltage is replaced by the gate signal calculated so as to suppress the overcurrent in order to directly control the gate signal and protect the inverter from overcurrent. Specifically, as shown in Fig. 4-6 (a), let the allowable current of the inverter be I^{max} (positive value I^{max+}, negative value I^{max-}), quasi permissible current I^{mar} (positive value I^{mar+}, negative value I^{mar-}), PWM modulation is performed by using a triangular wave located between I^{max} and I^{mar}. The positive overcurrent detection suppression signal is S^{+} and the negative overcurrent suppression signal is S^{-}. Then, when S^{+}=1, the gate signal is set to the negative side, and when S^{-}=1, the gate signal is set to the positive side. Since the target is a single-phase inverter consisting of two arms having four semiconductor elements, it is possible to prevent the inverter output current i^{inv} from deviating from the permissible current I^{max} by generating the gate signal so that the current in the direction opposite to the overcurrent flows. A logic circuit that generates gate signals from V_{PWM}, S^{+} and S^{-} can be realized by a majority decision circuit using NAND shown in Fig. 4-6 (b). The quasi-permissible current I^{mar} is desirably such a value to compensate for control delay and not distort the inverter output current i^{inv} at normal times. However, if the carrier frequency of the protection circuit is sufficiently high, it can be protected even if $I^{mar} \fallingdotseq I^{max}$. As described above, it is possible to protect the inverter without hindering the dynamic characteristics of the synchronous machine by eliminating the current control system that always interferes with the voltage reference value obtained from the swing equation and adding the function of controlling the gate signal only when overcurrent is generated. However, since the pseudo rotor angle θ_{inv} of the inverter behaves according to the swing equation, the inverter accelerates during failure occurrence as shown in Fig. 4-6 (b).

4.4 Other additional functions

4.4.1 Governor

Speed governor is a control device that maintain constant rotation speed in order to perform the stable parallel operation of synchronous generators. Governor maintains a constant rotation speed by detecting the deviation of the rotational speed. The governor free operation means the state that can be responded freely against variations of frequency by removing restrictions due to load limiter. Governor-free operation corresponds to load fluctuations of short fluctuation period of several tens of seconds to several minutes. The following is a governor model used in this study.

$$P_{gov} = \frac{K_{gov}}{1 + T_{gov}s}\left(\omega_{ref} - \omega_{inv}\right) \tag{4-6}$$

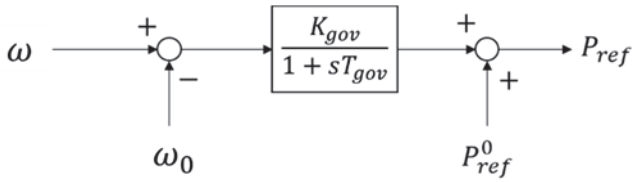

Fig.4-7 Block of governor

4.4.2 AVR

From the pseudo rotor angle θ_{inv} obtained as a solution to the swing equation, the virtual internal voltage of the single-phase synchronous inverter v^{inv*} is given by (4-7).

$$v^{inv*} = \sqrt{2}V^{inv}\sin\theta_{inv} \quad \text{..... (4-8)}$$

The effective value of the inverter internal voltage V^{inv} is adjusted by an automatic voltage regulator (AVR). AVR is designed by the control block with the first-order lag transfer function to the reference value as well as governor. It is assumed that the internal DC voltage of the inverter is maintained at a desired value by the DC / DC converter associated with the inverter and the power storage device. In order to control v^{inv*}

according to the magnitude of the system voltage, the sum of AVR output V^{avr} and detected system voltage V^{grid} is V^{inv}. In other words, the inverter promptly controls the magnitude of the output voltage v^{inv*} according to the system voltage, and controls the output voltage magnitude v^{inv*} to follow the reference value with a delay according to the AVR time constant T_{avr}. Equations (4-9) and (4-10) show the AVR output V^{avr} and the V^{inv} changing when the gain of AVR is K_{avr}, the time constant is T_{avr}, and the voltage reference value is V^{grid*}.

$$V^{avr} = \frac{K_{avr}}{1 + T_{avr}s}\left(V^{grid*} - V^{grid}\right) \quad \text{..... (4-9)}$$

$$V^{inv} = V^{grid} + V^{avr} \quad \text{..... (4-10)}$$

The system voltage V^{grid} is calculated by the equation (4-11) when the α-axis component of the interconnection point voltage of the inverter is v_α and the β-axis component is v_β.

$$V^{grid} = \sqrt{\frac{v_\alpha^2 + v_\beta^2}{2}} \quad \text{.....(4-11)}$$

The $\alpha\beta$ axis component of equation (4-11) can be extracted from a single phase waveform by using SOGI-QSG (second order generalized integrators-quadrature signal generator). However, note that the calculation delay on the value of V^{grid} is caused by the parameter k related to SOGI-QSG bandwidth. Since AVR also has a droop characteristic, it is necessary to compensate the reference voltage value V^{grid*} using an integrator in order to set the voltage deviation to zero.

4.4.3 Frequency controller

Fig. 4-2 shows a part of the control system of the single-phase synchronous inverter, and FFC (flat frequency control) refers to the block located at the lower left of Fig.4-2. The FFC computes the system frequency ω_{grid} using the PLL from the system voltage v_{grid} detected with the plug of Fig. 4-8 connected to the system, and the deviation from the inverter internal frequency ω_{inv} is $\Delta\omega$. Accelerate the inverter by performing PI control

on this $\Delta\omega$ and making it an auxiliary input to the set value P_{m0} of the pseudo machine input.

4.4.4 Plug and play function

Although the single-phase synchronous inverter can automatically operate synchronously as long as it is connected to the grid, we make the frequency and voltage equal to the system side before synchronization input and add a function to automatically turn on the interconnection switch in order to suppress sudden acceleration / deceleration and inrush current at interconnection. An overview of the Plug and Play function is shown in Fig.4-8. A switch and a plug are necessary for automatic synchronization input, and SW and plug are connected to the system via a filter. A voltage sensor of the inverter is installed between the SW and the plug. The Plug and Play function is realized by the following three steps.

Step 1: The inverter detects the system voltage v_{grid} by connecting the plug to the system. The system frequency ω_{grid} is calculated from v_{grid} by using PLL (pahse locked loop). The αβ axis component of v_{grid} is obtained by using stationary coordinate transformation, and the effective value V_{grid} is calculated.

Step 2: Accelerate the inverter and make the inverter internal frequency ω_{inv} follow the frequency ω_{grid} on the system side and the inverter output voltage V_{inv} to follow the system voltage $V_{grid.}$

Step 3: Close SW and complete synchronous input at the moment when the frequency of the voltage at both ends of SW and voltage effective value are equal and voltage phases are equal.

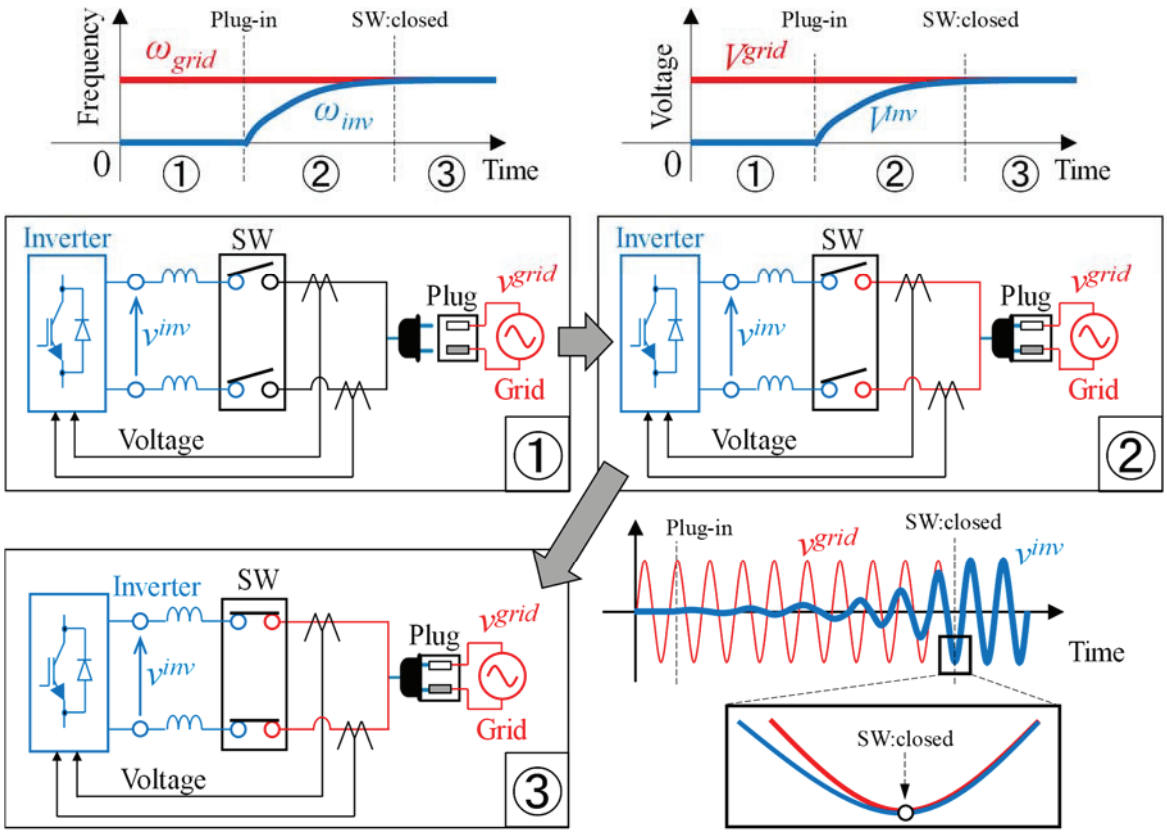

Fig. 4-8 The automatic synchronous connection

4.5 Small signal analysis

Since the proposed control system can realize the designed dynamic characteristics, SSI behaves faithfully to the Xd 'model of synchronous machine equipped with AVR and governor. In order to design the parameters of SSI, we derive the state equation near the equilibrium point in steady state. In this model, various parameters can be selected, but here it is assumed that the SSI is connected to the infinite bus via a transformer (turns ratio: 400/6600). Also, for simplicity, we do not consider PSS. Linearize this modelwith operating points (P_e, V_{inv}). SSI is a parameter, M_{inv} = 100, D_{inv} = 1000, V_{inv} = 400, V_{grid} = 6600, filter reactance X = 7.54 [Ω], K_{gov} = 100, T_{gov} = 0.2 [s], K_{avr} = 2, T_{gov} = 0.01 [s]. In steady state, the frequency and phase were ω_{inv} = 377 [rad / s] and θ_{diff} = 0.0475 [rad]. (2)

Step response (change to ω_{inv} = 377.6194 [rad / s]) is applied at response time t = 0.1 [s] to frequency fluctuation

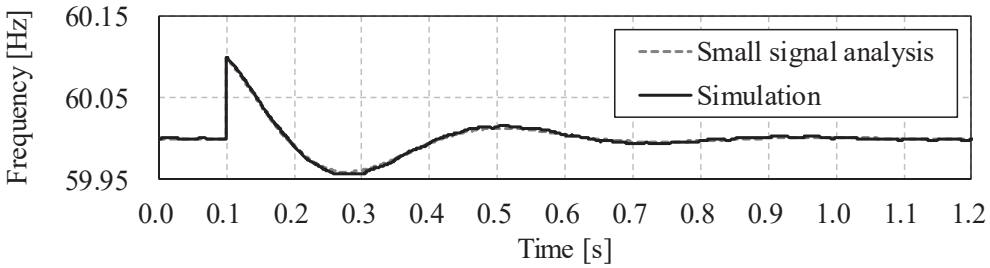

(a) Frequency

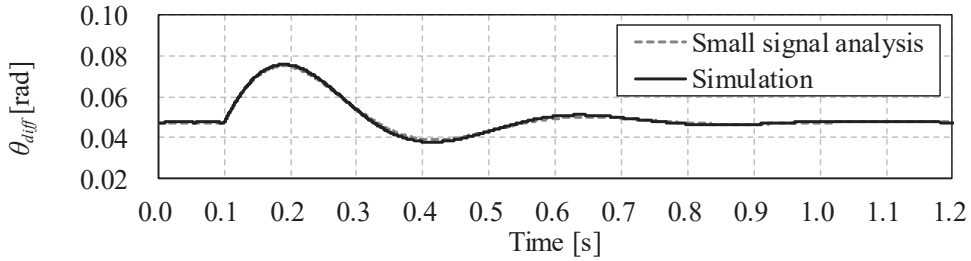

(b) Phase angle

Fig. 4-9. Response to the step variation of frequency.

I investigated the response of my shoulder. Fig. 4-9 is a comparison with numerical results of the behavior of SSI calculated by MATLAB / Simulink, and was calculated by the small signal analysis (a) Frequency (ω_{inv} / 2π) the theoretical value of (b) a phase (θ_{diff}) is there. It can be confirmed that the waveforms of the two are perfectly matched and the numerical calculation result agrees with the theoretical value, and the proposed control system can faithfully reproduce the dynamic characteristics designed in the core.

4.6 Numerical simulation

4.6.1 Simulation condition

In order to verify the function of the developed synchronous inverter, we constructed a power system model including a single-phase synchronous inverter on MATLAB /

Simulink, and whether the operation of single phase micro grid is stable. The simulation model is shown in Fig.4-9. There are three single-phase synchronous inverters, three-phase loads of 5000 [ohm] and single-phase loads of 5000 [ohm]. Three single-phase synchronous inverters are connected to infinite buses via filters and transformers, and switches are installed between them and the infinite bus. It is assumed that all three inverters are connected to the ab phase, so that a three-phase ground fault can be generated on the inverter side of the switchgear. The frequency reference value of the inverter is 60 [Hz], the reference value of the voltage effective value is 400 [V], and the pseudo machine input is Pm = 1,000 [W]. Same parameters are used for all inverters. The sampling time is 2.0 [μs], the carrier frequency is 15 k[Hz], the line impedance is 0.1 + j 0.1 [ohm], and the direct current side of the inverter is simulated with the direct current voltage source 800 [V]. The permissible current of the inverter is set to I^{max} = 35 [A], and the quasi-permissible current is set to I^{mar} = 34 [A]. Other conditions are shown in Table 4-1.

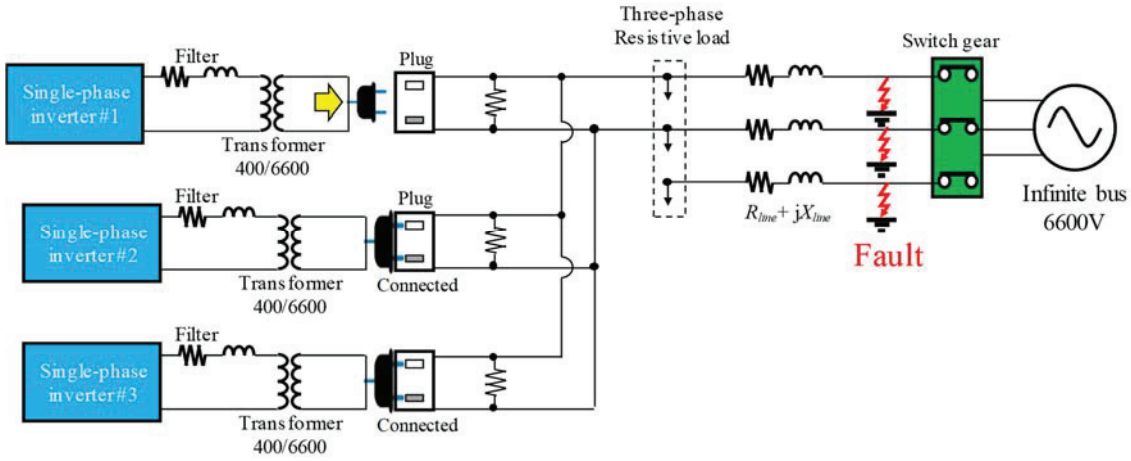

Fig. 4-9 Simulation model

Table 4-1 Simulation conditions

Governor	K_{gov} = 1000, T_{gov} = 0.5 [s]
AVR	K_{avr} = 2.0, T_{avr} = 0.2 [s]
Swing equation	M_{inv} = 100, D_{inv} = 5000
Filter	L = 20 [mH], R = 0.01 [ohm]

4.6.2 Result

For simplicity, it is assumed that the inverters # 2 and # 3 are already connected to the system, and the plug of the inverter # 1 is connected to the grid at time t = 0.0 [s]. After that, the switch is released at t = 4.0 [s], the operation is shifted to independent operation by three inverters, and the LFC signal is turned on at t = 6.01 [s]. Fig. 4-10 shows the output internal frequency of inverter # 1, Fig. 4-11 shows the output current of inverter # 1, and Fig. 4-12 shows the output voltage of inverter # 1. From Figs. 4-10, 11, and 12, it is understood that the inverter is interconnected after synchronizing the system with frequency and voltage. The Synchronization signal in Fig. 4-10 (a) is the synchronization signal shown in Fig.4-8 and realizes smooth synchronous linkage. Also, even when shifting to independent operation, the frequency reduction is suppressed by the damping characteristics of the inverter and the governor. At t = 6.00 [s], although the frequency deviation due to the droop characteristic of the governor remains approximately 0.05 [Hz], the frequency deviation is set to zero by LFC. A three-phase ground fault was generated at t = 6.00 [s] to 6.05 [s] without LFC function. The output voltage of inverter # 1 at this time is shown in Fig. 4-12 and the output current is shown in Fig.4-11. From Figs. 4-13 and 4-14, the output current of the inverter # 1 does not exceed the allowable current despite the severe instantaneous drop caused by the ground fault. From the above, it is confirmed that the proposed inverter protection system does not hinder the dynamic characteristics of the inverter in the steady state where failure does not occur, but protects the inverter appropriately from the overcurrent in case of failure.

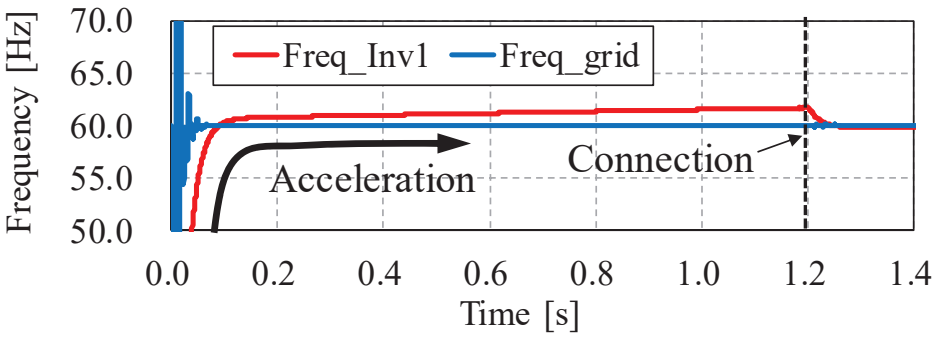

(a) At the connection

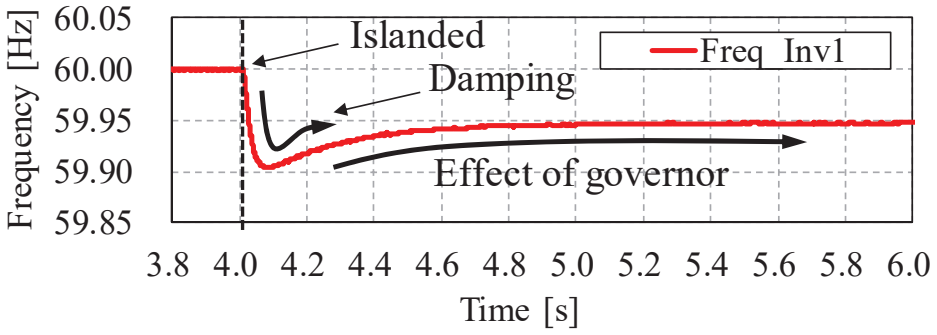

(b) At the islanded mode

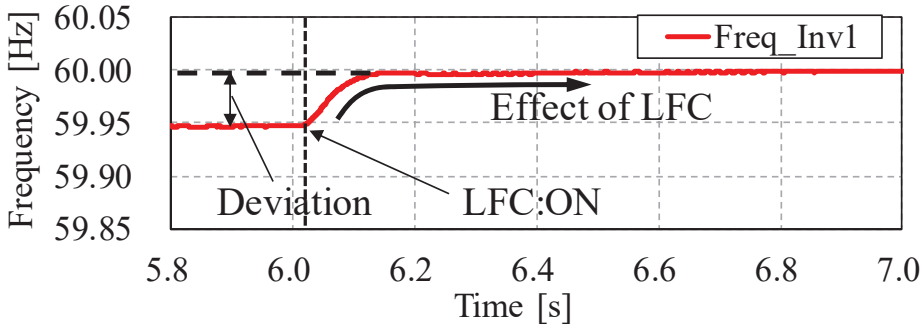

(c) At the FFC operation

Fig. 4-10 Frequency of the inverter #1

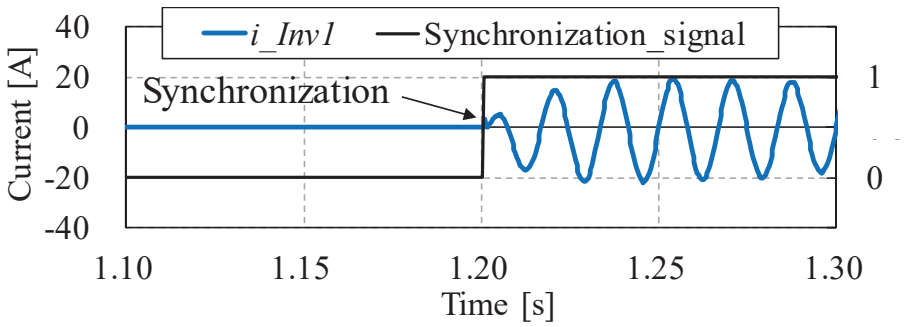

(a) At the connection

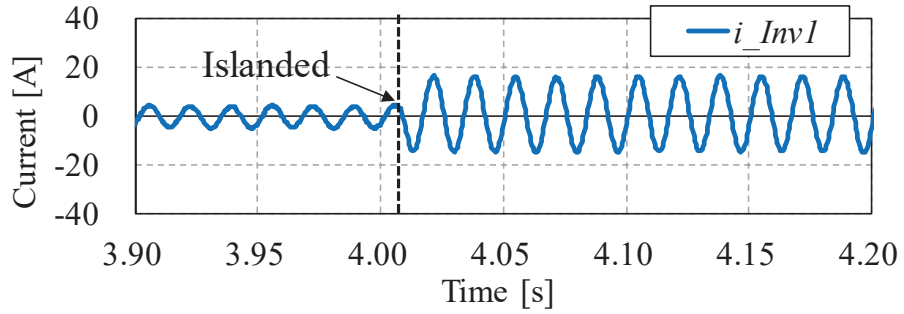

(b) At the islanded mode

Fig. 4-11 Output current of the inverter #1

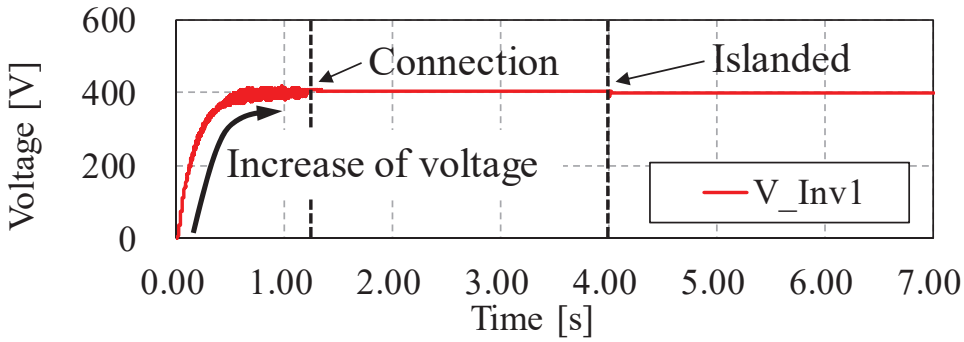

Fig. 4-12 Output voltage of inverter #1

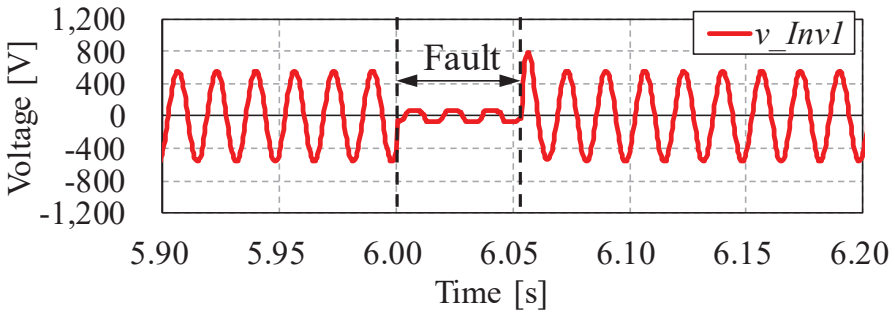

Fig. 4-13 Output voltage of inverter #1 at the fault

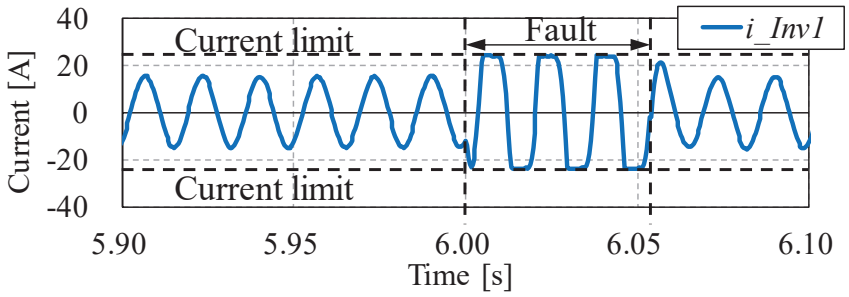

Fig. 4-14 Output current of inverter #1 at the fault

4.7 Hardware In the Loop (HIL) simulation

For realization of the single-phase microgrid, it is also necessary to verify the properly working of the developed controller in the experiment with disturbances such as sensor noises. In addition, the proposed controller is needed to be operated on real time. Therefore, from the viewpoint of efficient experimental verification, we employ Hardware In the Loop (HIL) test. In order to verify the effectiveness of the proposed controller, HIL simulations using as single-phase microgrid model are performed. The stabilization effect of the SSIs is compared with the case of inertia-less inverters. In this section, the effectiveness of SSI and overcurrent protection function in real time simulation using HIL are focused on.

4.7.1 Inertia-less inverter

A controller of the inertia-less inverter is developed. The controller consists of PLL, the orthogonal transformation circuit, dq transformation circuit, voltage controller, and current controller. Since the poor PLL cannot precisely detect frequency and phase angle under the islanded microgrid operation without rotating synchronous machines, SOGI-frequency-locked loop (FLL) is employed [66]. Fig. 4 shows the blocks of the employed SOGI-FLL, where ω_0 = 377 [rad/s], k = 1.42, γ = 2.22. v, v', qv', ω are input signal, filtered signal, 90° shifted signal, and frequency of the input signal, respectively. The phase angle θgrid can be calculated by (4-12).

$$\theta_{grid} = \arctan\frac{qv'}{v'} \tag{4-12}$$

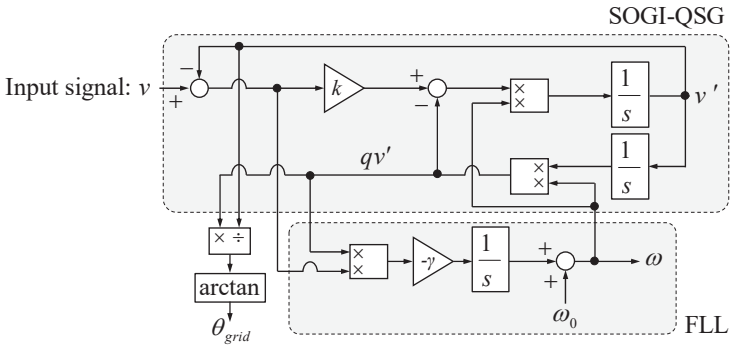

Fig. 4-15. SOGI-FLL

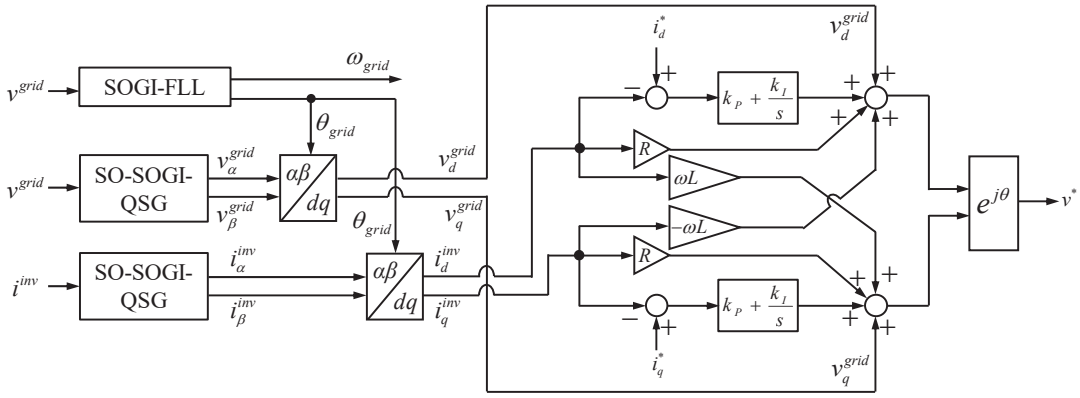

Fig. 4-16. The inertia-less inverter model.

θ_{grid} is used to transform alpha and beta components of grid voltage v_{grid} and current i_{inv} to dq components on the rotating reference frame as shown in Fig. 4-16. In order to avoid adverse effect of the distorted voltage and current, the alpha and beta components are calculated by SO-SOGI-QSG. The current controller with feedforward parts is shown in Fig. 4-16. i^* represents the reference value of the output current, PI controller is used in the current controller. The reference signal of the output voltage v^* can be calculated as the alpha components of the signal. k_P and k_I represent the gains of the PI controller. R and L are filter resistance and filter inductance, respectively.

4.7.2 HIL test system

Fig. 4-17 shows HIL test system. HIL is a technique used for the test of complex real-time embedded system. HIL simulation provides an effective platform to validate the developed controller in the experiment. The HIL system emulates the behavior of the SSI and the microgrid in real time. The signals, e.g. voltage, current, frequency, active power output, detected by sensors in HIL system are gathered by embedded SCADA system and monitored by users through A/D and D/A converters. The digital controller in the real world implementing the proposed controller computes pulse signals to drive gate of SSI based on the measured data in HIL system. The operator can monitor the behavior of the SSI and microgrid in real time, check the performance of the proposed controller, and discover bugs of the digital controller efficiently.

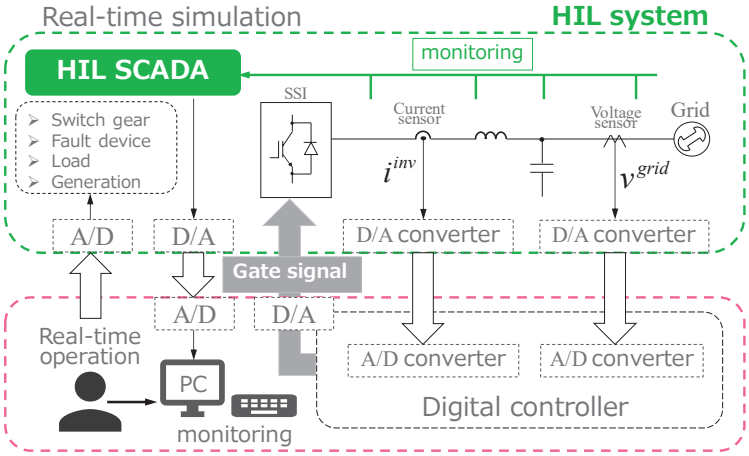

Fig. 4-17. HIL test system.

4.7.3 Experimental condition

The developed controller is coded by programming language C and implemented to a digital signal processing (DSP) board (PE-Expert4: Myway Plus Corp.). The computed gate signals based on the proposed controller are sent to a HIL real time simulation testing hardware (HIL402: Typhoon HIL Inc.). The simulator is connected to the PE-Expert4 through A/D and D/A convertors. The microgrid model is developed by GUI in the Typhoon HIL software on the Host-PC, and the model is then compiled and uploaded into the HIL402. HIL402 emulates physical states of the microgrid in real time and their signals are sent to the PE-Expert4. The proposed controller on the PE-Expert4 detects voltage and current signals on the microgrid and computes the gate signals to control the SSI on the HIL402. The constructed HIL simulation environment is shown in Fig. 4-18.

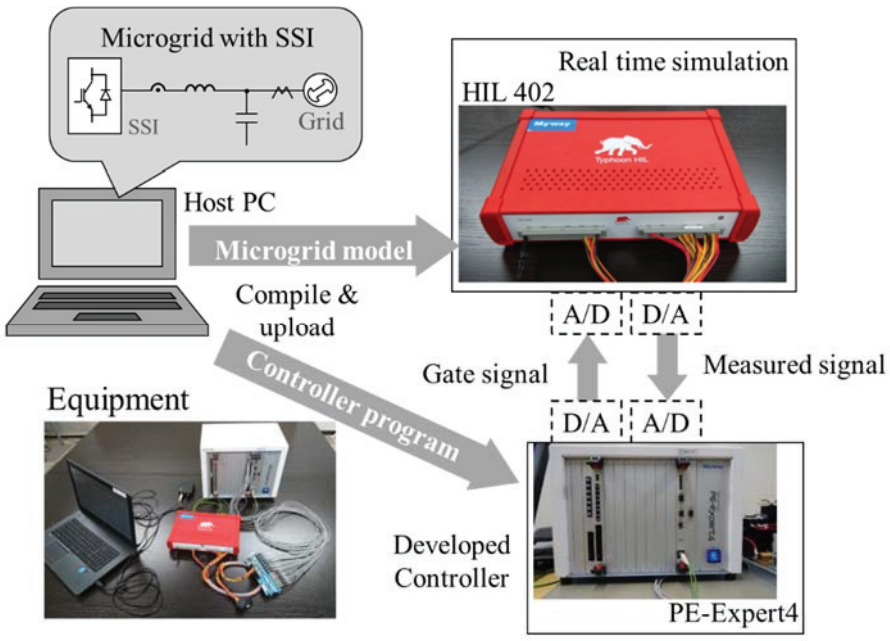

Fig. 7. Experiment condition

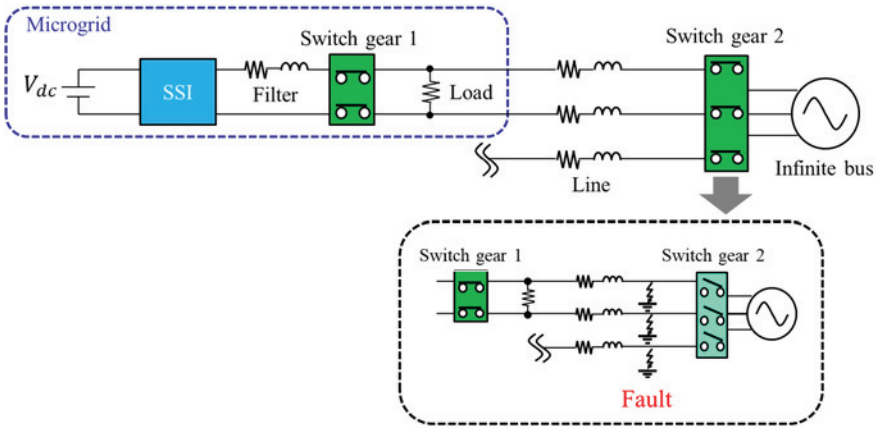

Fig. 4-19. Experiment condition

Fig. 4-19 shows the microgrid model used in the experiment. A SSI is connected to an infinite bus through the filter, the line, and switch gears. An initial state of the switch gear 1 is “open”, and the initial state of the switch gear 2 is “close”. After the start of the real-time simulation, the SSI accelerates and synchronizes with the infinite bus. After the synchronization, the close signal is sent to the switch gear 1 through the A/D convertor. After the SSI connects to the grid, the switch gear 2 is opened. By opening the switch gear 2, the microgrid is disconnected from the infinite bus. In the islanded operation, 3LG fault occurs at the point shown in Fig. 8. Parameters are set as follows: The constant DC voltage source (200 [V]) is on the DC side with both inertia-less inverter and SSI. The microgrid is connected to an infinite bus (rms value; 100 [V], 60 [Hz]) via switch gear. A single-phase resistive load (20 [Ω]) is located. K_{gov} = 1000; T_{gov} = 0.5 [s]; M_{inv} = 100; D_{inv} = 5000; Filter inductance L = 25 [mH], Filter resistance R = 0.1 [Ω]; Current limit I_{max} = 10 [A]; Fault duration time 0.05 [s].

4.7.4 Result

First, in order to confirm the stabilization effect by SSI, frequency, voltage and current of inertia-less inverter and SSI, when the infinite bus is disconnected, are shown in Fig. 4-20. Inertia-less inverter is synchronized with the grid by PLL. At 4.55 [s], the inverter

is disconnected from the infinite bus resulting in the islanding operation. The frequency of the microgrid is decreasing slowly after 4.55 [s] and it is not stabilized perfectly. Then, the frequency become approximately 59.98 [Hz]. The decrease in frequency can also be confirmed from the voltage waveform. Result of SSI is shown in Fig. 4-21. The decrease of frequency is reduced compared with the inertia-less inverter and it becomes stable soon. This is the influence from the governor and dumping added to the swing equation.

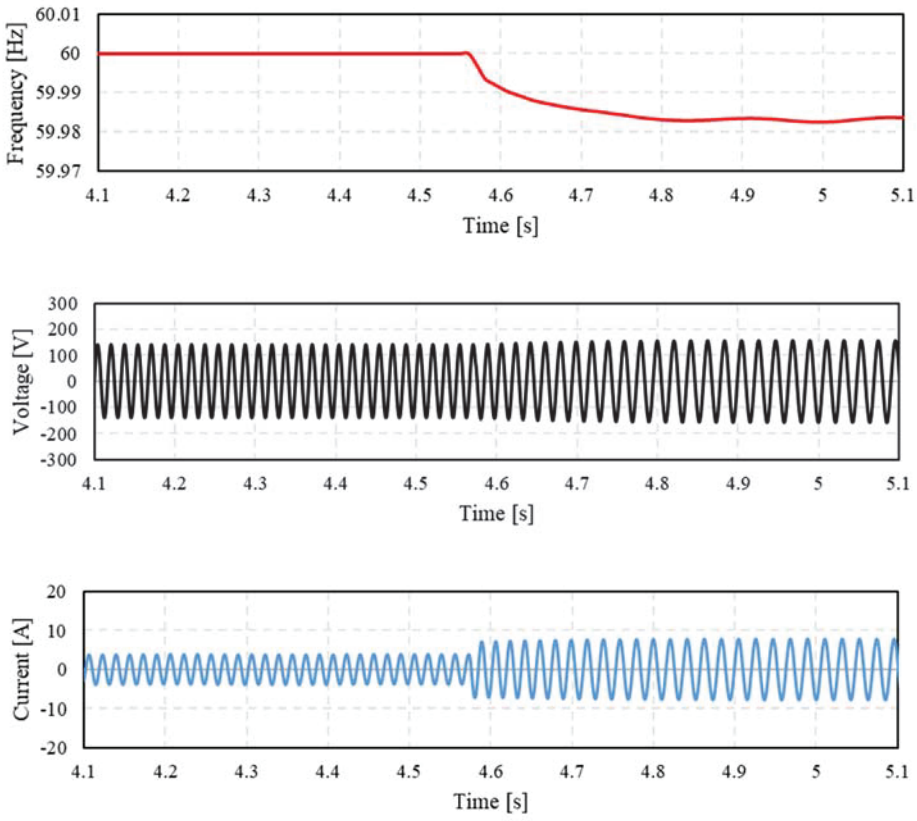

Fig. 4-20. Islanding operation with inertia-less inverter.

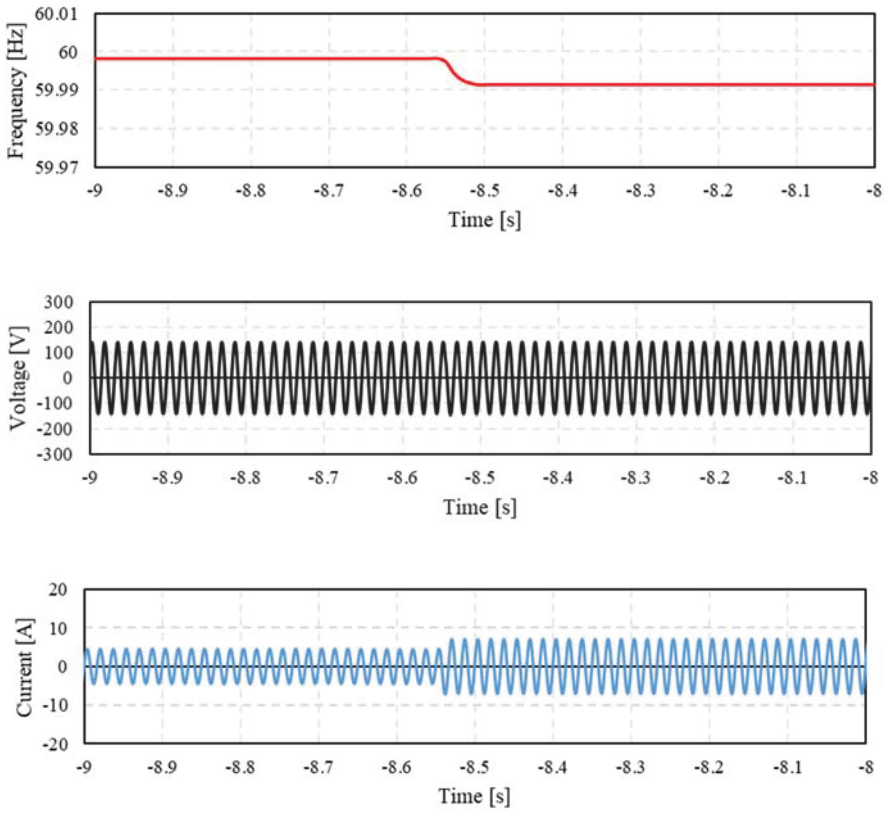

Fig. 4-21. Islanding operation with SSI.

Next, we confirm whether the overcurrent protection function works or not in real time by HIL simulator. When the fault occurs with only inertia-less inverter or SSI (islanding operation), we confirm the current difference. Fig. 4-22 shows frequency, voltage and current of inertia-less inverter and Fig. 4-23 shows that of SSI without protection. In Fig. 4-22, 3 LG is occurred at 17.90 [s]. It can be confirmed that the overcurrent is existed during the fault. In addition, at the moment the fault is cleared, a large surge voltage can be seen because PI controller is worked also during the fault and phase is largely shifted compared with grid. In Fig. 4-23, 3 LG is occurred at 6.98 [s]. The current is suppressed by swing equation but there are overcurrent. The result of SSI with protection is shown in Fig. 4-24. It is expanding to make it easy to confirm the effect of overcurrent protection. It can be confirmed that the current is limited by Imax = 10 [A]. It is protected with sufficient precision by swing equation and overcurrent protection function.

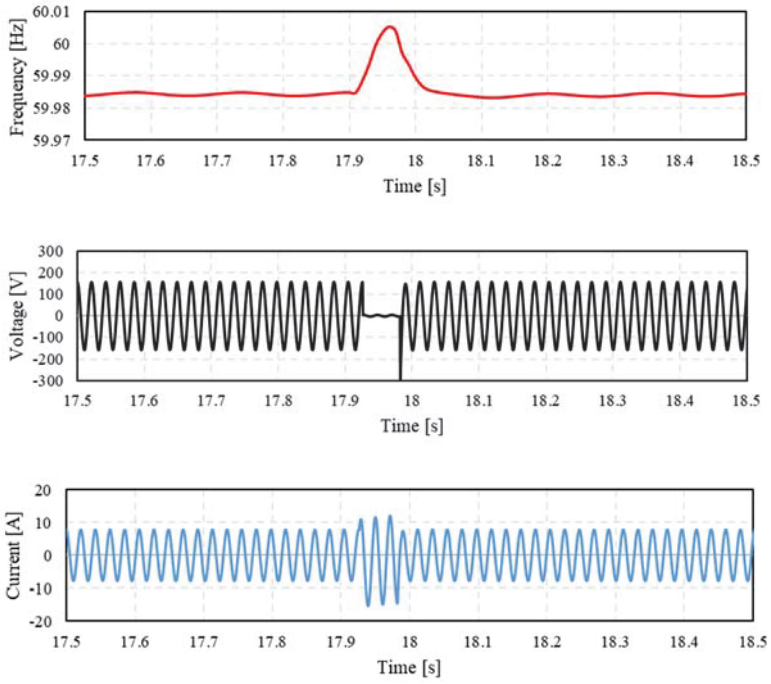

Fig. 4-22. Output of inertia-less inverter.

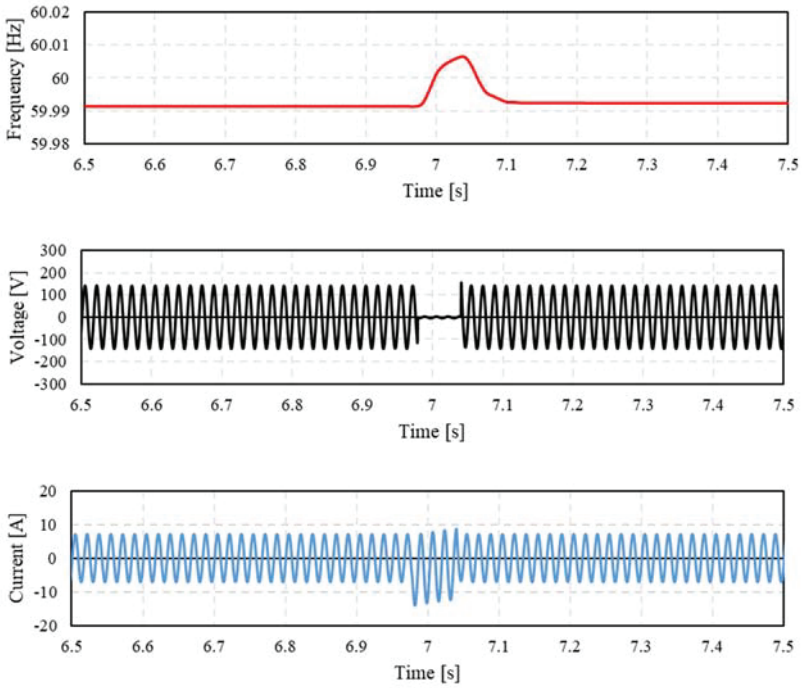

Fig. 4-23. Output of SSI without protection.

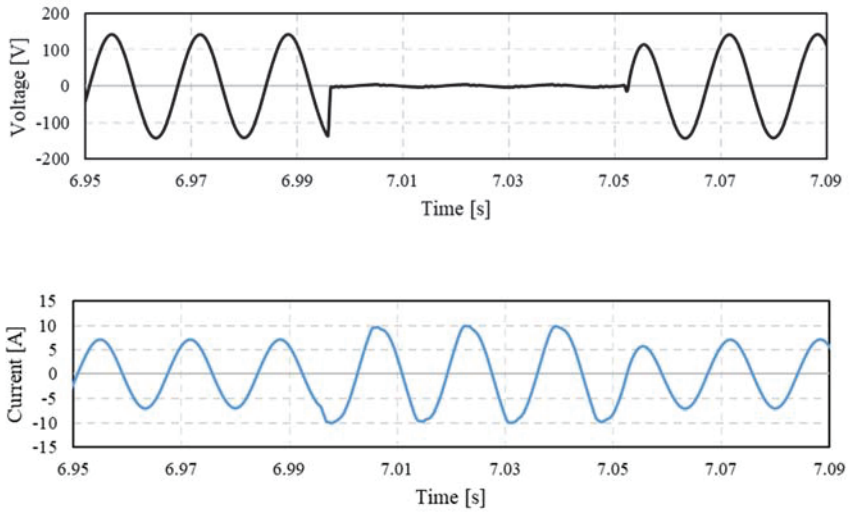

Fig. 4-24. Output of SSI with protection.

The problem of the proposed protection circuit was found by real time simulation using HIL. Therefore, we consider the cause and discuss how to design the protection circuit. Fig.4-25 shows the waveform when overcurrent protection does not work well. It can be seen that the current fluctuates finely around the limit. At this time, the inductance L of the filter is set to 10 [mH]. Thus, the current ripple becomes larger than when 25 [mH]. Since the PWM signal is directly controlled around the current limit, the influence of the ripple current is large. Therefore, it is necessary to consider not only cut-off frequency and ripple current but also overcurrent protection in designing the filter. However, sufficient protection can be achieved by providing a margin for the current limit in designing the overcurrent protection circuit. The degree of influence of the ripple current on the proposed protection circuit needs to be investigated in the future.

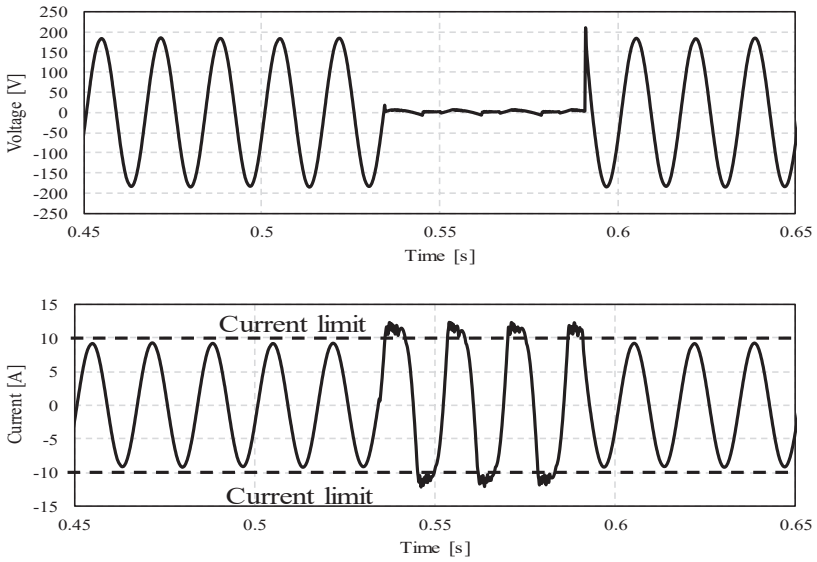

Fig. 4-25. Mismatch between protection circuit and filter

4.8 Summary

In this chapter, we propose the concept of a Core-shell type inverter, and as an example of the application destination, we conducted a study assuming a single-phase synchronizing power inverter. Specifically, we developed a control system for single phase synchronous power inverter to realize power system stabilization and emergency micro grid operation. Since the proposed control system has the advantage that it is possible to realize the desired synchronous machine characteristics designed and it does not involve impeding the dynamic characteristics by the multi-feedback loop which is difficult to adjust the optimal parameters, the system condition dynamically It is expected that cooperative design of multiple inverters in a changing single-phase microgrid becomes easy. Numerical calculation confirms seamless transition from grid interconnection mode to independent operation mode in case of emergency and that overcurrent suppression operates normally when line fault occurs and furthermore the performance of the proposed control system implemented in the actual machine I verified. We plan to carry out demonstration experiments on improving the resilience of the power

system by operating the proposed SSI under the experimental environment and using single phase micro grid in emergency.

Chapter 5

Conclusion

Chapter 1 explains the background and the problem of the present power system concerned with REs. Mega solar and domestic solar panels are being introduced in Japan because of poor energy resources. However, the amount of power generated by PV has uncertain as it depends on climate. Confidence intervals are defined to handle this uncertainty. By using this, it is possible to perform system simulation considering the uncertainty of PV. Since a large number of synchronous generators are connected to the grid, the system can be operated stably. System stability has steady state stability that takes into consideration the relatively slow state and transient stability to evaluate instantaneous stability. In this thesis, it will consider the transient stability from the next chapter to evaluate uncertainty. This chapter also describes our team project in Taoyaka program in order to realize future sustainable society.

Chapter 2 explains the stability of power system and its analysis methods. Conventional stabilization control methods are also explained. CCT is often used to evaluate transient stability. As a calculation method of CCT, there are a time domain simulation method that calculates by drawing a trajectory of stability and instability and an energy function method using transient energy when it critical situation. In this thesis, it evaluates stability by the simulation method with less CCT error. There are mainly two methods to improve the stability. One is a generator control and another is a FACTS control, which is a device using power electronics technology. After introducing the conventional control, the former is explained in Chapter 3 and the latter is explained in Chapter 4.

Chapter 3 proposes a novel approach, that is, the transient stability analysis and control methods based on CCTs. First, the characteristic of CCT is investigated when PV is introduced to conventional system. When simulation was performed using the power system model, it was confirmed that transient stability deteriorated due to uncertainty of

PV. From this result, the characteristics of the influence of uncertainty of PV on CCT were investigated. Also, as the output of PV fluctuates, it is necessary to adjust the output of the generator in order to maintain the supply and-demand balance. Therefore, its optimum generator control to improve CCT is considered. The effectiveness of CCT-DF is confirmed by comparison with the simulation method and it is applied to an actual control. Then, the transient stability control through CCT is studied based on CCT-DF by controlling generator outputs. This chapter also discusses formulation and solution of robust optimization problem for secure power system operation against REs uncertainties. This method is a control to improve the CCT without moving as much as possible from the economical operation state obtained from the economic load dispatch system. Then, the effectiveness is verified by simulation.

Chapter 4 proposes a new design of the synchronous inverter for improving power system stability. Assuming the future situation, it is expected that synchronizing power also decreases with the decrease of synchronous generators in operation. Thus, the synchronous inverter, which have synchronizing power similar to synchronous generator, is designed for improving power system stability. Since this thesis proposes a single-phase synchronizing power inverter, it can be flexibly used as compared with a three-phase inverter. This is because it can be directly applied to inverters for household PV which are thought to increase further in the future. Also, the proposed control system has an advantage that it does not disturb the characteristics of the generator to be mounted by improving the protection circuit. The conventional functions for voltage and frequency controls are also implemented in the inverter. It can be confirmed that the proposed inverter has the same characteristics as the small signal analysis. This makes it possible to analyze with effective value and design the optimum parameters of the inverter that can use the conventional system analysis method and contribute to system stabilization.

Appendix

Taoyaka Project

Our view of new community center

To support for the improvement and innovation of the traditional community centers, our team project considered to establish a new model of community center which is hoped to enhance the community's communication and to increase the community welfare by their own resources. The new community center, in our viewpoint, not only offer the common space for the local people to communication, but also provide the educational activities and experiments on the new technology (renewable energy and new farming technology), promote more mutual international understanding activities, introduce the new agricultural products, and also expand various commercial activities in which the local residents can sell their own products or the products from surrounding and peripheral areas, and exchange their professional skills, so on.

Local people and visitors can feel free to use community center and enjoy the products/services; furthermore, they can get information of new power facilities and apply in daily life. Community center is a place with multi-functional purposes and provide more convenience for users.

Fig. A-1 Concept of community center

Kodani village and the surroundings

Kodani village locates in the Takaya- cho, it is considered the rural area of Japan, with the number of the households is 1,677 (the crowded unit in Takaya - cho). The population were generated due to the Sanyo Main Line. 21..5% of the population are above 65. Unlike other depopulated area, Kodani locates in quite convenient place. It is not very far Saijo town and Hiroshima city (where there are many foreigners live, study and work) and Miyajima world heritage site (where many tourists will choose for one-day tour). It is also near the airport (people who want to go the airport by train have to stop in Siraichi station), near the highway where many passengers commute every day. Kodani village could also be treated as a new rural area where the decline is not so serious. However, it does face the same problems as other villages. The most serious problem is abandoned land and houses, how to deal with nature resources (bamboo and wild animals) and how to keep the traditional culture.

To deal with these problems, Kodani already set up its own organization and launch a

series of polices to overcome each problem. For instance, establishing new activities center to protect old heritage sites, cultural activities groups for drum performance and local handicrafts and agricultural groups for local farming industry and school education… etc. Their office website is http://www.kodani.org/, where you can find the latest activity and policy to support Kodani development.

Not only we found Kodani is a good place to foster local activities we also found some of the local households already set up a solar panel system and manage it by themselves for a few years. However, the application of the solar panel is still restricted to generating energy but not for daily life use. Meanwhile, Kodani area is next to the Sayo Express way and near to Kodani service area (shorten for SA, a place for express way passengers to take rest, consume and get information), local people from Kodani alreay open a vegetable market in SA. Based on these conditions, we think Kodani has good conditions for us to join community activities, build cooperation and apply our technical facilities.

Figure A-2 Solar panel site in Kodani village

Research aims

How to revive a rural area in disadvantaged area is often an important source for social science collections, as well as for researchers, policy makers, students. Therefore, it is also being a frequently discussed topic in onsite project. The aim of our study in Kodani and the depopulated area is try to contribute for rural development through a new model of community center. We try to figure out:

(1) How to enhance community vitality? Through joining and holding different activities, we want to invite more people to join local events and provide more chance for local communication.

(2) How to share technology information? Providing the 'easy and efficiency' technology that local residents can apply in their daily life or work.

(3) How to strength connections? Increase regional interaction through different stakeholders for example universities and SA/Michinoeki

(4) Future perdition of community center, what products/activities we should provide for local residents in the future?

Interdisciplinary aspect

Cultural aspect: enhancing the connections with people to activate of the region. Providing cultural exhibition/exchange activities. Hold experiential activities. Increasing local people's participation in community.

Technical aspect: Supporting for supplying renewable energy for the village activities (community center/ festivals/Introducing more information of solar panel for the local people…), information and technology sharing, online database and education.

Social aspect: providing the chance to build cooperation with outside institutions. Hold commercial activities to make profits for local people and sales exhibitions for local products. Systematic management of local community affairs.

Taoyaka Farm

Taoyaka farm is a test case of the community center we implemented for Kodani area. We borrowed land from the owner and built a farm. The overview is shown below.

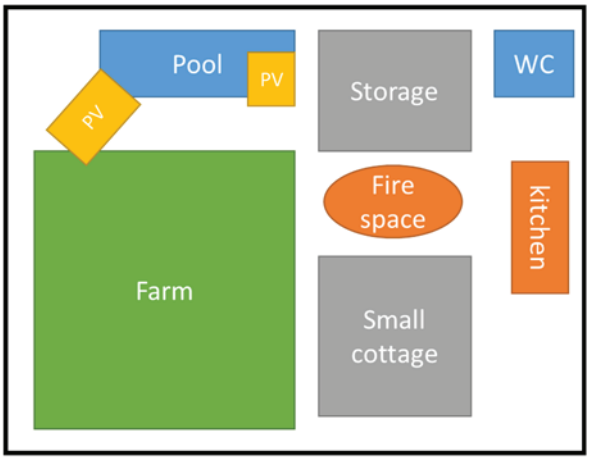

Fig. A-3 Construction of Taoyoka Farm

First, we set up a small hut and a toilet so that local residents can gather in the farm. Along with that, we installed a fire space so that a kitchen space and a bonfire can be made to make easy cooking. We also set up a storage space so that we can arrange the equipment. In addition, the PV panel is installed in the farm and the electric power in the Taya Farm is supplied from the PV panel. The pool is for hydroponic cultivation, and it is also operated by electric power from PV.

Fig. A-4 Actual Taoyaka Farm

Fig. A-5 A farm

Fig. A-6 During the construction of the pool

FigA-5 shows actual Taoyaka farm. We built such a farm in a residential area. Fig. A-6 is a picture when we were plowing. Since this land was not a field, it was necessary to include soil containing nutrients. Figure 3.4 is a picture we are making a foundation for pool and PV.

Fig. A-7 Completed picture of the pool

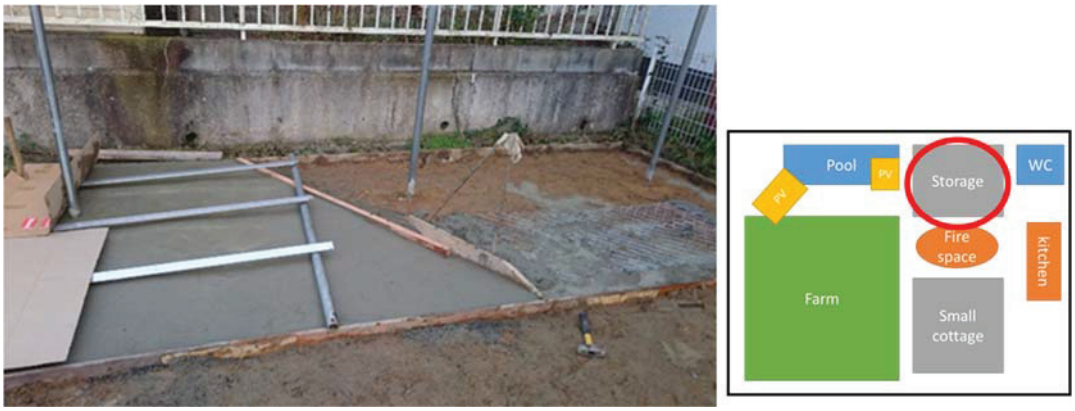

Fig. A-8 During construction of storage

Fig. A-9 Completed picture of the storage

Fig. A-7 is Completed picture of the pool. You cannot see PVs, but The PV is installed at the above of this picture. Fig. A-8 is a picture during construction of storage. We installed cement on the ground by ourselves. Fig. A-9 shows the storage with the roof installed.

Fig. A-10 Inside the small cottage

Fig. A-10 shows inside the small cottage. We made these facilities with local people.

There is a field in Taoyaka farm, so we can plant vegetables in the field and also harvest. The harvested products actually obtained by activities are shown below.

Cucumber, eggplant, radish, zucchini, bean, red pepper, strawberry, tomato, pumpkin, lemongrass, etc.

Fig. A-11 Vegetables harvested in Taoyaka farm

From Technical aspect:

Renewable energies don't emit CO2 gas, so it is eco-friendly generation. For example, photovoltaic generation, wind power generation, biomass generation, geothermal generation, and so on. we focus on PV, because PV is easy to install that is small size. It is optimal as a power generator installed in a disadvantageous area. Thus, PV is better generation system for local. Most people are interested in renewable energy. For example, there are solar home systems, mega solar, etc. And it is already installed many area and

houses. But that energy is just used vaguely and just sold to Power company. So we want PV to become more friendly and more properly for local people. Here, we suggest “Use solar power for agriculture from technical aspect.” Thus, our proposal is using hydroponic culture.

Hydroponic culture has many benefits, that is easy to cultivate, growth speed is fast, become big compare with soil.

How to use electricity from PV for hydroponic cultivation: If we want to harvest “Good vegetables” by hydroponic cultivation, we have to give oxygen and nutrients to roots in water. Thus, we adopted water pumps to solve this problem, and other solution is to use air pumps. Water pumps send oxygen to and circulate nutrients efficiently in water. Fig. A-12 shows construction of hydroponic culture of Taoyaka farm. There are main pool for vegetable and sub pool to keep water level. The main pool is the above the sub pool. There is a hole in the bottom of the main pool, and water is automatically falling. 1) Water are mixed with air in the sub pool, 2) there are water pumps to pumping up water to main pool. 3) Water flow is generated automatically. The PV supplies power to water pumps.

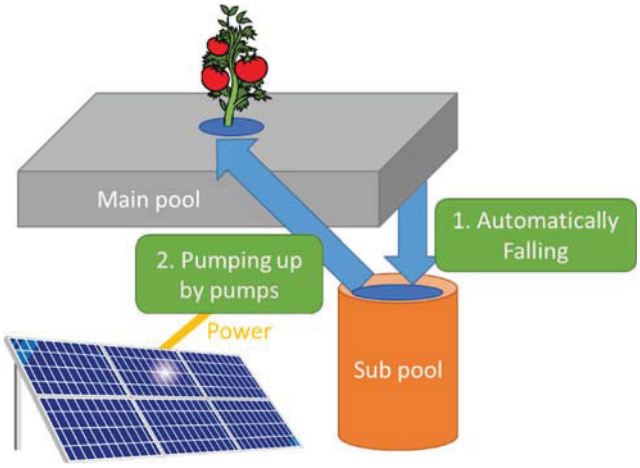

Fig. A-12 Hydroponic culture in Taoyaka farm

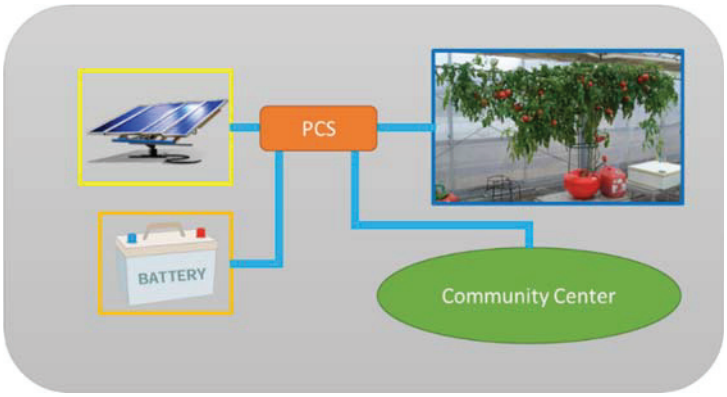

Fig. A-13 connection between PV, battery, hydroponic culture and community center

Fig. A-13 shows connection between PV, battery, hydroponic culture and community center in the future. Now, we connected PV, battery and hydroponic culture, because we had limited time. When the sun is shining, the PCS adjusts PV generated power and supplies power to the battery and pump. When the amount of PV generation drops, the battery supplies power to the pump, so the pump keeps running almost all day. This creates an important flow of water for hydroponic cultivation. The growth process of hydroponic tomato is shown below.

Fig. A-5 Growth process of hydroponic tomato

Acknowledgments

末尾ではありますが本研究を遂行するにあたりまして，お世話になりました電力・エネルギー工学研究室の方々に謝辞を述べさせていただきます。

本研究において，始終丁寧な御指導を頂きました餘利野直人教授に深く御礼申し上げます。また，本研究遂行中に有益な御助言，御意見を賜りました，造賀芳文准教授，佐々木豊助教，関崎真也助教に心より感謝の意を表します。

さらに，本論文を御査読して頂きました西崎一郎教授，高橋勝彦教授，塚井誠人准教授に厚く御礼申し上げます。

また本研究を進めるにあたりご協力頂きました松尾興祐氏に厚く御礼申し上げます。

最後に研究のみならず生活面でもアドバイスを頂いた本研究室の先輩方，並びに電力・エネルギー工学研究室の皆様に心より感謝の意を表し，謝辞とさせていただきます。

2019 年 1 月 18 日

中村　優希

References

[1] "Long-Term Energy Supply and Demand Prospect (draft)", Long-Term Energy Supply and Demand Prospect Subcommittee, Jun. 2015, in Japanese

[2] S. Eftekharnejad : V. Vittal, G.T. Heydt, B. Keel, and J. Loehr, “Imapact of Increased Penetration of Photovoltaic Generation on Power Systems“, IEEE Trans. on Power Syst., Vol. 28, No. 2, pp.893-901 (2013)

[3] Transistor Technology Editorial Department, "Fundamentals and Applications of Solar Cell Utilization", CQ Publisher (2011) in Japanese

[4] N. Taniguchi, “Power System Analysis - Modeling and Simulation “, The Institute of Electrical Engineers · Ohmsha (2009) in Japanese

[5] T. E. Dy Liacco : “System security: the computer’s role”, IEEE Spectrum, Vol. 15, No. 6, pp. 43-50 (1978)

[6] B. Stott and E. Hobson : “Power system security control calculations using linear programming, Part1&2”, IEEE Trans. Power App. Syst., Vol. PAS-97, No. 5, pp. 1713-1731 (1978)

[7] M. H. Banakar and F. D. Galiana : “Power system security corridors concept and computation”, IEEE Trans. Power App. Syst., Vol. PAS-100, no. 11, pp. 4524-4532 (1981)

[8] P. M. Anderson, et al : “Inter-Area Oscillations in Power Systems”, System Dynamic Performance Subcommittee Special Publication, IEEE Power Engineering Society, 95TP101 (1995)

[9] N. Yorino, H. Sasaki, Y. Tamura, and R. Yokoyama : “A Generalized Analysis Method of Auto-Parametric Resonances in Power Systems”, IEEE Trans. Power Systems, Vol. 4, No. 3, pp. 1057-1064 (1989)

[10] T. Athey, R. Podmore, and S. Virmani : “A Practical Method for Direct Analysis of Transient Stability”, IEEE Trans. Power Apparatus and Sys-tems, vol. PAS-98, pp. 573-584 (1979)

[11] H. D. Chiang and J. S. Thorp : “The closest unstable equilibrium point method for power system dynamic security assessment”, IEEE Trans. Circuits Syst,, Vol. 36, pp. 1187–1199 (1989)

[12] G. A. Maria, C. Tang, and J. Kim : “Hybrid Transient Stability Analysis”, IEEE Trans. Power Systems, Vol.5, No.2 (1990)

[13] Y. Xue, L. Wehenkel, R. Belhomme, P. Rous-seaux, M. Pavella, E. Euxibie, B. Heilbronn, and J. F. Lesigne : “Extended Equal Area Criterion Revised”, IEEE Trans. Power Systems, Vol. 7, No. 3 (1992)

[14] H. D. Chiang, C. C. Chu, and G. Cauley : “Direct Stability Analysis of Electric Power Systems Using Energy Functions: Theory, Applications, and Perspective”, Proceedings of the IEEE, Vol. 83, No. 11 (1995)

[15] R. T. Treinen, V. Vittal, and W. Kliemann : “An Improved Technique to Determine the Controlling Unstable Equilibrium Point in a Power System”, IEEE Trans. Circuit and Systems, Vol. 43, No. 4, pp. 313-323 (1996)

[16] J. T. Scruggs, L. Mili : “Dynamic gradient method for PEBS detection in power system transient stability assessment”, Int Jour of Electrical Power and Energy Systems, Vol. 23, No.2, pp. 155-165 (2001)

[17] Ancheng Xue, Shengwei Mei, Bangpeng Xie : “A comprehensive method to compute the controlling unstable equilibrium point”, IEEE Electric Utility Deregulation and Restructuring and Power Technologies, Third International Conference, pp. 1115-1120 (2008)

[18] H. Kita, K. Nishiya, J. Hasegawa, “On-line Preventive Control for Power System Transient Stability Based on the Energy Function Method”, IEEJ Trans. on Power and Energy, Vol. 110, No. 9, pp. 745-752, 1990

[19] A. Takimoto, “A Practical Preventive Control Methed for Transient Stability Based on Time Domain Simulation”, IEEJ Trans. on Power and Energy, Vol. 124, No. 12, pp. 1447-1453, 2004

[20] R. Umemura, H. Taoka, S. Kawasaki, and Y. Hondo, “The Prototype of Power-Synchronization Inverter for Dispersed Generation,” The Paper of Joint Technical Meeting on Power Engineering and Power System Engineering, IEEJ, PE-12-133/PSE-12-149, pp.55-59 (2012) (in Japanese)

[21] K. Sakimoto, Y. Miura, and T. Ise, “Characteristics of Parallel Operation of Inverter Type Distributed Generators Operated by a Virtual Synchronous Generator,” IEEJ Trans. on Power and Energy, Vol.133, No.2, pp.186-194 (2013) (in Japanese)

[22] L. Zhang, L. Harnefors, and H.P. Nee, “Power-Synchronization Control of Grid-Connected Voltage-Source Converters,” IEEE Trans. on Power Systems, Vol.25, No.2, pp.809-820 (2010)

[23] J. Zhu, C.D. Booth, G.P. Adam, A.J. Roscoe, and C.G. Bright, ”Inertia Emulation Control Strategy for VSC-HVDC Transmission Systems,” IEEE Trans. on Power

Systems, Vol.28, No.2, pp.1277-1287 (2013)

[24] K. Sakimoto, Y. Miura, and T. Ise, “Stabilization of a Power System including Inverter Type Distributed Generators by the Virtual Synchronous Generator,” IEEJ Trans. on Power and Energy, Vol.132, No.4, pp.341-349 (2012) (in Japanese)

[25] M. Hojo, R. Ikeshita, Y. Ueda, and T. Funabashi, “Effectiveness of a Self-Commutated Power Converter Emulating a Synchronous Machine,” The Paper of Technical Meeting on Power Engineering, IEEJ, PE-11-182, pp.7-10 (2011) (in Japanese)

[26] H. Akiyashi, M. Okamoto, E. Hiraki, and T. Tanaka, “A Three Phase PLL with Moving Average LPF,” The 62nd Chugoku-branch Joint Convention of Institute of Electrical and Information Engineers, pp.417-418 (2011) (in Japanese)

[27] L.N. Arruda S.M. Silva, and B.J.C. Filho, “PLL Structures for Utility Connected Systems”, 36th IAS Annual Meeting, IEEE, Vol.4, pp.2655-2660 (2001)

[28] T. Shintai. K. Sakimoto, Y. Hiura, and T. Ise, “Load Sharing Control by a Virtual Synchronous Generator Control with Reactive Power Control,” The Paper of Joint Technical Meeting on Power Engineering and Power System Engineering, IEEJ, PE-11-179/PSE-11-196, pp.79-84 (2011) (in Japanese)

[29] Y. Hirase, K. Abe, K. Sugimoto, and Y. Shindo, “A Grid Connected Inverter with Virtual Synchronous Generator Model of Algebraic Type,” IEEJ Trans. on Power and Energy, Vol.132, No.4, pp.371-380(2012) (in Japanese)

[30] Kawaguchi, A. Okui, H. Ikeda, and K. Matsuse, “Resonance Phenomenon in the DC Circuit of Large-scale Inverter System,” IEEE Trans. on Power and Energy, Vol.122, No.10, pp.966-974(2002) (in Japanese)

[31] Technical Report of IEEJ, No.869 (2002) (in Japanese)

[32] T. Matoba, R. Umemura, H. Taoka, S. Kawasaki, and J. Matsuki, “Basic Examination of the Synchronization Inverter for Distributed Generation,” IEEJ Annual Meeting, Vol.219, No.6, pp.390-391 (2012) (in Japanese)

[33] T. Shintai, K. Sakimoto, Y. Miura, and T. Ise, “Experimental Results of Reactive Power Control with Virtual Synchronous Generator Control”, IEEJ Annual Meeting, Vol.218, No.6, pp.388-389(2012) (in Japanese)

[34] Lidong Zhang, Lennart Harnefors, and Hans-Peter Nee, “Power-Synchronization Control of Grid-Connected Voltage-Source Converters”, IEEE Trans. Power Syst., Vol. 25, No. 2, pp. 809-820, 2010.

[35] Jon Are Suul, Salvatore D’Arco, and Giuseppe Guidi, “Virtual Synchronous

Machine-Based Control of a Single-Phase Bi-Directional Battery Charger for Providing Vehicle-to-Grid Services", IEEE Trans. Ind. App., Vol. 52, No. 4, pp. 3234-3244, 2016.

[36] Xin, Z., Wang, X., Qin, Z., Lu, M., Loh, P.C., and Blaabjerg, F.. "An Improved Second-Order Generalized Integrator Based Quadrature Signal Generator", IEEE Trans. Power Elect., Vol. 31, No. 12, pp. 8068-8073. 2016.

[37] J. M. Arroyo, and F. D. Galiana : "On the solution of the bilevel programming formulation of the terrorist threat problem", IEEE Trans. Power Syst., Vol. 20, No. 2, pp. 789–797 (2005)

[38] D. Bertsimas, E. Litvinov, X. A. Sun, J. Zhao, and T. Zheng : "Adaptive robust optimization for the security constrained unit commitment problem", IEEE Trans. Power Syst., Vol. 28, No. 1, pp. 52-63 (2013)

[39] A. Lorca, and X. A. Sun : "Adaptive robust optimization with dynamic uncertainty sets for multi-period economic dispatch under significant wind", IEEE Trans. Power Syst., Vol. 30, No. 4, pp. 1702–1713 (2015)

[40] J. Warrington, C. Hohl, P. J. Goulart, and M. Morari : "Rolling unit commitment and dispatch with multi-stage recourse policies for heterogeneous devices", IEEE Trans. Power Syst., Vol. 31, No. 1, pp. 187-197 (2016)

[41] E. Lannoye, D. Flynn, and M. O'Malley : "Evaluation of power system flexibility," IEEE Trans. Power Syst., Vol. 27, No. 2, pp. 922-931 (2012)

[42] J. Zhao, T. Zheng, and E. Litvinov : "A unified framework for defining and measuring flexibility in power system", IEEE Trans. Power Syst., Vol. 31, No. 1, pp. 339-347 (2016)

[43] J. Zhao, T. Zheng, and E. Litvinov : "Variable resource dispatch through do-not-exceed limit", IEEE Trans. Power Syst., Vol. 30, No. 2, pp. 820–828 (2015)

[44] Y. Okumoto, N. Yorino, Y. Zoka, Y. Sasaki, T. Yamanaka, and T. Akiyoshi : "An application of robust power system security to power system operation for high-penetration of PV", in Proc. of IEEE PES Innovative Smart Grid Technologies Conf., pp. 1-7 (2012)

[45] N. Yorino, Y. Sasaki, E.P. Hristov, Y. Zoka, and Y. Okumoto : "Dynamic load dispatch for power system robust security against uncertainties", in Proc. of 2013 IREP Symp., Crete, Greece, pp. 1-17 (2013)

[46] N. Yorino, M. Abdillah, T. Isoya, Y. Sasaki, and Y. Zoka : "A new method of evaluating robust power system security against uncertainties", IEEJ Trans. on

Elect.and Electron.Eng., Vol. 10, No. 6, pp. 636-643 (2015)

[47] N. Yorino, A. Muhammad, Y. Sasaki, Y, Zoka : "Robust Power System Security Assessment under Uncertainties Using Bi-Level Optimization", IEEE Trans. Power Syst., Vol.33, No.1, pp.352-362 (2017)

[48] N. Yorino, Y. Nakamura, M. Abdillah, Y. Sasaki, Y. Okumoto : "A Method for Evaluating Power System Security Region under Uncertainties and Its Application to Transient Stability Problem", in Proc. of 2017 IREP Symp., Porto, Portugal, pp. 1-15 (2017)

[49] N. Yorino, A. Priyadi, H. Kakui, and M. Takeshita : "A new method for obtaining critical clearing time for transient stability", IEEE Trans. Power Syst., Vol. 25, No. 3, pp. 1620-1626 (2010)

[50] A. Priyadi, N. Yorino, M. Tanaka, T. Fujiwara, H. Kakui, and M. Takeshita : "A direct method for obtaining critical clearing time for transient stability using critical generator conditions", European Trans. on Electrical Power, Vol. 22, No. 5, pp. 674-687 (2012)

[51] N. Yorino, E. Popov, Y. Zoka, Y. Sasaki, and H. Sugihara : "An application of critical trajectory method to bcu problem for transient stability studies", IEEE Trans Power Syst., Vol. 28, No. 4, pp. 4237-4244 (2013)

[52] P. Bhui and N. Senroy : "Real-Time Prediction and Control of Transient Stability Using Transient Energy Function", IEEE Trans. on Power Syst., Vol. 32, No. 2, pp. 923-934 (2017)

[53] H. Yoshida, R. Tachi, K. Takafuji, H. Imaeda, M. Takeishi, H. Taguchi, and K. Kusaba : "Development of Trunk Transmission Online Integrated Stability Control System (ISC)", IEEJ Trans. on Power and Energy, Vol. 137, No. 6, pp.434-445 (2017) (in Japanese).

[54] H. Yoshida, R. Tachi, K. Takafuji, et al.: 'Development of Trunk Transmission Online Integrated Stability Control System (ISC)', IEEJ Trans. on Power and Energy, Jun. 2017, 137, (6), pp.434-445, (in Japanese)

[55] C. Audet, P. Hansen, B. Jaumard, and G. Savard : "Links between linear bilevel and mixed 0–1 programming problems", Journal of Optimization Theory and Applications, Vol. 93, No. 2, pp. 273-300 (1997)

[56] IBM ILOG CPLEX optimization studio [Online]. Available:https://www-01.ibm.com/software/commerce/optimization/ cplex-optimizer.

[57] Standard model of electric power system, The institute of Electric Engineers of Japan

HP, http://www.iee.jp/pes/?page_id=132 (Dec. 20, 2018)

[58] Mahdi Ashabani and Yasser Abdel-Rady I. Mohamed, “Novel Comprehensive Control Framework for Incorporating VSCs to Smart Power Grids Using Bidirectional Synchronous-VSC,” IEEE Trans. Power Syst., Vol. 29, No. 2, pp. 943-957, 2014.

[59] Mahdi Ashabani and Yasser Abdel-Rady I. Mohamed, “Integrating VSCs to Weak Grids by Nonlinear Power Damping Controller With Self-Synchronization Capability,” IEEE Trans. Power Syst., Vol. 29, No. 2, pp. 805-814, 2014.

[60] Salvatore D’Arco and Jon Are Suul, “Equivalence of Virtual Synchronous Machines and Frequency-Droops for Converter-Based MicroGrids”, IEEE Trans. Smart Grid, Vol. 5, No. 1, pp. 394-395, 2014.

[61] S. M. Ashabani and Y. A.-R. I. Mohamed, “New family of microgrid control and management strategies in smart distribution grids—Analysis, comparison and testing,” IEEE Trans. Power Syst., Vol. 29, No. 5, pp. 2257–2269, 2014.

[62] Shinya Sekizaki, Naoto Yorino, Yutaka Sasaki, Yuki Nakamura, Yoshifumi Zoka and Ichiro Nishizaki, “A Basic Study on A Single Phase Pseudo-Synchronizing Power Inverter for Stabilization of Microgrid,” The papers of Technical Meeting on "Power Systems Engineering", IEE Japan vol.5, pp.121-126, PE-16-171/PSE-16-191, (2016).

[63] R. Teodorescu, M. Liserre, and P. Rodriguez, Grid Converters for Photovoltaic and Wind Power Systems. New York, NY, USA: Wiley. (2011)

[64] Technical Report of IEEJ, No.869 (2002)

Publications

主論文	既発表論文番号
1　Introduction: Power system on introduction of renewable energy	A-1,2 B-1-10
2　Stabilization control for power system	A-1,2 B-1-10
3　Transient stability analysis and control for power system by using CCT	A-2 B-4,7
4　Stabilization control by synchronous inverter	A-1 B-1-3,5,6,8-10
5　Conclusion	A-1,2 B-1-10

引用既発表論文

A　学術論文誌掲載論文

[A-1]　関﨑真也, 餘利野直人, 佐々木豊, 松尾興祐, 中村優希, 造賀芳文, 清水敏久, 西﨑一郎, "電力系統安定化と非常時のマイクログリッド運用を目的とした特性非干渉型単相同期化力インバータの提案と実験的検証," 電気学会論文誌Ｂ（電力・エネルギー部門誌）, Vol. 138, No. 11, Nov. 2018.

[A-2]　中村優希, 餘利野直人, 佐々木豊, 造賀芳文, "CCT Distribution Factor を利用した過渡安定度監視と予防制御," 電気学会論文誌 B（電力・エネルギー部門誌）, Vol. 139, No. 3, Mar. 2019 (発行予定).

B　国際会議発表論文

[B-1]　Shinya Sekizaki, Yuki Nakamura, Yutaka Sasaki, Naoto Yorino, Yoshifumi Zoka, and Ichiro Nishizaki, "A Development of Pseudo-Synchronizing Power VSCs Controller for Grid Stabilization," *19th Power System Computation Conference* (*PSCC*), Genoa, Italy, Jun. 2016, pp. 1-7.

[B-2]　Shinya Sekizaki, Naoto Yorino, Yuki Nakamura, Yutaka Sasaki, Yoshifumi Zoka, and Ichiro Nishizaki, "A Theoretical and Experimental Study on Pseudo-synchronizing Power Inverter," *The International Conference on Electrical Engineering '16* (*ICEE2016*), Okinawa, Japan, Jul. 2016, pp. 1-6.

[B-3] Yuki Nakamura, Naoto Yorino, Shinya Sekizaki, Yutaka Sasaki, and Yoshifumi Zoka, "A Development of Power System Stabilizer using Synchronizing Power on VSC," *The International Conference on Electrical Engineering '16* (*ICEE2016*), Okinawa, Japan, Jul. 2016, pp. 1-6.

[B-4] Naoto Yorino, Yuki Nakamura, Abdillah Muhammad, Yutaka Sasaki, and Yoshiharu Okumoto, "A Method for Evaluating Power System Security Region under Uncertainties," *10th Bulk Power Systems Dynamics and Control Symposium – IREP2017*, Espinho, Portugal, Aug. 2017, pp. 1-15.

[B-5] Shinya Sekizaki, Yutaka Sasaki, Naoto Yorino, Yoshifumi Zoka, Yuki Nakamura, and Ichiro Nishizaki, "A Development of A Single-phase Synchronous Inverter for Grid Resilience and Stabilization," *7th Innovative Smart Grid Technologies* (*ISGT Asia 2017*), Auckland, New Zealand, Dec. 2017, pp. 1-5.

[B-6] Yuki Nakamura, Shinya Sekizaki, Yutaka Sasaki, Kosuke Matsuo, Naoto Yorino, Yoshifumi Zoka, and Ichiro Nishizaki, “A development of single-phase synchronous inverter for microgrid operation”, *International Workshop on Power Engineering in Remote Islands* (*IWPI2018*) *in Okinawa*, Feb. 2018, pp 1-6.

[B-7] Yuki Nakamura, Naoto Yorino, Yutaka Sasaki, and Yoshifumi Zoka, "Transient Stability Monitoring and Preventive Control based on CCT," *IEEE International Symposium on Devices, Circuits and Systems* (*ISDCS2018*), Kolkata, India, Mar. 2018, pp. 1-6.

[B-8] Kosuke Matsuo, Shinya Sekizaki, Yutaka Sasaki, Naoto Yorino, Yuki Nakamura, Yoshifumi Zoka, and Ichiro Nishizaki, "An Experimental Study of Single-phase Synchronous Inverter with Hardware in the Loop Simulation," *The International Conference on Electrical Engineering* (*ICEE2018*), Seoul, Korea, Jul. 2018, pp. 1-6.

[B-9] Shinya Sekizaki, Kosuke Matsuo, Yuki Nakamura, Yutaka Sasaki, Naoto Yorino, Yoshifumi Zoka, and Ichiro Nishizaki, "Stabilization of Microgrid with Multiple Inverters," *10th IFAC Symposium on Control of Power and Energy Systems* (*CPES2018*), Tokyo, Japan, Sep. 2018, pp. 1-6.

[B-10] Shinya Sekizaki, Kosuke Matsuo, Yutaka Sasaki, Naoto Yorino, Yuki Nakamura, Yoshifumi Zoka, Toshihisa Shimizu, and Ichiro Nishizaki, "A Development of Single-phase Synchronous Inverter and Integration to Single-phase Microgrid effective for frequency stability enhancement," *10th IFAC Symposium on Control of Power and Energy Systems* (*CPES2018*), Tokyo, Japan, Sep. 2018, pp. 1-6.